

# The Messenger



No. 146 – December 2011

VST and OmegaCAM commissioned  
Four-telescope interferometry with PIONIER  
Spectra of extremely metal-poor stars  
Ly-alpha luminosity function at high redshift





# The VLT Survey Telescope Opens to the Sky: History of a Commissioning

Massimo Capaccioli<sup>1,2</sup>  
Pietro Schipani<sup>2</sup>

<sup>1</sup> Department of Physical Sciences,  
University Federico II, Naples, Italy

<sup>2</sup> INAF–Capodimonte Astronomical  
Observatory, Naples, Italy

Commissioning team members:

Massimo Dall’Ora<sup>1</sup>, Sergio D’Orsi<sup>1</sup>, Laurent Marty<sup>1</sup>,  
Carmelo Arcidiacono<sup>2,3,5</sup>, Javier Argomedo<sup>3,4</sup>,  
Jacopo Farinato<sup>5</sup>, Demetrio Magrin<sup>5</sup>, Roberto  
Ragazzoni<sup>5</sup>, Gabriele Umbrico<sup>6</sup>

<sup>1</sup> INAF–Capodimonte Astronomical Observatory,  
Italy, <sup>2</sup> INAF–Bologna Astronomical Observatory,  
Italy, <sup>3</sup> INAF–Arcetri Astronomical Observatory,  
Italy, <sup>4</sup> ESO, <sup>5</sup> INAF–Padua Astronomical Observatory,  
Italy, <sup>6</sup> University of Padua, Italy

The VLT Survey Telescope (VST) is now ready to undertake its mission. After a long gestation, the telescope has revealed its power, providing image quality and resolution beyond expectation. This achievement has been made possible by a motivated team of scientists and engineers who have brought the VST to its current state of readiness for survey science. This paper briefly reviews the latest stages of the project and the characteristics of the VST, and lists the scientific programmes for the observing time guaranteed by ESO to the Italian community in return for the procurement of the telescope.

## Introduction

The VLT Survey Telescope (VST) is a wide-field optical imaging telescope with a 2.61-metre aperture, operating from the ultraviolet to the near-infrared ( $z'$ -band) with a corrected field of view of 1 degree by 1 degree. Views of the VST in its dome are shown in Figures 1, 2 and 3. Conceived for the superb environment of the Paranal Observatory (Figure 4), it features an  $f/5.5$  modified Ritchey–Chrétien optical layout, a two-lens wide-field corrector with the dewar window acting as a third lens or, alternatively, an atmospheric dispersion compensator coupled with a single-lens wide-field corrector plus the dewar window, an active primary mirror (Figure 5), a hexapod-driven secondary

mirror, and an alt-azimuthal mounting. Its single focal plane instrument, OmegaCAM, is a large format (16k × 16k pixels) CCD camera contributed by the OmegaCAM consortium (see Kuijken, p. 8).

The VST is the result of a joint venture between ESO and the Capodimonte Astronomical Observatory (OAC) in Naples, formerly an independent institution, and, since 2002, part of the Italian National Institute for Astrophysics (INAF). It is the largest instrumental project carried out by Italian astronomy for ESO and the first active optics telescope completely designed in Italy, from scratch, and by a fistful of engineers.

Here we briefly describe the final stages of the project before its completion and report on the scientific programmes devised by the INAF community for the guaranteed time observing (GTO). For the earlier history see Capaccioli et al. (2003, 2005).

## Early development

The VST project was proposed by OAC to ESO in 1997 and began in 1998 with the signature of a Memorandum of Understanding (MoU) establishing the dues and rights of the partners. OAC committed to procuring the telescope and providing up to two of its personnel to support the operation of the facility. In return, OAC (now part of INAF) was entitled to receive a proportional share of the total VST observing time plus a number of nights at one VLT Unit Telescope (UT). ESO committed itself to provide the facilities needed to house and run the telescope at Paranal, to cooperate with OAC in setting the specifications and interfaces of the telescope, to procure the transport of the instrument from Italy to Chile, to secure the proper CCD camera, and to commission the complete VST system. Moreover ESO took responsibility for the operation and maintenance of the VST for a period of ten years.

In the summer of 2011 ESO and INAF amended the MoU and agreed on the following share for the INAF–GTO: 10% for the first four years of the telescope’s life, 15% for following two years, and 20% for the remaining four years (percentages

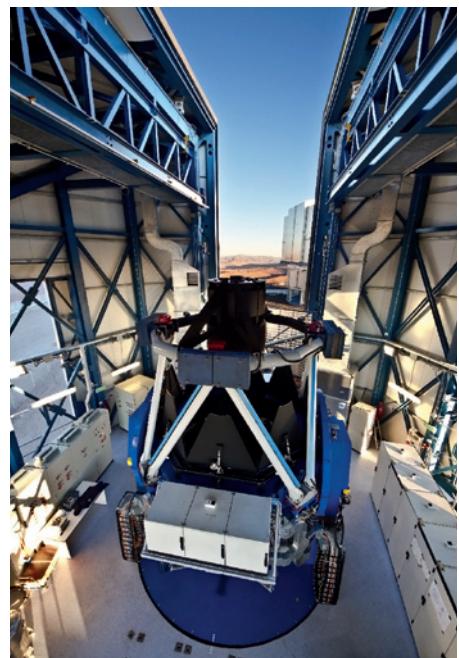


Figure 1. A view of the VST inside its enclosure, surrounded by the electrical control cabinets. UT4 and the Atacama desert are visible in the background.

to be calculated at the net of the Chilean time). These numbers reflect the effort made by INAF to boost the ESO Public Surveys, and take into account the delays in the project. INAF was also granted a number of hours, equivalent to 28 nights at one VLT UT, to be evenly distributed over an interval of ten years and to be used exclusively for follow-up programmes for INAF–VST surveys.

The development of the project was marked by two major accidents which have extended the schedule significantly: the first back in 2002, when the primary mirror (M1) was literally shattered during its transfer by ship to Chile. Recovery from this took almost four years, while the Russian firm LZOS, which had very successfully manufactured the first mirror, completed an exact replica. In addition to the time delay, it had grave collateral effects on the motivation of the VST technology team at OAC and on the budget (see Capaccioli et al., [2005], for more details).

In 2002 the Italian observatories were merged into the National Institute for Astrophysics, which had the critical mass to sustain OAC in this dramatic phase of



Figure 2. The VST from above. The M1 cover is open and the primary mirror is visible with its baffle. On top, the back side of the hexapod driving M2 is visible. The observation doors with the wind screen are seen on the right side of the picture.

the project. In addition to money, INAF provided managerial and technological support using the knowhow available in its other structures, increasing the staff complement by bringing in people, mainly from the Padua Observatory. In late 2005 INAF also created an *ad hoc* institute, based at Capodimonte and named VSTceN, to coordinate the project, which was placed under the direction of Massimo Capaccioli, former OAC director and the principal investigator of the VST.

By March 2006 the new primary mirror, with which the active optics sub units had to be carefully matched, had safely reached the Paranal Observatory, and by the end of the year an ESO audit team spent about one month with the OAC team in Naples and concluded that the telescope mount and the tracking system, pre-assembled at the MecSud firm in Scafati, were ready for shipping to Chile, which was done during 2007. The telescope was then re-integrated and tested at Paranal. In the same year, the Critical Design Review (CDR) of the primary and secondary mirror systems,

which should have given the green light to these crucial units, was globally unsuccessful. Of course, the immediate feeling at OAC was of considerable disappointment! But looking back, this failure marked the turning point for the later success. The key problem identified by the ESO reviewers was a lack of proper systems engineering in the project, which had been diluted by the considerable efforts made on the single subsystems.

### Recent progress

Starting from mid-2007, the primary and secondary mirror support systems were extensively reconsidered by INAF–OAC at the systems engineering level, transferring the technical leadership to P. Schipani and establishing a new team with some of the engineers who had already been working on the project. The re-design of the active optics system was further complicated by two stringent conditions: to minimise the changes and the expenditures and to close out the activities as soon as possible.

This strategy led to success: in a little less than two years, including manufacturing and tests, all the parts of the telescope still in Italy received the green light to be shipped to Chile. The telescope error budget was revisited and the

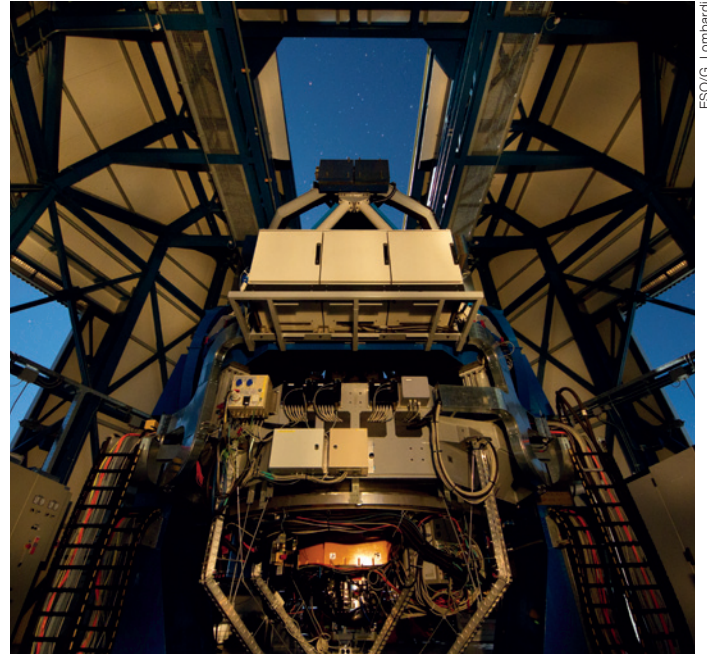


Figure 3. The VST as seen from the observing floor. The OmegaCAM instrument and its control cabinets are in the lower section, interfaced to the telescope at the Cassegrain focus.

concept of the primary mirror support and safety system redesigned, with regard to performance, reliability, and maintenance operations. The error budget was modified, adopting ambitious, but realistic, capabilities for the telescope subsystems. Two major simplifications were introduced into the active optics subsystems. The 24 lateral active supports in the M1 cell were replaced by passive astatic levers, and three lateral fixed points were introduced. In addition, the piezoelectric plate, with five degrees of freedom, coupled to the hexapod for the accurate positioning of the secondary mirror (M2) was eliminated, with no real loss of accuracy and a major gain in reliability and operability.

The primary mirror support system design, the control software and the electronics were updated by INAF–OAC, and the new mechanical parts were designed by Tomelleri srl, the firm which also re-cabled the cell, under VSTceN requirements and supervision. The earthquake safety system, previously overlooked, was designed in a joint effort led by INAF–OAC, which made the analysis jointly with BCV srl, and with full support



from ESO's Technology Division, while the mechanical design was committed to Tomelleri srl.

The concept of the secondary mirror support system was also significantly updated by INAF–OAC in order to improve reliability and performance. The mechanics of the hexapod were slightly improved by ADS International srl, while the modification of the control electronics was shared between ADS for the leg electronics and VSTceN for the Local Control Unit. New control software was written at INAF–OAC, replacing the old version made obsolete by the new hardware. At the end of 2008 the secondary mirror support system was effectively tested at system level and shipped to Chile, where in early 2009 it was installed at the telescope and verified on site. The secondary mirror could now perform relative displacements along the optical axis with a precision of about  $0.1\ \mu\text{m}$  (budget:  $0.5\ \mu\text{m}$ ), and in the XY-plane with precision of  $1\text{--}2\ \mu\text{m}$  (budget:  $5\ \mu\text{m}$ ) at any altitude angle.

Both the primary and the secondary mirror support systems were extensively tested in Italy in all gravity conditions using tilting test devices, undergoing severe qualification of both performance and reliability. A good MTBF (mean time between failures) was assessed by intensive tests on a subset of ten M1

Figure 4. The total complement of telescopes on the Paranal platform: the UTs and the auxiliary telescopes are joined by the latest addition of VST on the right side (north-east).



actuators, simulating years of work of the support systems with uninterrupted 24-hour testing performed for several weeks at an accelerated rate.

#### New accident, new recovery

In early 2009 the support system was ready to be shipped. Unfortunately, another major transport accident occurred. The vessel carrying the mirror cell, which had left Livorno at Easter, was delayed around Toulon by a general average. Two months passed before the ship set out again for Chile, but once the load reached Paranal it became apparent that a fair amount of water had penetrated the moisture barrier bag protecting the M1 cell and had caused severe damage.

The cell had to be re-imported back to Italy for re-manufacturing and qualification of the whole system, and, in particular, of the most critical component of the whole telescope, the primary mirror supports. This phase ended with successful system tests in April 2010. The accident had further shifted the schedule of the project back by one year. The recovery activity was supposed to be a “mere” repetition of the work already done but, surprisingly, the replacement of some obsolescent commercial components by nominally identical parts caused unexpected problems which were solved by changes in the control system. In the end the primary mirror supports turned out to have very good differential

force setting capability; they perform small differential force adjustments generally with an error of just  $\pm 0.2\ \text{N}$ , better than expected (budget:  $\pm 0.5\ \text{N}$ ).

With a few months of hard work, in early 2009 a team composed of people from Padua (Observatory and University), Capodimonte and INAF Headquarters, together with the industrial support of Tomelleri srl, completed the work on the remaining subsystems: adapter/rotator, probe optics, Shack–Hartmann wavefront sensor, atmospheric dispersion corrector (ADC), were all tested and debugged for the electromechanical part. The technical CCD systems were also put into operation. These units were shipped to Chile in mid-2009 and reassembled on site.

Meanwhile, other activities continued. The telescope control software was improved and tested, using the VLT control model facility at ESO Headquarters; a cabling plan was prepared and then followed during the integration; some parts of the cooling system were revisited because the old design did not fulfill all the real needs; the active optics operating model was studied in detail; the wavefront sensing was simulated; much optomechanical integrated analysis was carried out; the software interface with OmegaCAM was tested; the transfer function of the axes was measured both in Naples and again in Paranal, giving an altitude-locked rotor eigenfrequency of  $9\ \text{Hz}$ , in reasonable agreement with the control simulations; and many much less significant activities were also performed.

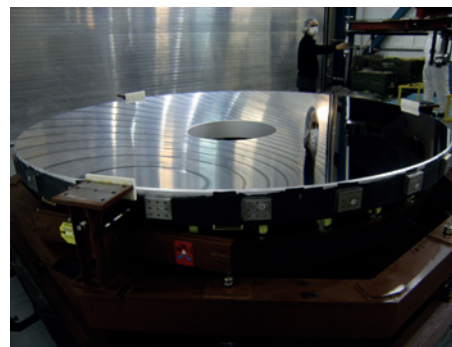


Figure 5. The 2.6-metre VST primary mirror in the coating plant.



## Recent years in Chile

The reintegration in Paranal was performed in three different steps, always in strict collaboration with ESO. The first was the installation of the hydrostatic bearing system for the azimuth rotation and of the telescope mount, which ended in 2008. In 2009 the remaining parts of the telescope were shipped, but only the secondary mirror support system was put in place, due to the damage to the primary mirror cell. The missing work was completed in 2010 when the mirror cell returned to Paranal (never had a mirror cell travelled so much!), allowing the installation of the mirrors, adapter/rotator and ADC. The mirrors were coated and installed in the telescope with the close collaboration of ESO, Tomelleri srl and ADS International srl. The missing parts of the cooling system were also installed by EIE srl.

By the end of 2010 the telescope was integrated and pre-aligned. There were some missing details, but also great urgency: the commissioning team therefore accepted that the missing aspects would be taken care of in parallel with the night work, starting in January 2011. Then a fourth large integration step was taken: the installation of the camera in March 2011 by the OmegaCAM consortium, with some involvement of the VST commissioning team for the electro-mechanical interfaces and the final balancing of the telescope. The latter is now balanced with a remarkable 3.6-tonne counterweight on the top ring, which fortunately did not detract from the good tracking performance.

## Commissioning

Commissioning is the last fundamental step, i.e. the transformation of a big piece of iron and glass into a telescope. At the time of writing, this stage has just been successfully completed.

The commissioning of the telescope and of its camera should take place together, because OmegaCAM needs a working VST to be tuned and vice versa. The management of this interaction between the teams of OmegaCAM, ESO and VST could have become critical. But the good

relationships established with the other teams nullified this risk: a human addition to a technical success in this case. The INAF team, composed of about ten people from Capodimonte, Padua and Arcetri, enjoyed the collaboration with OmegaCAM and ESO, as well as with the Dalkia engineering people hired in Paranal (the first light photo is shown as Figure 1 in Kuijken p. 8).

It must be added that the relatively small mirror diameter does not simplify things much with respect to a 8–10-metre telescope; in fact, it can make life even harder due to lack of space and reduced accessibility. Nevertheless, the commissioning of the VST was planned to take only a few months, including the camera commissioning. Everybody knew that this was an ambitious goal, but not unrealistic, for two reasons. First, the massive amount of preparatory work: there was little to invent from scratch on the mountain. Second, ESO support: the INAF team could always count on the Paranal people. In addition, one of the best ESO telescope control experts and the Garching guru of active optics joined the team. The commissioning plan was strictly followed and completed on time. Nevertheless, at the end of the scheduled activities, we realised that the image quality of the telescope on the whole field of view could be improved by additional shimming, discussed below, which was done in July 2011.

## Pointing and tracking

Work on the axis control loops was expected to proceed smoothly, because the loops had already been successfully tuned in Italy in 2006 and we were confident we could do it again. This was the case: no real show-stoppers were encountered; also for the pointing model and autoguiding, which of course had never been tested before. The pointing accuracy is at the level of 1 arcsecond root mean square (rms), with a best score of 0.8 arcseconds so far. The tracking axes have a blind tracking error against their own encoders of the order of a few  $10^{-2}$  arcseconds rms, lower than specification. The VST guiding system with its guide probe is fully operational and enables an image centroid error on the

guide probe smaller than 0.1 arcseconds. Good performance was also maintained during windy nights, with wind speeds up to 18 m/s, by closing the ventilation doors and using the wind screen.

## Active optics

The active optics was indeed an exciting part of the job. That system had been the major recent concern; we had to prove the effectiveness of the new concepts that we had implemented for the primary and secondary mirror support systems. This was relatively straightforward. After two nights of work we had successfully converted the Shack–Hartmann aberration angles into M1 and M2 coordinates and the active optics loop had been closed: we could already reduce the amount of aberration we saw on the workstation panels. But still there was a hidden problem, which we only discovered some weeks later: the Shack–Hartmann sensor suffered from static aberrations in the non-common path, which was dominant for some modes with respect to the real aberrations of the telescope. In other words the measurement was corrupted, but we were able to make a software fix.

Another major improvement was also necessary: by design the primary mirror support has no passive system that automatically compensates for the change of axial weight. This caused, as expected, incorrect forces on the three axial fixed points if no action was taken, especially at large zenith angles, generating trefoil aberration. The other M1 aberration modes proved to be much more stable. In order to be compliant with any operational scheme, we removed the root cause of the trefoil with a background software task that makes the system astatic. The active optics system is now fully operational: the aberration coefficients measured by the Shack–Hartmann sensor can usually be reduced to an acceptable level in two iterations.

## Alignment

The alignment was one of the hardest parts of commissioning, because the wide



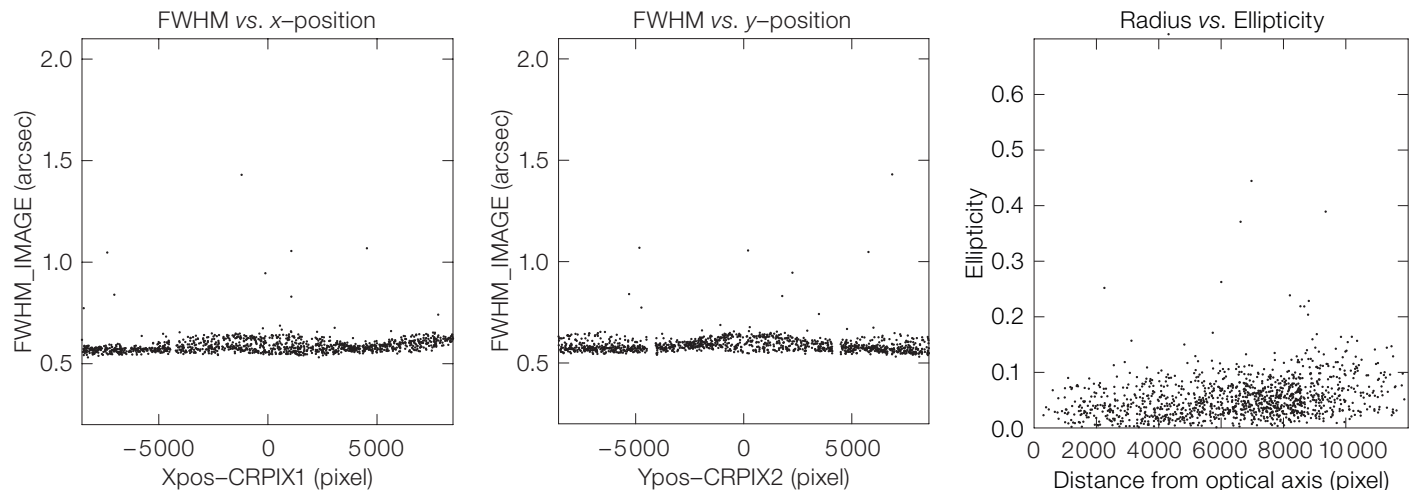


Figure 6. Image full width at half maximum vs.  $X$  offset (left) and  $Y$  offset (centre) are shown to be homogeneous after the alignment of rotator and optical axes. The image ellipticities, shown at right as a function of radial offset, are mostly within 10%.

field imposes much tighter requirements than for a normal telescope. We could remove a large amount of off-axis astigmatism by aligning M2 with M1: once we knew the correct measure, the correction was easily implemented using the hexapod. But the telescope still suffered from a focus gradient. Indeed, after the installation of the camera, a misalignment between the rotator and the optical axis was clearly detected. This had negligible effects on about 70% of the image, but caused a degradation on one side of the mosaic, which was out of focus. This problem could only be solved by shimming the rotator flange, with a lot of mechanical work and some suspense over the angle of the shims, which was fortunately correct! Now the image quality is homogeneous over the whole mosaic as expected by design (see Figure 6).

### Prospects

During commissioning the telescope has reached a good level of performance, as discussed above. Last but not least, the system has regularly worked for the whole duration of these activities with a technical downtime less than we could optimistically have expected for such a phase. The VST commissioning process has finally concluded with the Preliminary Acceptance Chile (PAC) being granted by ESO.

As a consequence of all this testing and the concomitant reliability, the telescope is already delivering seeing-limited images, with seeing measured by the Astronomical Site Monitor down to 0.4 arcseconds. Thus, it is now ready to survey the sky, and we are ready to work on the images using both AstroWise, the software package developed by the OmegaCAM consortium, and VST-Tube, another package designed at OAC to process VST images specifically. This latter package is an automated pipeline going from the raw exposures to fully calibrated co-added images, and extraction of catalogues with aperture and point spread function photometry. A set of tools allows us to administrate the data and check the quality of the intermediate and final products. VST-Tube comes with a Graphical User Interface to facilitate the interaction between data and user. The capabilities of this software have been recently proven as it was applied to produce the monochromatic images combined by ESO for the picture of the globular cluster Omega Centaurus (front cover image). In passing we note that a preliminary reduction of these images leads to limiting stellar magnitudes that are perfectly consistent with the expectations.

### Acknowledgements

The proposal, study, design, and realisation of the VST telescope was the result of the joint effort of a number of people who are acknowledged here as a whole. The following list is just for the last few years. Even so, it is quite long and we run the risk of forgetting someone (for which we apologise in advance).

For the ESO Paranal and Garching team: Ueli Weilenmann, Andreas Kaufer, Octavio Lavin, Ricardo Parra, Matteo Pozzobon, Mario Tapia, Thomas Szeifert, Juan Osorio, Ismo Kastinen, Guillermo Valdes, Ivan Munoz, Stephane Guisard, Lothar Noethe, Franz Koch, Michael Mueller, Michael Esselborn, Henri Bonnet, Jaime Alonso, Gerd Hudepohl, Toomas Erm, Dietrich Baade, Olaf Iwert, Cristian Romero, Duncan Castex, Christophe Geimer, Miguel Riquelme, Steffen Mieske, Fernando Selman, Stefan Sandrock, Frederic Gonte, Guillaume Blanchard, Gerardo Ihle, Arno Van Kesteren, Nicolas Haddad, Andrew Wright, Alex Segovia, Pierre Sangsasset;  
for the Dalkia team: Yerco Juica, Luis Romero, Cristian Garrido, Edu Fernandez;  
for the Tomelleri Srl team: Raffaele Tomelleri, Pierfrancesco Rossetti, Francesco Perina, Stefano Recchia, Alessandro Da Ronco;  
for the ADS International srl team: Daniele Gallieni, Pierluigi Fumi, Enzo Anaclerio, Paolo Lazzarini;  
for the EIE team: Gianpietro Marchiori, Andrea Busatta, Cristina Battistel.

Key people who, in various fields, helped to rescue of the telescope project at various stages, from CDR to the integration in Chile, are: Massimo Brescia, Davide Fierro, Giacinto De Paris, Francesco Perrotta and Paolo Vettolani.

Special thanks are due to Jason Spyromilio and Roberto Tamai for their constant constructive criticism.

Last but not least, Konrad Kuijken and the whole OmegaCAM team were great partners in the telescope+camera commissioning.

The Italian Ministry of University and Research (MIUR), the Italian National Institute for Astrophysics (INAF) and the Regione Campania, are acknowledged for their financial support.

### References

- Capaccioli, M., Mancini, D. & Sedmak, G. 2003, Mem. SALT, 74, 450
- Capaccioli, M., Mancini, D. & Sedmak, G. 2005, The Messenger, 120, 10



## Appendix: Overview of INAF–GTO Surveys

Nicola R. Napolitano<sup>1</sup>

<sup>1</sup> INAF–Capodimonte Astronomical Observatory, Naples, Italy

The VST/OmegaCAM facility provides multi-band images of unprecedented quality, suitable for the investigation of a range of cutting-edge issues, such as the constituents of the Milky Way and its companion galaxies, the structure of nearby galaxies, galaxy formation processes in different environments from the field through clusters to superclusters, the search of intermediate redshift supernovae, the search/study of Active Galactic Nuclei (AGNs) and quasars, and finally the study of dark matter distribution in the Universe by weak lensing. Of course, based on previous experience with survey telescopes, a major outcome can also be expected from serendipitous discoveries.

The science division of VSTceN (for several years led by Juan Alcalá Estrada) has cooperated with the PIs of the INAF–GTO survey programmes with the aim of monitoring their degree of competitiveness. Following revision in 2008 some of the surveys were dropped. In 2009, just before the accident to the VST cell, INAF and VSTceN organised a workshop in Naples to discuss the current programmes and gather new ideas for VST–GTO exploitation. This led to a call for letters of intent. A comprehensive summary of the projects was presented at the ESO VST Public Surveys and GTO Programmes Review meeting in 2010 resulting in a synthesis which took into account the synergies among GTO projects and ESO Public Surveys. Brief summaries of the INAF–GTO programmes follow.

### SUDARE: Supernova diversity and rate evolution

PI: Enrico Cappellaro (INAF–Padua Observatory)

The aim of the survey is to measure the rate of the different types of supernovae (SNe) at redshift  $z \sim 0.3$ – $0.6$  and, by comparison with local rates, probe the evolution of SN diversity with cosmic time. Statistics of SNe in different environments and as a function of redshift are a key test of the coherence of stellar evolution theory, SN explosion mechanisms and the relation between nucleosynthesis and galaxy evolutionary scenarios, through some of their basic ingredients, namely star formation history, chemical enrichment, and feedback effects. The project is also intended to build up experience and test tools that will be needed for future all-sky synoptic surveys.

### STEP: The SMC in Time: Evolution of a Prototype interacting late-type dwarf galaxy

PI: Vincenzo Ripepi (INAF–Capodimonte Observatory)  
The intent is to derive the color–magnitude diagrams of the oldest population of the Small Magellanic Cloud (SMC) down to 1–2 magnitudes below the main sequence turn-off. This will help to break the age–metallicity degeneracy and recover the star formation history of the galaxy and of the Magellanic Bridge. Classical variable stars (RR Lyrae, Cepheids, anomalous Cepheids,  $\delta$ -Scuti stars, etc.) will be used as population tracers, especially in the unexplored region of the Bridge. The survey, which is synergic with the VISTA Public Survey VMC, will also shed light on the first stages of star formation by securing a complete mapping of pre-main-sequence objects.

### STREGA@VST: Structure and evolution of the galaxy

PI: Marcella Marconi (INAF–Capodimonte Observatory)  
This survey addresses the issues of the formation mechanisms in the Galactic halo by: i) tracing tidal tails and haloes around stellar clusters and galaxies; ii) mapping extended regions of the southern portion of the orbit of the Fornax dwarf galaxy; iii) possibly identifying new very faint stellar systems using recent techniques developed by the Sloan Digital Sky Survey (SDSS). Stellar tools will be used to achieve the science objectives: variable stars (RR Lyrae and long-period variables), turn-off and main sequence stars.

### Extension in the $u'$ -band of the WINGS Survey (Wide field Imaging of Nearby Galaxy clusters Survey)

PI: Mauro D’Onofrio (University of Padua)  
The survey aims at obtaining deep  $u'$ -band images for  $\sim 50$  galaxy clusters in the redshift range  $0.04 < z < 0.07$ , which already have complete  $B$ ,  $V$ ,  $J$ ,  $K$  and spectroscopic information from the WINGS survey. The  $u'$ -band imaging of the WINGS clusters gives a first chance to study in detail the star formation activity in a statistically significant sample of cluster galaxies and to establish the correlations between such activity and the galaxy morphology (from  $V$ -band imaging) and masses (from  $K$ -band data), and the link with the environment.

### VST-ACCESS (A Complete CEnsus of Star formation and nuclear activity in the Shapley supercluster)

PI: Paola Merluzzi (INAF–Capodimonte Observatory)  
This is a multiband ( $u'$ ,  $g'$ ,  $r'$ ,  $i'$ ,  $z'$ ) survey project aimed at determining the importance of cluster assembly processes in driving the

evolution of galaxies (down to  $M^* = +6$ ) as a function of their mass and environment, by covering a field of 23 square degrees centred on the core of the Shapley supercluster ( $z = 0.048$ ). It will be possible to track the evolution of galaxies from field to filaments and groups up to the cluster cores and to investigate what is the primary location for galaxies to be transformed. The survey will extend the multi-wavelength (far-ultraviolet to far-infrared) ACCESS survey ongoing in the super-cluster core.

### VOICE: VST optical imaging of the CDFS and ES1 areas

PI: Giovanni Covone & Mattia Vaccari (Universities of Naples & Padua)  
VOICE is a multiband ( $u'$ ,  $g'$ ,  $r'$ ,  $i'$  to  $AB \sim 26$ ) optical survey of the central regions of the Chandra Deep Field-South (CDFS) and ES1 fields (8 square degrees in total). These areas are of paramount interest for the community as they have been, and will be, targeted by deep ultraviolet (GALEX–DIS), near-infrared (VISTA–VIDEO), mid-infrared (Spitzer–SERVS and Spitzer–SWIRE), far-infrared (Herschel–HerMES), and radio (ATCA–ATLAS) surveys. The uniform and deep optical coverage still missing on these fields will be suitable for galaxy formation studies out to  $z \sim 1$  and for gravitational lensing.

### VEGAS: VST survey of Elliptical Galaxies in the South hemisphere

PI: Massimo Capaccioli (University of Naples Federico II)  
This deep multiband VST survey of nearby elliptical galaxies in the southern hemisphere is expected to reach 27.5, 27.0, 26.2 mag arcsecond<sup>-2</sup> in  $g'$ ,  $r'$ ,  $i'$ , respectively. The aim is to: i) trace the light distribution out to ten effective radii ( $R_e$ ); ii) derive colour gradients and measure the surface brightness fluctuation gradients out to a few  $R_e$ , for stellar population characterisation; and iii) obtain a full census of the satellite systems (globular clusters and dwarf galaxies) out to 20% of the galaxy virial radii.

### A VST-OmegaCAM survey of Local Group dwarf galaxies

PI: Enrico Held (INAF–Padua Observatory)  
The survey aims at carrying out a multiband ( $B$ ,  $V$ ,  $i'$ ,  $u'$ ) wide-field survey of southern Local Group dwarfs, extending well beyond the current nominal tidal radii. The survey will represent the most complete mapping of dwarf galaxies and provide useful targets for follow-up spectroscopy as well as an insight into the variations of the stellar populations. The proposal is based on both OmegaCAM and INAF–GTO.



# OmegaCAM: ESO's Newest Imager

Konrad Kuijken<sup>1</sup>

<sup>1</sup> Leiden Observatory, the Netherlands

Team members:

Ralf Bender<sup>1</sup>, Bernard Muschiello<sup>1</sup>, Wolfgang Mitsch<sup>1</sup>, Reinhold Häfner<sup>1</sup>, Hans-Joachim Hess<sup>1</sup>, Ulrich Hopp<sup>1</sup>, Ivica Ilijewski<sup>1</sup>, Helmut Kravcar<sup>1</sup>, Enrico Cappellaro<sup>2</sup>, Andrea Baruffolo<sup>2</sup>, Alessandro Bortolussi<sup>2</sup>, Laura Greggio<sup>2</sup>, Carlo Magagna<sup>2</sup>, Paolo Bagnara<sup>2</sup>, Enrico Cascone<sup>3</sup>, Harald Nicklas<sup>4</sup>, Reiner Harke<sup>4</sup>, Walter Wellem<sup>4</sup>, Klaus Reif<sup>5</sup>, Günther Klink<sup>5</sup>, Philip Müller<sup>5</sup>, Henning Poschmann<sup>5</sup>, Dietrich Baade<sup>6</sup>, Olaf Iwert<sup>6</sup>, Claudio Cumani<sup>6</sup>, Sebastian Deiries<sup>6</sup>, Christoph Geimer<sup>6</sup>, Guy Hess<sup>6</sup>, Jean-Louis Lizon<sup>6</sup>, Robert Niemeczek<sup>6</sup>, Javier Reyes<sup>6</sup>, Armin Silber<sup>6</sup>, Edwin A. Valentijn<sup>7</sup>, Kor Begeman<sup>7</sup>, Danny Boxhoorn<sup>7</sup>, Fabrice Christen<sup>7</sup>, Ewout Helmich<sup>7</sup>, Gijs Verdoes Kleijn<sup>7</sup>, John McFarland<sup>7</sup>, Gert Sikkema<sup>7</sup>, Erik Deul<sup>8</sup>, Roeland Rengelink<sup>9</sup>

<sup>1</sup> Universitäts-Sternwarte München, Germany,

<sup>2</sup> INAF-Osservatorio Astronomico di Padova, Italy,

<sup>3</sup> INAF-Osservatorio Astronomico di Capodimonte,

Napoli, Italy, <sup>4</sup> Universitäts-Sternwarte Göttingen,

Germany, <sup>5</sup> Sternwarte der Universität Bonn,

Germany, <sup>6</sup> ESO, <sup>7</sup> Kapteyn Institute, Groningen,

the Netherlands, <sup>8</sup> Leiden Observatory,

the Netherlands

OmegaCAM, the 300-megapixel wide-field optical camera on the new VLT Survey Telescope (VST), was commissioned between March and August of this year. This new capability in ESO's arsenal takes images of 1 degree by 1 degree patches of the sky, at 0.2 arcseconds per pixel resolution and of image quality well-matched to the natural seeing on Paranal. The commissioning and OmegaCAM's scientific niche as a high image quality, ultra-violet-sensitive wide-field survey instrument are briefly discussed.

## Getting to first light

On 27 March, after several weeks of intense technical preparations, the moment was finally reached: OmegaCAM had been attached to the new VLT Survey Telescope, everything was cabled up, and the first sky exposure could be taken. We sent the command, and a minute later the 32 CCDs of OmegaCAM started to read out, and the image built up on the screen. Thirty-five seconds later it was done: OmegaCAM had achieved first light! Figure 1 captures the team in the control room following first light.



Figure 1. The OmegaCAM and VST teams in the makeshift control room in the VLT building, after achieving first light on 27 March 2011.

Getting to this point had been a long and sometimes rocky road. When we started the project, more than ten years ago (see Kuijken et al., 2002), the expectation had been that the VST would be operational by 2005 at the latest — but fate and shipping companies decided otherwise (see Capaccioli & Schipani, p. 2). In the end OmegaCAM was completed and delivered to Garching in 2006, and has patiently waited in storage since then for its place at the VST Cassegrain focus. Because of this long wait, it is easy for us to forget how much work went into the project in its early years, and in particular into the optical and mechanical design, filter procurement, electronics, instrument control and data flow software... as well as project meetings, writing documents, reviews, writing documents, ESO progress meetings, writing documents, etc. (Not being a hard-core instrumentalist myself, if I had known at the beginning what would be involved, I might well have shied away). But it all came together on 27 March 2011, when it quickly became clear that we had a nicely working instrument, in operation, on a great new telescope. In fact, even on the first night we managed to obtain images on which the stars were as sharp as 0.6 arcseconds! Although it took some time after that point to complete the alignment and achieve good focus over the full field of view, this was a very promising start.

## The OmegaCAM project

The VST was designed as a single-purpose facility, for making images of large chunks of the sky. Its optical design foresaw a camera, fully integrated into the design and optimised along with the telescope (for example, the dewar entrance window of the camera is actually a spherical lens). After a call for ESO community consortia to provide this camera, the OmegaCAM project was born in 1999.

OmegaCAM is at its heart a 32-CCD detector mosaic, with each three-edge butttable 2k by 4k CCDs manufactured by e2V, consisting of almost 300 million pixels in total. The array samples a full square degree at 0.21 arcseconds per pixel resolution, with minimal gaps between the devices.

In addition to the science CCDs the focal plane also contains four auxiliary CCDs used for guiding and wavefront sensing (seen in Figure 2b on both sides of the array). A filter exchange mechanism permits observations through any one of 12 filters, and a large shutter is used to define precisely the length of the exposures. Figure 3 shows a schematic of the camera. On account of space constraints (not so surprising given that the filters are very large, some 30 cm x 30 cm!), OmegaCAM does not store the filters in a traditional wheel, but in two stacks on either side of the focal plane. A purpose-built robotic mechanism picks out the desired filter and positions it in front of the detectors. OmegaCAM comes with



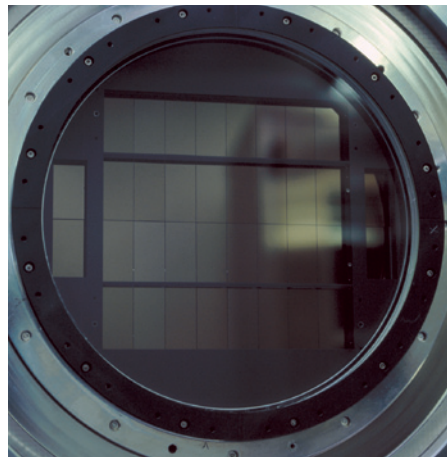
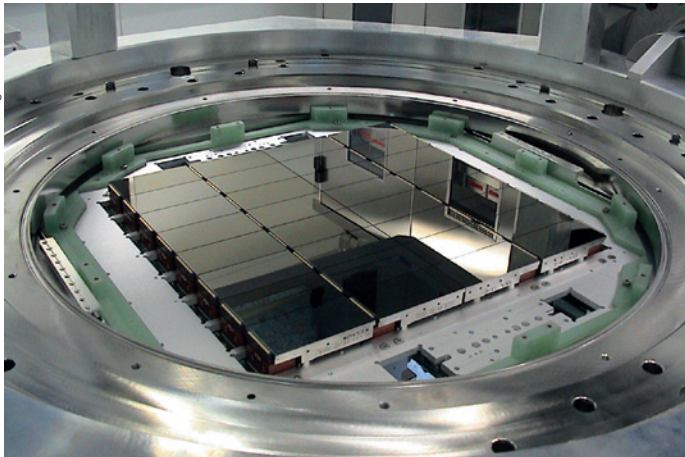


Figure 2. The detector mosaic at the heart of OmegaCAM. Left: A view of the open mosaic, populated with test devices in the lab. Right: The final science CCD array in its dewar ready for installation in the instrument.

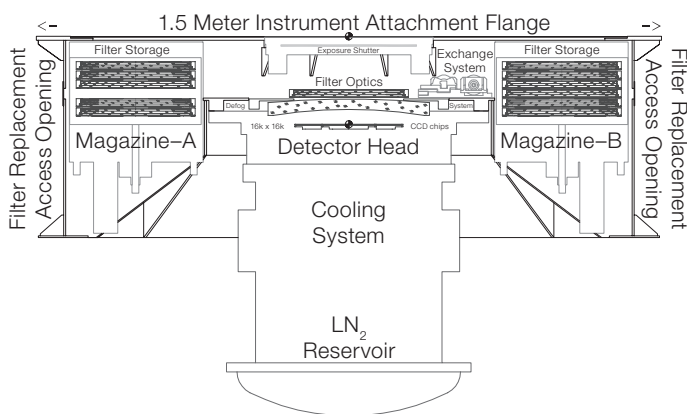


Figure 3. Schematic view of the main components of OmegaCAM.

tions for controlling the instrument functions, power, alarm signals, and of course the data connections from the CCDs to the readout electronics. It is very fortunate that there will be no other instruments on the VST, since connecting up the instrument is quite a job — see Figure 4!

### Scientific niche

Even though OmegaCAM started operation quite a bit later than originally planned, it is still scientifically very powerful, despite of competition from other observatories.

OmegaCAM is the largest wide-field imager in the southern hemisphere: while this will surely change in the future, for the moment we can take advantage of the fact that many of the other “pixel monsters” (particular the Megacams on the Canada France Hawaii Telescope [CFHT] and MMT, and Pan-STARRS) are in the north. Furthermore the operational synergy with the VLT and VISTA should not be underestimated: ESO now has an unrivalled “survey system” that covers  $u$ - $K$ -bands from a superb site. The  $u$ -band sensitivity is high, because of the choice of CCDs in OmegaCAM; new optical wide-field imagers are concentrating on redder sources and are increasingly sacrificing  $u$ -band sensitivity for the near-infrared. Zero points and filter throughput curves for the VST/OmegaCAM system are listed in the appendix to this article; many more details are available in the user manual<sup>1</sup> maintained by the ESO user support group<sup>2</sup>.



Figure 4. Cables, cables, cables... OmegaCAM behind the VST.

broad Sloan  $u$ ,  $g$ ,  $r$ ,  $i$ ,  $z$  and  $B$ ,  $V$  filters, as well as a Strömgen- $v$  and several narrowband filters. Many of the narrowband filters are segmented, with four quadrants that each have a different bandpass; a special calibration filter with  $u$ ,  $g$ ,  $r$ ,  $i$  quadrants for extinction measure-

ments is also part of the set. A large tank for liquid nitrogen to cool the detectors completes the “raw” instrument.

Surrounding the instrument is a true spider’s web of cables and tubes, which supply cooling water, electronic connec-



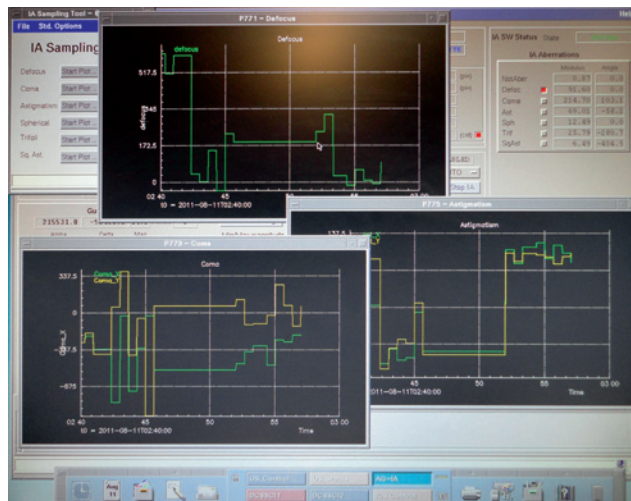
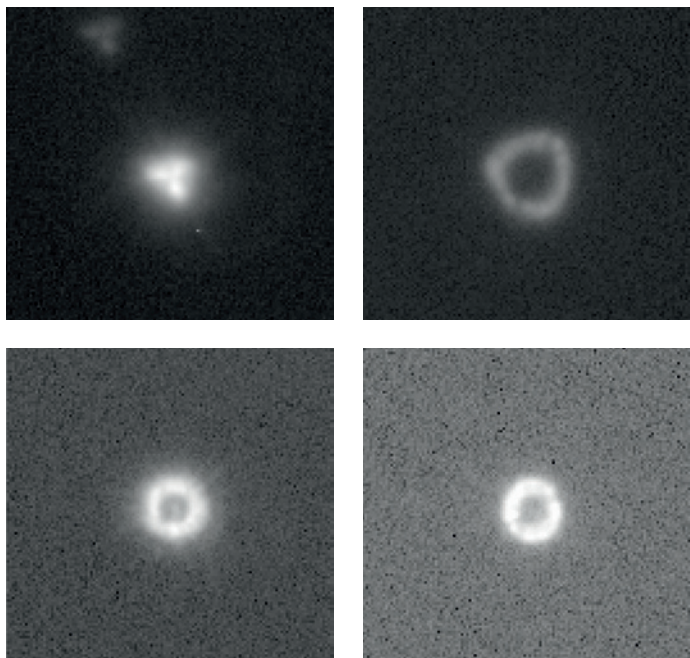


Figure 5. Left: Before (top) and after (bottom) pictures of the pairs of defocused star images recorded on the OmegaCAM image analysis CCDs. In the ideal case both doughnuts should be round and of the same size. Right: Automatic displays of the calculated aberrations on the instrument control panel.

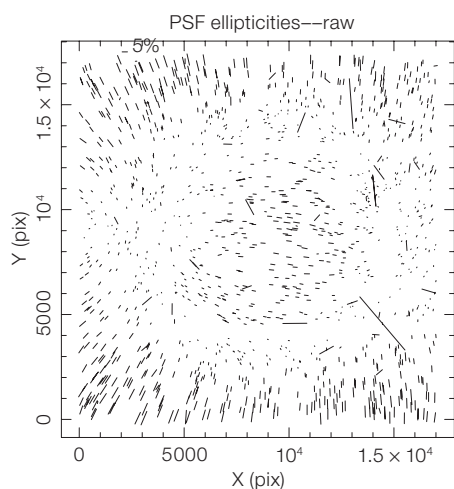


Figure 6. Illustration of the superb image quality of the VST/OmegaCAM system, represented here as a map of ellipticity vectors over the full field. The residual pattern in the (small!) ellipticities is a consequence of the slight curvature of the focal plane combined with small field astigmatism. The size of the stellar images over the field varies less than 5% over the full field and is equal to the outside DIMM seeing measurements, even in this 0.6-arcsecond-seeing image.

But the strongest reason for the scientific niche occupied by OmegaCAM and the VST is image quality. Many of the largest imaging surveys — at least in cosmology — are focussing on understanding the growth of structure, as a probe of dark

energy. One of the most powerful ways to measure this is by means of gravitational lensing, a difficult technique that relies on superb image quality (as it is based on measuring the shapes of galaxies as accurately as possible). Paranal offers excellent seeing much of the time, and the VST and OmegaCAM have been designed explicitly to take full advantage of the natural seeing. The combination of a fully active telescope, wavefront sensing in OmegaCAM, an optical design with little aberration over the full field and a constant plate scale, a deployable atmospheric dispersion corrector, and flexible scheduling to take optimal advantage of the best seeing periods make this a unique facility. Much of the later work in the commissioning of the telescope and camera was rightly concentrated on realising this image quality: meticulously aligning the telescope optical axis with the instrument rotator, making sure OmegaCAM is parallel to the flange, and fine-tuning the real-time wavefront sensors in the instrument.

The wavefront sensors provide a robust way of maintaining the telescope focus on the science array. They work by registering star images that are significantly out of focus: for this purpose two auxiliary CCDs are mounted out of the focal plane, one 2 mm above and one 2 mm below. Stars

show up as doughnut-shaped on these CCDs, and by insisting that both “doughnuts” have exactly the same shape, the telescope focus is forced to lie exactly halfway between these planes (see Figure 5). Similarly, higher-order aberrations can also be measured from the way the doughnuts are distorted into elliptical or triangular shapes. Using these “image analysis CCDs”, aberrations are continuously measured during scientific exposures, and as soon as the shutter is closed the telescope is corrected, ready for the next exposure.

The other two auxiliary CCDs are mounted in focus, and make up an auto-guider that guides using two stars on either side of the field (so that the centre of the image remains on track). Together the two guide CCDs and the two image analysis CCDs ensure the best possible image quality on the 32 science arrays. This is exemplified in Figure 6, where a map of the image ellipticity across the field is shown.

#### Data flow and calibration

Calibrating wide-field images accurately can be tricky, particularly since an open wide-field telescope provides many paths for stray light, and interference filters



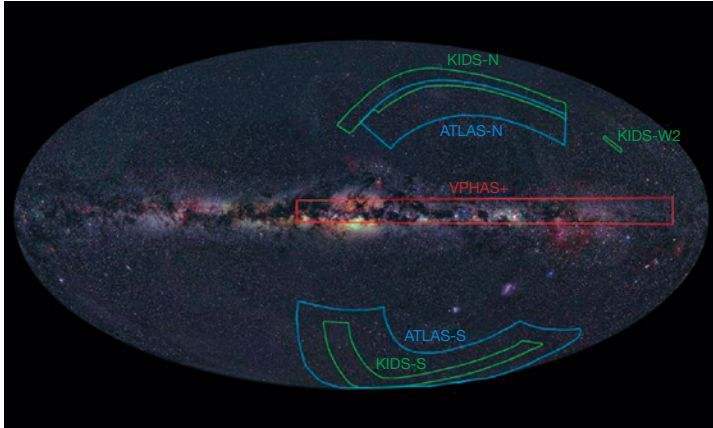


Figure 7. (Top) Sky projection of the three public surveys that will take most of the VST's observing time in the first three years: VPHAS+ which will study the Galactic Plane, ATLAS which can be seen as a southern twin to the Sloan Imaging Survey, and KiDS, a deep/wide cosmological survey. See Arnaboldi et al. (2007) for more details.

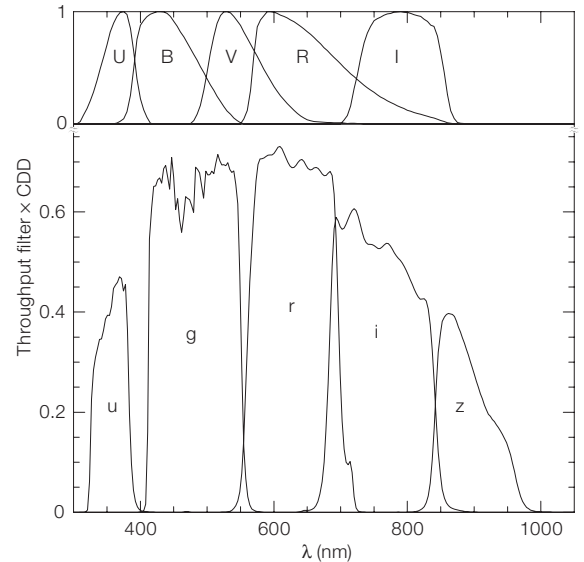
can lead to strange reflections. Initial efforts have already resulted in photometric calibrations that are accurate to a few percent (see the Table of zero points in the Appendix), and with experience and more data this number should improve further. We have established photometric secondary standard fields, a square degree in size each, along the celestial equator and these, together with frequent observations of the celestial pole, will be the backbone of the nightly photometric calibration.

Our delivery to ESO included pipeline modules with which the instrument scientists will be able to monitor the image quality and photometric performance of the instrument. The quick-look capability that this provided during commissioning, as well as an experimental implementation of the newly laid EVALSO high-speed internet link to Paranal (see Filippi, 2010), made it possible for us to have an entire “back office” in Groningen looking over our shoulders and analysing the data on the fly, despite the considerable data volumes. Sometimes there are advantages to schedule slips: this would have been impossible in 2005!

### Looking ahead

Now that OmegaCAM is about to enter operations, we can look forward to

Figure 8. (Right) The throughput of the entire VST system for the broadband Sloan filters in OmegaCAM is shown (lower) with the passbands of the standard Johnson-Cousins UBVRI filters shown for comparison (upper).



many results. The first few years will be devoted to three public surveys (see Figure 7 and Arnaboldi et al., 2007), to guaranteed time for the camera and telescope teams, and to Chilean programmes. With our guaranteed time we will initially focus on mapping the young galaxy clusters in the Hercules supercluster, capturing the full extents of dwarf spheroidals and globular clusters in the Galaxy, and searching for very short-period binary stars as possible supernova Ia progenitors.

After many years of patience and preparation, the harvest can finally begin!

### Appendix: Filter characteristics

The throughput curves of the workhorse broadband Sloan filters are reproduced in Figure 8. Approximate zero points (they vary from CCD to CCD by of the order of 0.1 mag) are given in the table.

FILTER	Zero point (AB mag, 1 e <sup>-</sup> /s)
u	23.9
g	25.8
r	25.7
i	25.2
z	23.8
B	25.7
V	25.5

### Acknowledgements

OmegaCAM was designed, built and commissioned by a consortium of institutes from the Netherlands,

Germany and Italy, with significant contributions from ESO. The mechanical design was led by Harald Nicklas (Göttingen), the shutter by Klaus Reif (Bonn), electronics by Achim Hess (München), instrument control software by Andrea Baruffolo (Padua) and data flow and calibration software by Edwin Valentijn (Groningen). Olaf Iwert (ESO) led the work on the detector system, including the CCD mosaic and Jean Louis Lizon (ESO) led the cooling system. Project management was done for most of the project by Bernard Muschielok (München), after initial efforts from Don Hamilton and Günter Wiedemann. Ralf Bender (München) and Enrico Cappellaro (Padua) served as co-PI's. Our ESO project scientist was Dietrich Baade. Much of the funding was provided by NOVA, the BMBF and INAF.

I wish to express my sincere thanks to all of the OmegaCAM team for sticking with the project over the years, and for helping to deliver what I am sure is going to turn out to be a fantastic science machine. Working more closely with the VST team in the final year of the project, particularly with Pietro Schipani and his commissioning team, was a joy. Observing the Paranal operation up close, juggling the running of an observatory with learning to accommodate a new facility and helping to solve problems, was an eye-opening experience. Many thanks to all.

### References

- Arnaboldi, M. et al. 2007, *The Messenger*, 127, 28
- Filippi, G. 2010, *The Messenger*, 141, 2
- Kuijken, K. et al. 2002, *The Messenger*, 110,15

### Links

- <sup>1</sup> OmegaCAM manuals: <http://www.eso.org/sci/facilities/instruments/omegacam/doc/index.html>
- <sup>2</sup> OmegaCAM at the VST web page: <http://www.eso.org/sci/facilities/paranal/instruments/omegacam/>



# PIONIER: A Four-telescope Instrument for the VLTI

G rard Zins<sup>1</sup>  
 Bernard Lazareff<sup>1</sup>  
 Jean-Philippe Berger<sup>2</sup>  
 Jean-Baptiste Le Bouquin<sup>1</sup>  
 Laurent Jocou<sup>1</sup>  
 Sylvain Rochat<sup>1</sup>  
 Pierre Haguenaue<sup>2</sup>  
 Jens Knudstrup<sup>2</sup>  
 Jean-Louis Lizon<sup>2</sup>  
 Rafael Millan-Gabet<sup>3</sup>  
 Wes Traub<sup>4</sup>  
 Myriam Benisty<sup>5</sup>  
 Alain Delboulbe<sup>1</sup>  
 Philippe Feautrier<sup>1</sup>  
 David Gillier<sup>1</sup>  
 Philippe Gitton<sup>2</sup>  
 Pierre Kern<sup>1</sup>  
 Mario Kiekebusch<sup>2</sup>  
 Pierre Labeye<sup>6</sup>  
 Didier Maurel<sup>1</sup>  
 Yves Magnard<sup>1</sup>  
 Mickael Micallet<sup>1</sup>  
 Laurence Michaud<sup>1</sup>  
 Thibaut Moulin<sup>1</sup>  
 Dan Popovic<sup>2</sup>  
 Alain Roux<sup>1</sup>  
 Noel Ventura<sup>1</sup>

<sup>1</sup> Institut de Plan tologie et d'Astrophysique de Grenoble (IPAG), OSUG, Universit  Joseph Fourier, Grenoble, France

<sup>2</sup> ESO

<sup>3</sup> NASA Exoplanet Science Institute, California Institute of Technology, Pasadena, USA

<sup>4</sup> Exoplanet Exploration Program, Jet Propulsion Laboratory, Pasadena, USA

<sup>5</sup> Max-Planck-Institut f r Astronomie, Heidelberg, Germany

<sup>6</sup> Laboratoire d'Electronique et Technologies de l'Information (LETI), Grenoble, France

PIONIER, developed by the Institut d'Astrophysique de Grenoble (IPAG) and installed at the VLT Interferometer, is a near-infrared (1.5–2.4  $\mu\text{m}$ ) instrument that allows the beams from four telescopes to be recombined for the first time, thus permitting high angular resolution imaging studies at an unprecedented level of sensitivity and precision. At the heart of the instrument is an integrated optics beam combiner (IOBC) that splits and recombines the four incoming signals, provid-

ing excellent compactness and stability. The IOBC has been developed by IPAG and the Laboratoire d'Electronique et Technologies de l'Information. PIONIER was successfully commissioned in October 2010, 12 months after being approved by ESO as a visitor instrument. With the baselines up to 130 metres offered by the VLTI, PIONIER can resolve structures less than 3 milliarcseconds across. The scientific motivation behind PIONIER is outlined, the instrument is described and illustrative scientific results from the first year of operation are presented.

## Introduction

Since October 2010, the visitor instrument PIONIER has been recombining the light of all four beams of the Very Large Telescope Interferometer (VLTI), enabling new science at the highest angular resolution.

Infrared interferometry has been one of the baseline goals for the Paranal Observatory since its inception. Major milestones have been the first fringes between VLT Unit Telescopes (UTs) in March 2001, and the first fringes between the Auxiliary Telescopes (ATs) in February 2005. The VLTI infrastructure is currently structured for four telescopes. The AMBER instrument (commissioned in 2004) allows three-telescope operation, leaving the full potential of the VLTI yet to be realised.

For about the last ten years, the Laboratoire d'Astrophysique de l'Observatoire de Grenoble (LAOG), now merged into the Institut d'Astrophysique de Grenoble (IPAG<sup>1</sup>) and the Laboratoire d'Electronique et Technologies de l'Information (LETI<sup>2</sup>), has been developing integrated optics components for infrared interferometry. One outcome of this effort was a four-beam *H*-band combiner. This integrated combiner opened an opportunity for the PIONIER instrument, which has been designed to exploit the full potential of the VLTI array in preparation for the arrival of the second generation instruments GRAVITY (see Eisenhauer et al., 2011) and MATISSE (Hofmann et al., 2008). The main observational motivation is the possibility of using four telescopes simultaneously, which provides six visibilities and three independent closure phases per

wavelength channel and one closure amplitude, whereas a three-telescope combiner only provides three visibilities and one closure phase. The remarkable success of the four-telescope (4T) CHARA interferometer (Monnier et al., 2007) has demonstrated that such an increase in *uv*-plane coverage significantly improves the capability to reconstruct a "model-independent" image from the observables, so-called aperture synthesis imaging.

In November 2009, PIONIER was approved as a visitor instrument by the ESO Scientific and Technical Committee. Less than twelve months later, the completed instrument was brought to Paranal; see ESO Announcement 1081<sup>3</sup>.

## Scientific motivation

The initial core science goals of PIONIER were to provide spatially resolved diagnostics, at the level of 1 astronomical unit (AU), for the close environments of planet-forming stars. This capability will place direct constraints on the physical conditions at the distances from the star where planets may form. The PIONIER target list spans different evolutionary stages of planet-forming environments around stars of different masses. The dusty environments of massive and intermediate-mass (Herbig AeBe) young stars are ideal candidates for aperture synthesis since their angular extent is of the order of 10 milliarcseconds (mas). The direct or modelled images provide unique diagnostics to constrain the structure of the inner rim of their protoplanetary discs. Of particular importance is the possibility of obtaining direct images of the morphology of the dust/gas inner disc rim (and in particular its vertical structure and possible clumpiness), and of studying the dust's properties and the role of extended scattering envelopes in the global radiative energy balance.

PIONIER's sensitivity allows the "T Tauri barrier" to be broken and opens the way to direct spatially resolved observation of young solar analogues that have demanded more sensitivity than currently available for VLTI near-infrared (NIR) observations until now. T Tauri stars with discs at different evolutionary stages

are a focus of PIONIER observations, with a particular emphasis on obtaining direct diagnostics of the presence of planet-forming signatures, such as huge gaps in the emission. PIONIER observations have proved to be remarkably complementary to constraints provided by advanced disc-modelling using Spitzer and Herschel data, since they allow an unambiguous constraint on the inner disc boundary and radial emission. Furthermore PIONIER aims at reaching a closure phase accuracy sufficient to hunt down stellar, substellar and maybe hot planetary companions and to contribute to the statistical study of multiplicity in planet-forming environments. In a similar vein, PIONIER is designed to push visibility precision to a level where it can reveal the hot dust component that has been recently pinpointed around debris-disc host stars (e.g., Absil et al., 2009).

The sensitivity and mapping capability of PIONIER also opens new territories requiring milliarsecond direct or parametric mapping, such as for interacting binaries, stellar surfaces, Wolf-Rayet stars, etc.

### System overview

Each of the beams from the VLTI switchyard first enters the injection and optical path delay unit (IOPDU, see Figure 1), where the *H*-band light is reflected from a dichroic mirror, while the *K*-band light is transmitted to the VLTI infrared image sensor (IRIS) guiding camera. The roles of the *H*- and *K*-bands can be exchanged in a planned extension to *K*-band observation. The following elements on the signal path are a flat mirror on a piezo stage with a 400  $\mu\text{m}$  travel, a piezo tip-tilt mirror with a bandwidth of 100 Hz and a throw of  $\pm 200$  arcseconds that responds to input from IRIS, a shutter, a birefringence compensation plate, and an off-axis parabola for injection into an optical fibre. Other elements, not on the signal path, are used for alignment or spectral calibration.

The integrated optics beam combiner (see Figures 2 and 3) takes the four input signals and delivers 12 outputs (24 for the ABCD variant): six baselines times two phase states:  $a + b$  and  $a - b$ . The

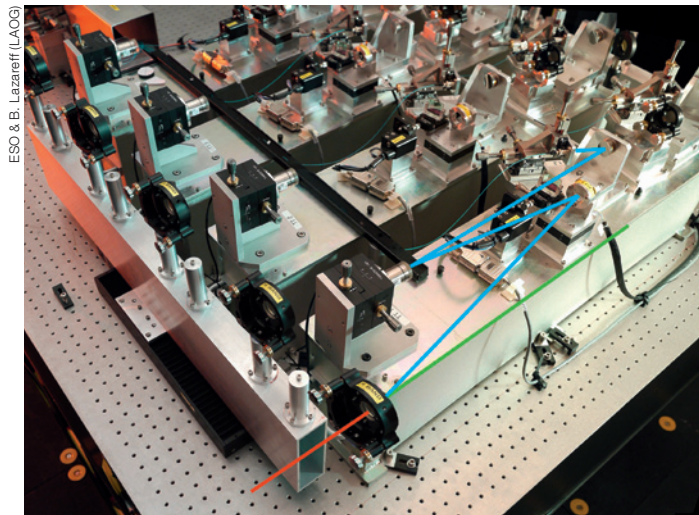


Figure 1. Partial view of the PIONIER IOPDU. The beam from the VLTI switchyard is split by a dichroic plate. The *K*-band is transmitted to the IRIS guiding camera, while the *H*-band beam (blue line) is reflected and follows the path: OPD piezo (used to modulate the optical path and scan the fringes), tip-tilt stage (used to track the focal plane position of the target), birefringence compensation plate, and finally an off-axis parabola for injection into the optical fibre, on its way to the beam combiner.

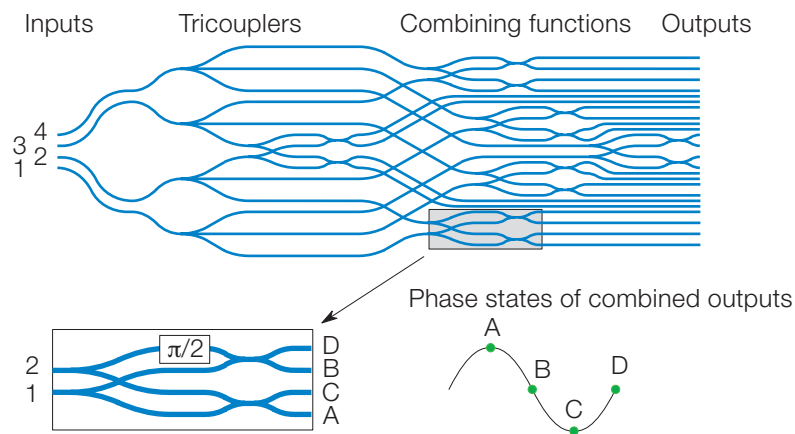


Figure 2. Top: schematic of a 4T-ABCD combiner. Each input is divided in three to interfere with other inputs in an elementary combining block. Bottom left: detail of one combining block. Each input is further divided in two; after a  $\pi/2$  phase shift is applied in one arm, pairwise combinations are made in

couplers. Bottom right: representation of the four (relative) phases achieved in the four outputs. In a simplified version, called 4T-AC, the Y-junction and  $\pi/2$  phase shift are omitted; so each pairwise combiner has only two outputs instead of four.

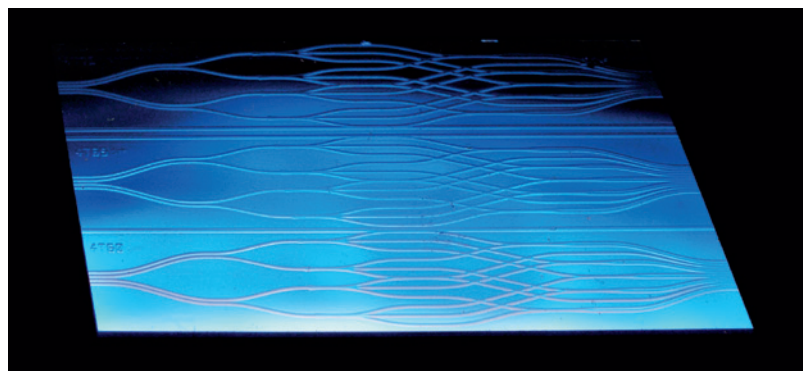


Figure 3. Picture of a 4T-AC integrated optics beam combiner. The buried optical waveguides are revealed by small deviations from surface flatness,

amplified by the specular lighting. Beam propagation is left to right.



outputs of the IOBC are imaged by 1:1 relay optics onto the detector; a dispersing prism and/or a Wollaston polarisation separator can also be inserted. Two available prisms can disperse the  $H$ -band over 7 pixels (for spectral resolution  $R \sim 40$ ) or three pixels (for  $R \sim 20$ ).

The detector is a  $128 \times 128$  Rockwell PICNIC in a commercial liquid nitrogen cryostat, both kindly on loan from JPL. After amplification and 16-bit numerical conversion, the signal is acquired by the detector control system (DCS).

### Integrated optics combiner

The interferometric combination is achieved in a thumb-sized integrated optics element. This silica-on-silicon chip embeds a single-mode optical circuit capable of combining four beams in a pair-wise scheme. There are four main drivers for this choice: 1) single-mode spatial filtering associated to proper photometric monitoring provides significant improvements in the accuracy of the observables; 2) the extreme compactness of the chip ensures excellent stability of the instrument response; 3) the complex circuit is permanently aligned and only requires the adjustment of the light injection and the output on the detector (unlike discrete component optics); 4) different designs can be swapped and tested with minimal realignment.

The basic design is described in detail in Labeye et al. (2006), Labeye (2009) and Benisty et al. (2009). The four incoming beams are each split into three and rearranged in six pairs. For each pair (baseline), a “static-ABCD” combining cell is implemented. It generates four phase states simultaneously (nominally in quadrature), for a total of 24 outputs. This combiner can be used both in fringe-scanning mode (VINCI-like) or ABCD-like mode (PRIMA-like). Such combiners have been developed for the  $H$ -band and for the  $K$ -band (Jocou et al., 2010). These are the most complex interferometric circuits ever used on-sky.

To increase the signal-to-noise and the readout speed in fringe-scanning mode, a variant has been designed using only the A and C outputs ( $\pi$  phase difference);

that variant (AC) is currently in operation. The combiner is fed by polarisation-maintaining single-mode  $H$ -band fibres, whose lengths have been equalised with an accuracy of  $20 \mu\text{m}$ , so that they introduce a negligible differential chromatic dispersion.

### Polarisation control

A collateral effect of using polarisation-maintaining fibres to carry the signal from the injection unit to the integrated combiner is that such fibres are strongly birefringent, accumulating a phase difference between their principal axes at a rate of one turn every few millimetres. Even if the lengths of the fibres are carefully matched, and they are taken from the same fabrication batch, their birefringence will not match to a fraction of a wavelength. The differential optical path difference (OPD) between fringes in orthogonal polarisations was measured and found typically to be a few wavelengths. In the initial design, the two linear polarisations were spatially separated by a Wollaston prism, and detected separately. This approach of course carries penalties in both signal-to-noise and readout speed.

It was decided to insert a birefringent plate into the signal path between the tip-tilt mirror and the injection parabola (see Figure 1). This plate is made from lithium niobate, a uniaxial material that has good transmission in the  $H$ - and  $K$ -bands. Each plate is  $X$ -cut, i.e. the extraordinary axis is in the plane of the plate. Without going into detailed calculations, it is apparent that:

- (a) When the plate is perpendicular to the beam, it introduces a differential OPD between the two polarisations, which is the product of the plate thickness and the difference of refractive indices for the ordinary and extraordinary rays ( $n_o - n_e$ );
- (b) If the plate is tilted, for example about the  $n_o$  axis, the two polarisations will follow different geometrical paths and experience different optical indices, with a net differential OPD that depends upon the inclination.

Lithium niobate is a suitable material for this application because its birefringence

( $n_o - n_e$ ) =  $-0.073$  is large enough at  $1.6 \mu\text{m}$ , with only a small wavelength dependence (a quality not shared by quartz). The compensation plates are  $2 \text{ mm}$  thick and tilted typically by  $20^\circ$ . In practice, the Wollaston is inserted, then the inclination of the plates is adjusted so that both the wavepacket envelopes and the individual fringes coincide between the two polarisations on each of the six baselines. The Wollaston is removed for all observations, and the co-aligned fringes from both polarisations are detected jointly on the same detector pixel.

### Camera and readout electronics

The scientific requirements for the camera are low noise (faint targets), high speed (atmospheric phase coherence time typically a few milliseconds) and large dynamic range. Our implementation strives to meet these requirements as far as the intrinsic parameters of the detector allow.

The PICNIC detector has a spectral response extending from  $850 \text{ nm}$  to  $2500 \text{ nm}$ , with a quantum efficiency of  $60\text{--}65\%$ . Two filter wheels are located inside the cryostat. The first one defines the bandpass:  $H$ -band ( $1.5\text{--}1.82 \mu\text{m}$ ) or  $K$ -band ( $2.0\text{--}2.36 \mu\text{m}$ ). The second wheel, generally in the “open” position, carries neutral density (ND) filters for  $\text{ND} = 0.6$ ,  $\text{ND} = 1.4$ , and  $\text{ND} = 2.0$  that are inserted when observing bright objects. The PICNIC detector has the interesting property of non-destructive readout: it is possible to perform sequentially partial integrations without an intervening reset. See the section “Observing modes”.

A differential amplifier (gain  $\times 10$ ) inside the cryostat provides a good immunity against common-mode electrical perturbations. Differential signal wiring is preserved up to the inputs of a fast ( $250 \text{ ns}$ ) 16-bit analogue-to-digital (A/D) converter in the warm electronics. The patterns for the various timing and housekeeping signals of the detector (line, pixel, reset, etc...) are updated at a clock rate of  $5 \text{ MHz}$ , which provides reasonably fine-grained control of the timing.

The minimum detector readout time per pixel (typically  $6 \mu\text{s}$ ) is set by the intrinsic time constant of the PICNIC array. Repeating A/D conversions (duration  $0.25 \mu\text{s}$ ) on the same pixel up to eight times, reduces the readout noise. Detection gain and noise of the detector were characterised by the standard mean–variance method. In essence, the detector gain, expressed in A/D units (ADU) per electron can be calibrated exploiting the known statistics of electron counts: variance = mean. Table 1 summarises the detector characteristics.

Parameter	Value (median)
Gain ADU/e <sup>-</sup>	0.26
Readout noise e <sup>-</sup>	18.5 (a)
Readout noise e <sup>-</sup>	15.2 (b)

**Table 1.** Measured electronic gain and readout noise of the PICNIC detector. Two values are given for the readout noise: (a) for zero illumination, but including the variance of the dark current; (b) excluding the contribution from the dark current.

### Instrument control

Although PIONIER is a visitor instrument, the control software is fully compliant with the ESO VLT standards, and consists of standard components such as observation software (OS), instrument control software (ICS) and detector control software (DCS). This compliance allows full interoperability with all sub-systems of the VLT, enabling rapid installation at the telescope site and easing the operations of the instrument. PIONIER is thus operated at Paranal as other VLT instruments.

However, PIONIER introduces several interesting innovations:

**Programmable logical controller (PLC) for the ICS** — Due to constraints on the project, such as a tight budget, space requirements and thermal dissipation, it was decided to use an embedded programmable controller (PC) from the company Beckhoff instead of traditional VME-based local controller units (LCUs) running VxWorks. This computer is an industrial PLC, controlling distributed input/output components through the EtherCAT fieldbus. The VLT software has been extended to support fieldbus technology (IC0 fieldbus extension). Device drivers have been developed to control



**Figure 4.** Part of the PIONIER/VLTI team taking a break during the instrument commissioning.

the instrument functions like stepper motors, lamps, shutters and sensors via EtherCAT terminals (Kiekebusch et al., 2010).

**DCS** — The detector front-end and video electronics used in PIONIER are not the standard system, normally provided by ESO. Therefore it has been necessary to re-implement the software controlling the detector. This software is a multi-threaded application whose design is inspired from the new generation controller (NGC) DCS, developed by ESO. The customised DCS implemented for PIONIER is compatible with the NGC interface, to make integration with the OS transparent. This application is in charge of driving the detector by generating the clock patterns for the different readout modes (simple, double and Fowler sampling), to acquire detector data and drive the piezo to synchronise OPD modulation with detector readout cycles. It is also in charge of pro-

cessing and delivering detector data to all clients requiring this, such as the real-time display (RTD) or the alignment control software (ACS; see below).

**ACS** — A dedicated software component, called the alignment control software, has been implemented to perform alignment tasks. This consists of: 1) optimising the flux injection into fibres by creating a map of fluxes and fitting a Gaussian to find the maximum; and 2) performing fast guiding to compensate for turbulence using positional errors delivered by IRIS through the reflective memory network (RMN). This software runs on the detector LCU for fast communication with the DCS. In this way, it is possible to perform flux injection optimisation in a very efficient way; less than 20 seconds per beam is achievable in most cases.

**RTD scope** — In fringe-scanning mode, the RTD scope application retrieves data from the DCS for each scan sequence, displays it to the user and computes the OPD which is forwarded back to the DCS



for group delay tracking. This application, running on the instrument workstation, has been implemented by PIONIER scientists using the Yorick tool, which provides advanced functions for data processing and display.

**Ethernet-based controllers** — The controllers for the piezo and for the tip-tilt devices, are the E-712 and E-517 digital controller modules from the company Physik Instrumente. These are driven through transmission control protocol/internet protocol (TCP/IP) interfaces. This solution offers more flexibility than the analogue interface normally used. The devices can be controlled from any system that has an Ethernet interface and there is no cable length limitation between the controller and the driving system, which is the DCS. PIONIER performance tests have been done up to 2 kHz with good results with this system.

### Observing modes

Almost all observations are made in the so-called Fowler mode. Following a reset of the detector, a series of  $N_{read}+1$  readouts are performed (at the maximum rate performed by the detector and electronics), defining  $N_{read}$  consecutive integration periods. This sequence takes typically a few hundred milliseconds. The base value of  $N_{read}$  is 512, under fair to good atmospheric conditions. For sources weaker than  $H = 6$  mag,  $N_{read}$  is increased (more integration time per fringe), Simultaneous with the readouts, the piezo stages are scanned following a linear ramp, with respective throws  $-3A$ ,  $-A$ ,  $+A$ ,  $+3A$ , so that the OPD for any baseline is swept over an amplitude of  $2A$ ,  $4A$ , or  $6A$ . The default value is  $A = 40 \mu\text{m}$ .

For very bright sources ( $H < 0$  mag), when the minimum time for a Fowler scan would saturate the detector, a series of separate reset-read-read sequences are performed during the piezo scan, with an extra overhead from the extra reset and read operations. For each integration period, the number of pixel detectors acquired is 12 or 24 (number of IOBC outputs) times the number of spectral channels: 1 (no dispersion), 3 (lower resolution prism) or 7 (larger resolution prism). Table 2 lists the time per scan in various

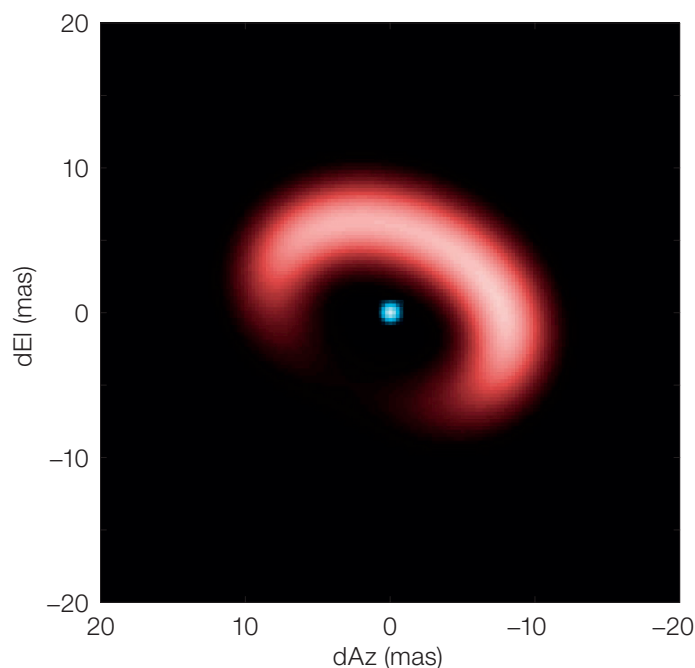


**Figure 5.** A parametric model reconstruction of the circumstellar environment of the Be star HD45677. The different “colours” of the star and circumstellar matter pose a challenge to existing image reconstruction techniques; a simple parametric model gives a reasonable fit to the observed visibilities and closures. The ring-shaped emission in the  $H$ -band is thought to originate at the inner boundary of the circumstellar disc, where the intense radiation of the star causes the sublimation of interstellar dust grains.

configurations with the currently used AC beam combiner. The actual elapsed time may be longer due to overheads, e.g., evaluation of wave packet position.

$N_{read}$	$N_s$	$N_{disp}$	$t(ms)$
512	1	1	126
512	1	7	383
2048	1	1	294
2048	8	1	366

**Table 2.** Duration of one scan, in various configurations.  $N_{read}$  is the number of readouts in one scan;  $N_s$  is the number of repeated A/D conversions for one pixel;  $N_{disp}$  is number of wavelength channels, when a dispersing prism is used.

### Integrated data flow

Although it is a visitor instrument, PIONIER follows the ESO data flow as far as possible. From the high-level point of view, PIONIER is operated via the broker of observing blocks (BOB) that executes observing blocks (OBs) fetched from the standard P2PP ESO software. OBs can be conveniently generated by the ASPRO2<sup>4</sup> preparation software from the Jean-Marie Mariotti Center (JMMC). This tool automatically fetches the target coordinates, proper motions, magnitudes and other parameters from the Centre de Données Stellaires (CDS) database. This saves time and avoids typing errors.

The PIONIER data reduction software is publicly available<sup>5</sup> as a YORICK package; see Le Bouquin et al. (2011) for more information. It converts the raw FITS file produced by the instrument into calibrated visibilities and closure phases written in the standard OIFITS format. Angular diameters of calibration stars are automatically recovered from published catalogues. Consequently, the final products are science-ready and can be directly handed over to software such as LITpro<sup>6</sup> (model fitting) or MIRA<sup>7</sup> (image reconstruction).

The PIONIER data reduction software runs in the background during the night. The science-ready outputs are available about 30 minutes after the beginning of the observations, once the first calibration star has been observed. This allows the data quality to be assessed and decisions are taken accordingly. This is also a powerful tool to quickly identify bad calibration stars, such as previously unknown binaries, and re-execute an additional calibration. Finally, we were sometimes able to obtain an image reconstruction of the observed target even before the end of the night.

To optimise the scientific return of PIONIER in the medium term, we maintain a simple archive at IPAG, which

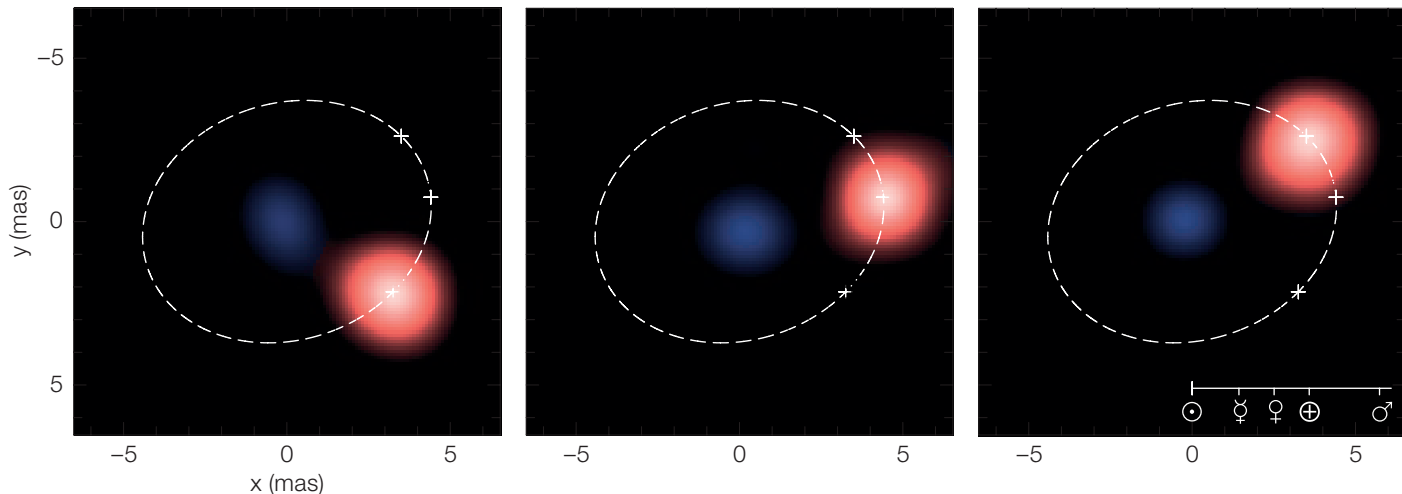


Figure 6. Multi-epoch image reconstructions of the symbiotic binary SS Lep (see Blind et al. 2011 and ESO release 1148). The system is composed of a cool red giant in orbit around a hot blue dwarf with a period of 235 days. The stars are so close that several episodes of mass transfer occurred in the recent past of the system, explaining the so called "Algol paradox", where the most massive component (A dwarf) is also the least evolved. The size of the inner Solar System is shown for reference.

includes both the raw FITS files and the science-ready OIFITS products.

### PIONIER results

Capitalising on previous developments and available experience, PIONIER was built in about one year, providing the capability to recombine all four VLTI beams for the first time. First fringes on-

sky were obtained five days after we started unpacking the transport boxes and two hours after the instrument received the VLTI beams. A number of scientific programmes have been executed during the first year of operation; examples of results are shown in Figures 5 and 6. PIONIER not only bridges the gap to VLTI second generation instruments, but may also serve as a testbed for certain aspects of these instruments.

### References

Abil, O. et al. 2009, ApJ, 704, 150  
 Benisty, M. et al. 2009, A&A, 498, 601  
 Blind, N. et al. 2011, A&A, 536, A55  
 Eisenhauer, F. et al. 2011, The Messenger, 143, 16  
 Jocou, L. et al. 2010, Proc. SPIE, Volume 7734  
 Hofmann, K.-H. et al. 2008, SPIE, 7013, 122

Labeye, P. et al. 2006, in Silicon Photonics, Proc. SPIE, 6125, 161  
 Labeye, P. 2009, PhD dissertation, INPG, <http://arxiv.org/abs/0904.3030>  
 Le Bouquin, J.-B. et al. 2011, A&A, 535, A67  
 Monnier, J. D. et al. 2007, Science, 317, 342

### Links

- <sup>1</sup> Institut de Planétologie et d'Astrophysique de Grenoble (IPAG): <http://ipag.obs.ujf-grenoble.fr/>
- <sup>2</sup> Laboratoire d'Electronique et Technologies de l'Information (LETI): <http://www-leti.cea.fr/>
- <sup>3</sup> ESO announcement 1081: <http://www.eso.org/public/announcements/ann1081/>
- <sup>4</sup> ASPRO2 preparation software: [http://www.jmmc.fr/aspro\\_page](http://www.jmmc.fr/aspro_page)
- <sup>5</sup> PIONIER data reduction software: <http://apps.jmmc.fr/~swmgr/pndrs>
- <sup>6</sup> LITpro model fitting software: <http://www.jmmc.fr/litpro>
- <sup>7</sup> MIRA image reconstruction software: <http://www-obs.univ-lyon1.fr/labo/perso/eric.thiebaut/mira.html>



Panoramic view of the Very Large Telescope Interferometer (VLTI) tunnel, showing two delay lines.



# Sparse Aperture Masking on Paranal

Sylvestre Lacour<sup>1</sup>  
 Peter Tuthill<sup>2</sup>  
 Michael Ireland<sup>2,3</sup>  
 Paola Amico<sup>4</sup>  
 Julien Girard<sup>4</sup>

<sup>1</sup> Observatoire de Paris, Meudon, France

<sup>2</sup> Sydney Institute for Astronomy, Sydney University, Australia

<sup>3</sup> Australian Astronomical Observatory, Epping, Australia

<sup>4</sup> ESO

The new operational mode of aperture-masking interferometry was added to the CONICA camera four years ago. Over the years, the masks — pieces of metal only two centimetres wide — have opened an unprecedented observational window for the NACO instrument. In comparison to the full aperture, they deliver superior point source function calibration, rejection of atmospheric noise and robust recovery of phase information through the use of closure phases. In the resolution range from about half to several resolution elements, masking interferometry sets the benchmark for the present state of the art worldwide in delivering high fidelity imaging and direct detection of faint companions. The technique and observational applications to imaging of circumstellar discs and exoplanets are outlined.

As its name suggests, aperture masking consists of putting a mask at the entrance pupil of a telescope. We could have placed a mask with the physical size of the primary (M1) mirror on the VLT Unit Telescope 4 (UT4). Instead, we have placed a precision fabricated sheet of thin steel inside the CONICA camera in a plane conjugate to the telescope's aperture. On NAOS–CONICA (NACO), there are four masks available. Each one completely blocks the incoming light except for a number of small circular holes. One mask has seven holes, two have nine holes, and one has 18 holes. For example, the 7-hole mask transforms the 8-metre VLT primary into an array of small telescopes each 1.2 metres in diameter. Instead of 49 m<sup>2</sup> of light-collecting power, only seven times 1.13 m<sup>2</sup> of the reflective

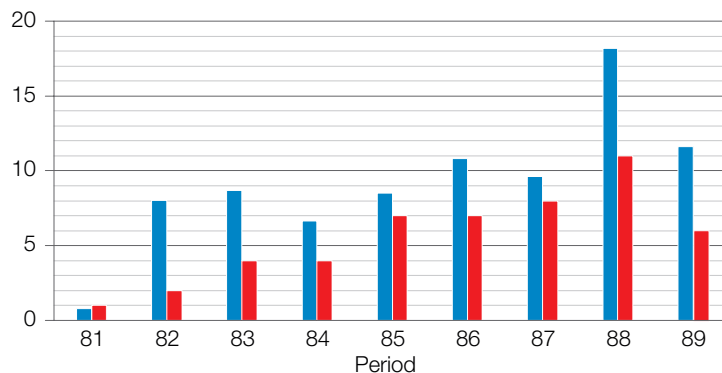


Figure 1. In blue, the percentage of SAM proposals with respect to the total number of NACO proposals submitted. Over the last two periods, 224 NACO proposals have been submitted, of which 33 required the use of SAM (approx 15%). In red, the

number of SAM PIs for proposals that were accepted by the Observing Programmes Committee and eligible for technical feasibility. This is one of the major successes of recent years: the aperture masking community is getting wider.

surface of UT4 is used — this is only 16%. At first thought, discarding 80% of the valuable stellar photons seems pure madness, and it is true that on faint targets, when observations are limited by photon noise, aperture masking is detrimental. However, it is in the speckle-dominated domain, where atmospheric turbulence and instrumental defects limit the signal-to-noise, that the real power of sparse aperture masking (SAM) is manifest. The steady increase in popularity of this mode is a clear indication of its relevance in this domain, as demonstrated by the histogram of VLT SAM proposals and Principal Investigator (PI) statistics of over nine semesters shown in Figure 1.

The simplest way to explain the principle of aperture masking is to consider the wavelike nature of light. In order to form a perfect image, the incoming starlight must be perfectly coherent, with flat wavefronts spanning the area of the aperture. With an 8-metre-class telescope, attaining perfect correction becomes difficult, even with a functioning adaptive optics (AO) system. With SAM, the requirement is less stringent, because the wavefront has to be flattened only within the size of a hole. Even though the image of a star looks like a “snowflake” on the detector (see Figure 2), the high frequency information from interference between the hole pairs can be recovered through techniques involving computation of the bispectrum and closure phases. In other words, SAM makes an

instrument more robust to any large optical aberration over the pupil, such as atmospheric noise or instrumental non-common path errors. Figure 2 shows the application of SAM to resolving the close separation binary star HD9129Aab, itself part of a wide separation binary.

A second advantage of SAM is that it exploits Fourier transform techniques to dramatic effect. To many astronomers, Fourier techniques are sometimes regarded as an arcane and difficult way to perform science. However here they provide one of the best ways to increase the resolution of a telescope. Images can be thought of as an ensemble of multiple spatial frequencies: the highest ones give the image its sharp edges, and the lowest ones give the broad distribution. Observationally, the recovered information from a filled telescope pupil is weighted towards recovery of the lower spatial frequencies resulting in the well-known Rayleigh resolution limit of  $1.2 \lambda/D$ , where  $\lambda$  is the wavelength of the light and  $D$  the imaging aperture. With Fourier analysis, the information contained in the highest frequencies can be extracted, giving access to resolutions down to  $\lambda/2D$ . This process is called Fourier deconvolution, a difficult technique when working on full-aperture images (but not impossible, i.e. as in speckle interferometry). The superiority of aperture masking comes from the fact that non-redundant masks make an image with only a few unique spatial frequencies. The complex amplitudes of

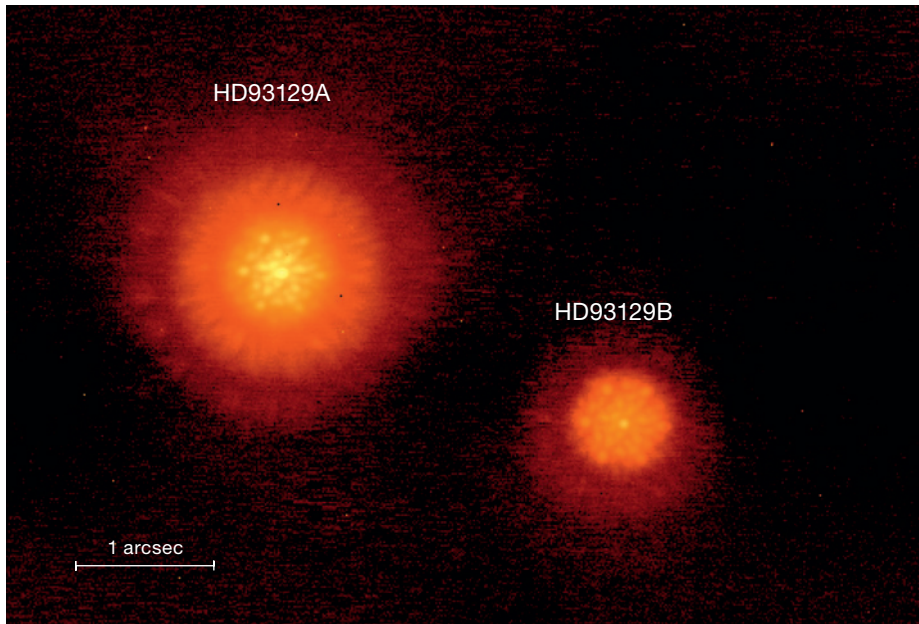
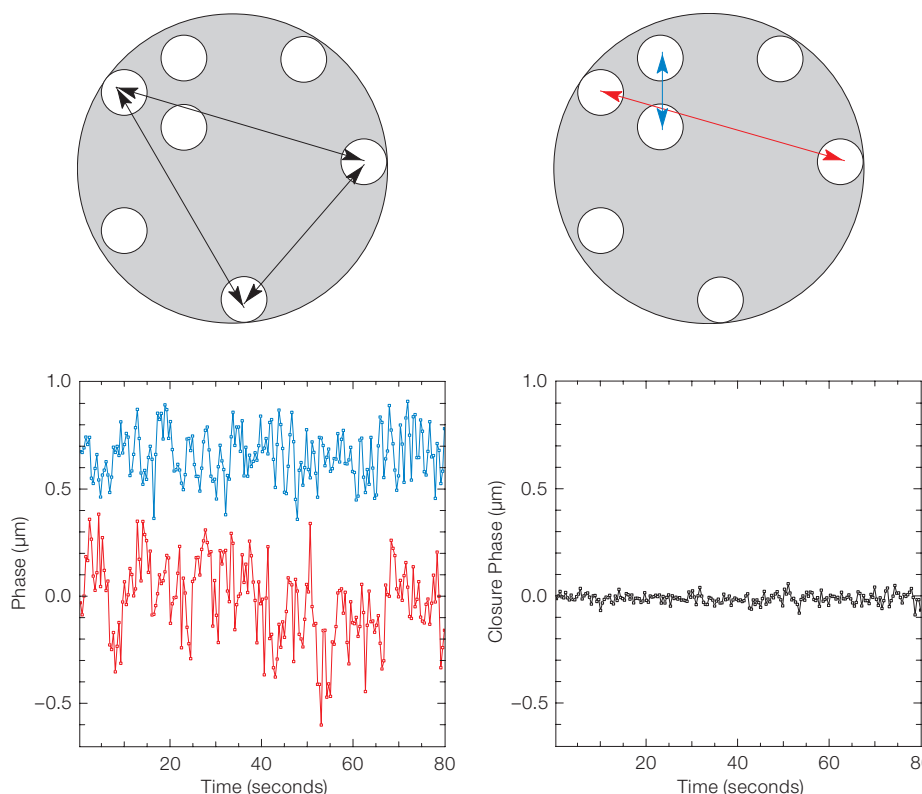


Figure 2. NACO-SAM observations of the HD93129A and B visual binary (angular separation 2.76 arcseconds). SAM is not needed to split the AB pair; classical imaging would have served better here. But SAM is able to resolve the HD93129Aab pair with 0.034 arcsecond separation — almost one hundredth of the separation of the binary depicted. The Aab pair is embedded within the diffraction

pattern of HD93129A. HD93129A appears as an Airy pattern (of size given by the diffraction of the 1.2-metre holes — thus 800 mas in *K* band), interlaced with high frequency fringes. Only through careful Fourier processing can the phase of the fringes be determined to reveal the presence of the third component (Sana et al., 2011).



each frequency are accurately measured thanks to the fact that each one is produced by a single pair of holes. Amplitudes are more stable to seeing fluctuations, and phase aberrations can be subtracted thanks to the use of closure phase (see Figure 3). The use of closure phase is one of the key strengths of aperture masking as it yields an observable that is only affected by the astronomical object, and is robust to any residual optical phase aberration. By recording as many low frequencies as high frequencies, the detection limit of aperture masking is constant at any separation down to an inner working angle of  $\lambda/2D$ , more than twice that commonly expected for a single-dish telescope.

The point to remember about aperture masking is that its key discovery space, when compared to other imaging methods, lies at scales close to the diffraction limit of the telescope. Here we present notable scientific and instrumental successes, which give a broad view of the capabilities and potential of the SAM observational modes.

### Imaging with unprecedented details

The proof of the pudding is in the eating: to test the capability to recover full images at diffraction-limited resolutions of relatively complex targets, we observed VY CMa with the 18-hole mask. With respect to the other masks, this mask gives the best Fourier coverage, but restricts observations to relatively bright systems. An alternate mask geometry which has proved to be very

Figure 3. For each pair of apertures in the 7-hole mask, a set of fringes of a given spatial frequency is observed on the detector. The ensemble image created by many such overlapping fringe packets is illustrated in Figure 2. The phase of the fringes, which for a perfect optical system would be zero everywhere, corresponds to residual aberrations in the pupil. Actual NACO phase data are shown in the lower left panel for two different pairs of holes (red and blue baselines, marked by arrows on the pupil image), exhibiting phase residuals of the order of 300 nm. On the lower right panel, instead of the phase we plot the closure phase. This is the sum of three phases of three baselines formed by three separate holes (the triangle is given by black arrows in the pupil image). For the example dataset, most of the phase noise coming from uncorrected seeing disappears, leaving a closure phase residual of 10 nm; an improvement by a factor of 30.



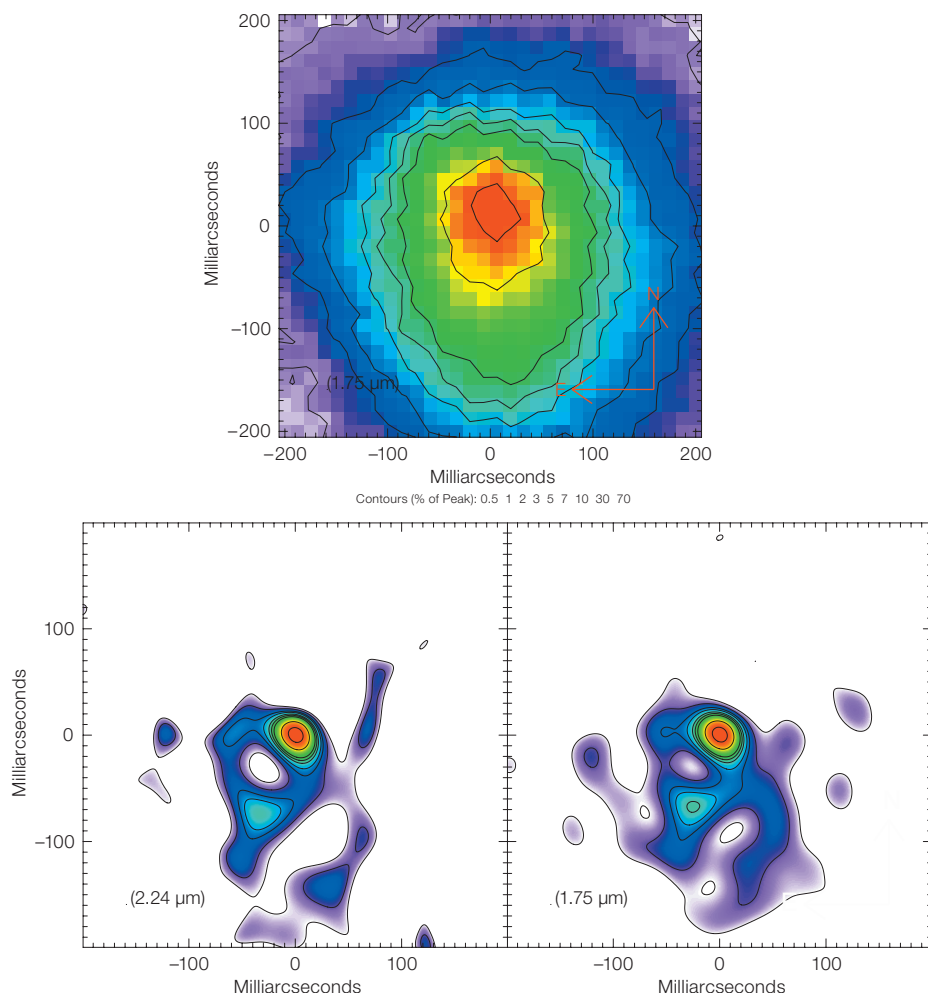


**Figure 4.** Images of the extreme mass-losing supergiant VY CMa. Upper panel: *K*-band image with the full telescope pupil of UT4 and adaptive optics system correction. Lower panels: *K*- and *H*-band images recovered with NACO-SAM data. There is some correspondence between the AO-only and SAM, but the fine detail and diffraction-limited structures appearing in the masking data cannot be seen in the AO image. (Data taken in March 2008).

successful for the imaging of fainter complex targets is an annular geometry: this forms one possible upgrade path now being explored with ESO staff.

For comparison, we obtained imaging observations using the full telescope pupil taken only minutes apart from the SAM data. We used the shift-and-add algorithm to stack these data into a final resultant best image. The images are shown in Figure 4. There is some correspondence between the AO-only and SAM images, in that there is evidence for

a similarly skewed centre of brightness in the AO image. However, the fine detail and diffraction-limited structures appearing in the masking data cannot be seen in the AO-only image. It is possible that more real structure may be recovered with deconvolution using a carefully recorded point spread function (PSF) frame, but this procedure has proved to be controversial in the past, and can lead to spurious structures. Note that the asymmetric structures reproduced in the SAM images are nearly identical to those found by the Keck telescope over a decade ago (also with aperture masking, Monnier et al., 1999).

#### Hunting for exoplanets

Although the exoplanet hunting season has been declared open for quite a while, the field of direct imaging is just begin-

ning to get exciting. With the discovery of Beta Pictoris b (Lagrange et al., 2010), a new race has commenced, towards the detection of ever younger planets. We hope new discoveries will provide clues about the formation of the Earth, that existing observations (including 2M1207b [Chauvin et al., 2004] or HR8799bcd [Marois et al., 2008]) have not been able to provide. But the problem is that planets which formed like the Earth are faint and close to their parent stars, requiring imaging at very small angular separations. Techniques like angular differential imaging (ADI), spectral differential imaging (SDI) or coronagraphy all gain in power as the planet-to-star separation increases. On the other hand, SAM is able to perform well in the region from several  $\lambda/D$  down to separations as small as  $0.5 \lambda/D$  (Lacour et al., 2011). It turns out that this separation range is a particularly valuable one. When imaging the nearest populations of young stars, AO surveys to date can be criticised for doing little more than proving that planets are rare in wide orbits, where they are not expected to form anyway. (Beta Pictoris is an exception because of its extreme proximity to the Sun). SAM on the other hand has demonstrated the ability to probe Solar System scales (Evans et al., 2011), successfully revealing companions and brown dwarfs at resolutions commensurate with the diffraction-limited core.

At the vanguard of the revolution in high-contrast imaging was the discovery of T Cha b. T Cha is a young star (only  $\sim 7$  million years old) with a transition disc (Huélamo et al., 2011). Transition discs are so named because they mark the transition between protostellar discs (formed with the star) and a debris disc (created by subsequent planetary collision — see illustration in Figure 5, upper). Transitions discs are protoplanetary discs with gaps, or put another way, transition discs are made of at least two discs: an inner disc and an outer disc separated by a region which has been cleared of material. Most transition discs have only recently come to scientific attention particularly due to the work of the Spitzer telescope. Astronomers have observed these discs with intense interest in the hope of finding a gravitating body responsible for the creation of the

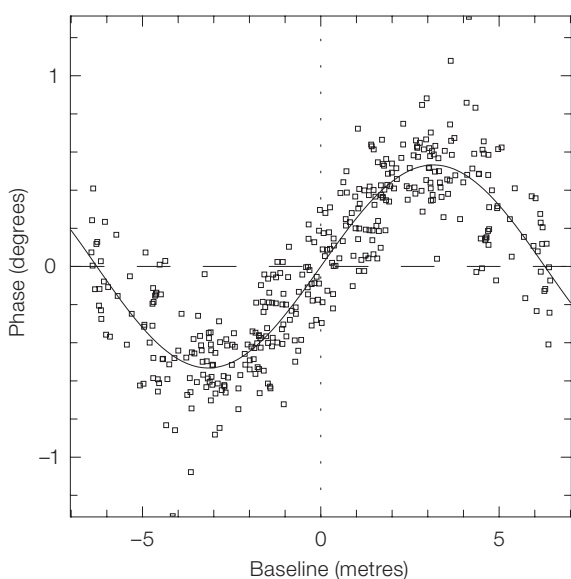
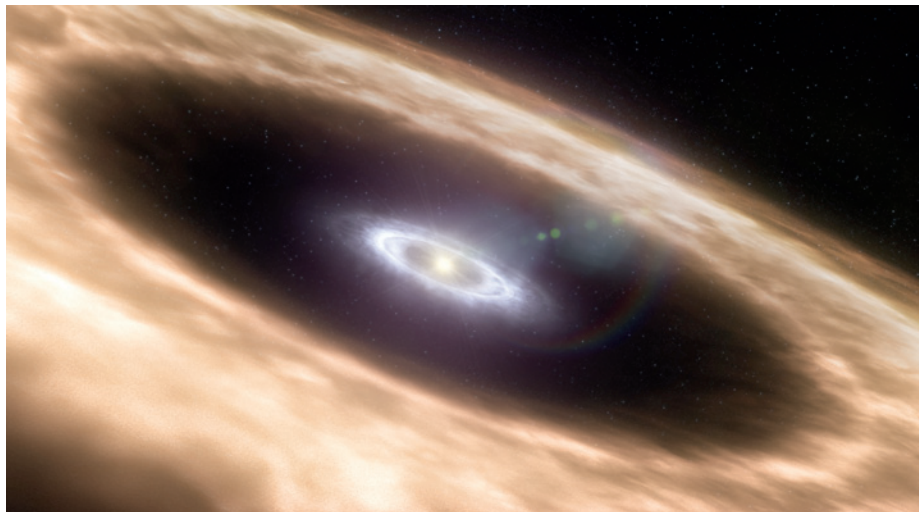


Figure 5. Artist's impression of a transition disc is shown (upper). In the case of T Cha, the inner disc is 0.1 AU in radius, and the outer disc 7.5 AU (according to modelling by Olofsson et al. [2011]). Inside the gap, at a distance of 6.7 AU from the central star, aperture masking revealed a young orbiting body (Huélamo et al., 2011). The closure phase values are plotted as a function of the spatial frequency in the lower panel. The flux ratio in the *L*-band is below 1/100, and the separation is 60 mas (while  $\lambda/D$  is equal to 100 mas).

a second similar object has been observed in the gap of LkCa 15 (Kraus & Ireland, 2011), also thanks to aperture masking — but on the Keck telescope this time.

### SAMPol

In the optical/infrared, celestial targets usually exhibit a polarised signal due to scattering or reflection of light. Common astronomical objects studied through polarimetry include young stellar objects, evolved mass-losing stars and Solar System bodies. The polarised signature is very difficult to observe where such scattering occurs in the immediate vicinity of a star (as opposed to an extended nebula), as can often be the case. This is because light from different spatial regions, each of which may be highly polarised, often adds together with polarisation vectors to cancel out any net signal when the final stellar image is formed. The integrated polarisation from even highly polarised stellar targets is therefore rarely more than a few percent, despite the fact that parts of their circumstellar environments probably emit nearly completely polarised light.

What is needed to overcome this problem is an observing method capable of preserving polarised signals which arise from regions which may be only milliarcseconds apart on the sky. Utilising SAM mode with the polarising Wollaston prisms and halfwave plates already installed as part of the CONICA optics complement, we have commissioned a powerful new observing mode, christened SAMPol. Calibration precision is dramatically enhanced thanks to differential techniques (the camera records both polarisations simultaneously). The halfwave plate can be used to exchange the polarisation states of the two images produced by the Wollaston, allowing for a high degree of resilience against instrumental and seeing-induced sources of measurement error.

In order to test the ability of SAMPol to recover signals from high resolution polarised sources, several late-type giants including L2 Pup were observed utilising the differential interferometric polarimetry method. The masking diffraction pattern

gap, a scenario that would constitute the youngest sign of planet formation. The problem lies in the fact that the gap is at a few astronomical units (AU), and the closest of the star formation associations (like  $\rho$  Ophiucus or  $\eta$  Cha association) are at least 100 pc distant, which implies that an angular resolution of  $\sim 50$  milliarcseconds (mas) is needed to probe the gap. This resolution corresponds to  $\lambda/D$  for the VLT telescopes in the near-infrared (NIR), a regime which is problematic for most classical high dynamic range imaging techniques.

Exploiting the SAM mode on NACO, we have probed within the gap of T Cha, and, for the first time, managed to discover the presence of such a body

through closure phase (see Figure 5, lower). At 6 AU from the central star (slightly above  $\lambda/2D$ ), this object is right within the gap. But as is often the case with a new breakthrough in observational capability, new discoveries generate more questions than they answer and the nature of the T Cha system is an enigma. Currently the true nature of the body (planet, brown dwarf, low-mass star?) is not known, but its existence is likely to be linked to the presence of the gap. The object is profoundly red, relatively easy to detect in the *L*- and *M*-bands (3–5  $\mu\text{m}$ ), but almost invisible at 2  $\mu\text{m}$ . It does not compare well with any contemporary models of planet formation. This object is thus likely to open a new window on planet formation. To add to the mystery,



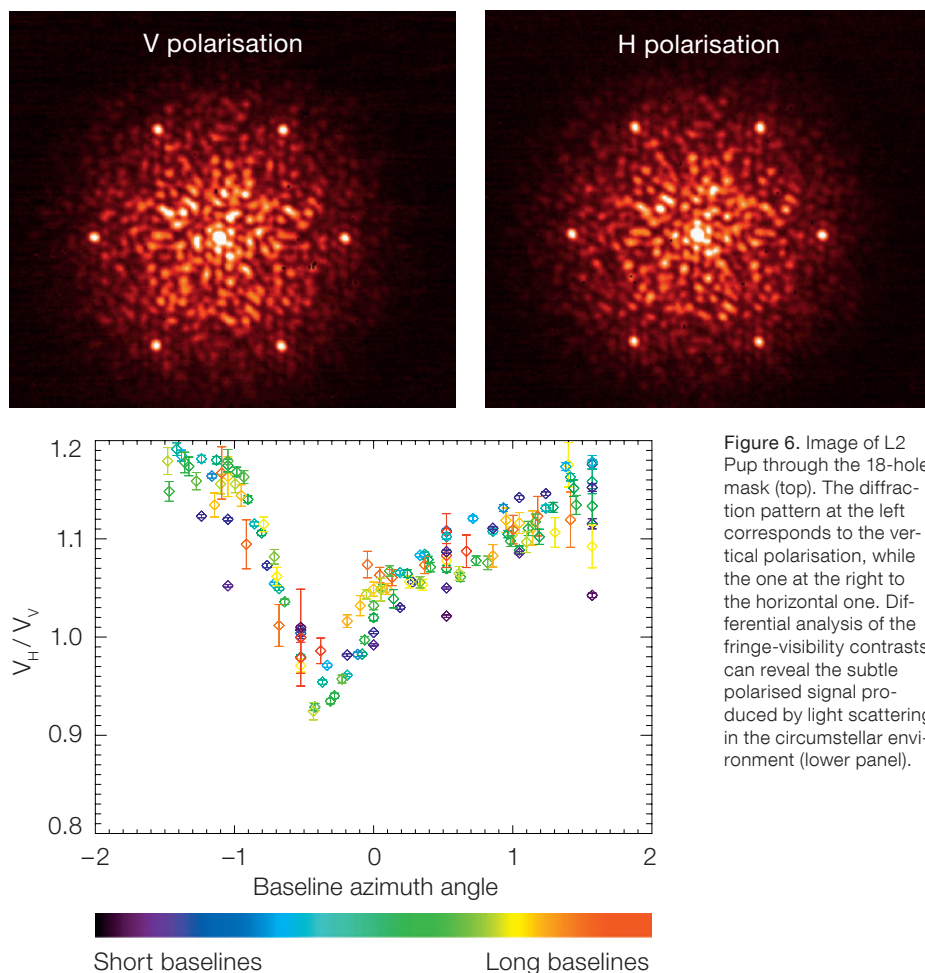


Figure 6. Image of L2 Pup through the 18-hole mask (top). The diffraction pattern at the left corresponds to the vertical polarisation, while the one at the right to the horizontal one. Differential analysis of the fringe-visibility contrasts can reveal the subtle polarised signal produced by light scattering in the circumstellar environment (lower panel).

produced by the star appears twice on the detector thanks to the use of the Wollaston prism (see Figure 6, top). After reduction of the raw data, the final observables can be obtained as ratios of visibilities in different polarisation states (Figure 6, lower; and Norris et al., 2011). The data can be compared with models of scattering to understand the features of the polarisation data.

#### Prospects for aperture masking at the VLT

Aperture masking allows imaging with a formal resolution limit twice as good as a full telescope pupil, while simultaneously delivering observables such as closure phase, which are very resilient to instrumental aberrations. For these reasons, SAM has a future at long wavelengths, as well as in the field of extreme AO.

A SAM mode for the VISIR instrument recently passed the final design review. No schedule for implementation has been yet agreed, but most of the implementation task is software development (another advantage of SAM mode is the simplicity of the hardware). The utility of aperture masking at  $10\ \mu\text{m}$  is sometimes debated, because it is a common — although false — view that the telescopes deliver a nearly perfect beam at mid-infrared wavelengths. It is correct that if the full optical chain were perfect, there would be no need for aperture masking. But the truth is that whatever the wavelength, there are still aberrations which will limit the dynamic range at very small separations. Aperture masking will always bring an additional level of robustness compared to full aperture imaging. Moreover, the mask will be cold, and as such, will decrease both the

stellar light and sky background in proportion, thus preserving this particular signal-to-noise term.

A second project is an upgrade of the SPHERE instrument. SAXO, the SPHERE extreme AO system, will produce an extremely well-corrected wavefront from infrared to visible wavelengths. SAM would double the resolution capabilities of the instrument. At short wavelengths, thanks to an angular resolution of 10 mas at 600 nm, the SAM mode on ZIMPOL would probe the structures of polarisation in young discs or circumstellar shells to unprecedented fine angular scales. The mode is not yet officially accepted by the SPHERE consortium; but such an implementation could happen through an upgrade, or as a visitor instrument mode. It is amazing to think that these new capabilities can be obtained with such a modest hardware investment (a photo of the mask is shown in Figure 7). At longer wavelengths, a mask in front of the SPHERE integral field spectrometer (IFS) would enable a method to characterise companions detected at offsets around  $\lambda/D$  for wavelengths from 0.9 to  $1.7\ \mu\text{m}$ . Moreover, the IFS will offer new possibilities with SAM for phase calibration, which could be used to provide even higher dynamic range.

Presently, the main challenge facing aperture masking is the issue of calibration. On NACO, the current dynamic range of the SAM mode is currently limited to 500 ( $\Delta\ \text{mag}\ 6.7$ ) at  $\lambda/D$  for stars down to magnitudes 7 or 8. For brighter

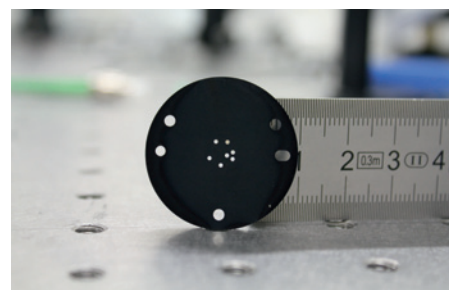


Figure 7. ZIMPOL 7-hole mask for the SPHERE instrument. The mask is 3 cm in diameter for a pupil of 6 mm. Each hole is 825  $\mu\text{m}$  in diameter, which, scaled to M1, corresponds to 1.1 metres projected onto the primary mirror. Combined with the extreme AO system of SPHERE, this mask should allow polarisation structures to be characterised down to a resolution of 10 mas.

stars we are limited by our capacity to calibrate the closure phase (~ 0.3 degrees). On a star of the magnitude of Fomalhaut, aperture masking is capable of delivering closure phases with a scatter below 0.03 degrees, but calibration still dominates the error, preventing us from reaching the theoretical limit of 10 magnitudes in contrast. An important step forward for a new generation of aperture masking instruments would be to understand

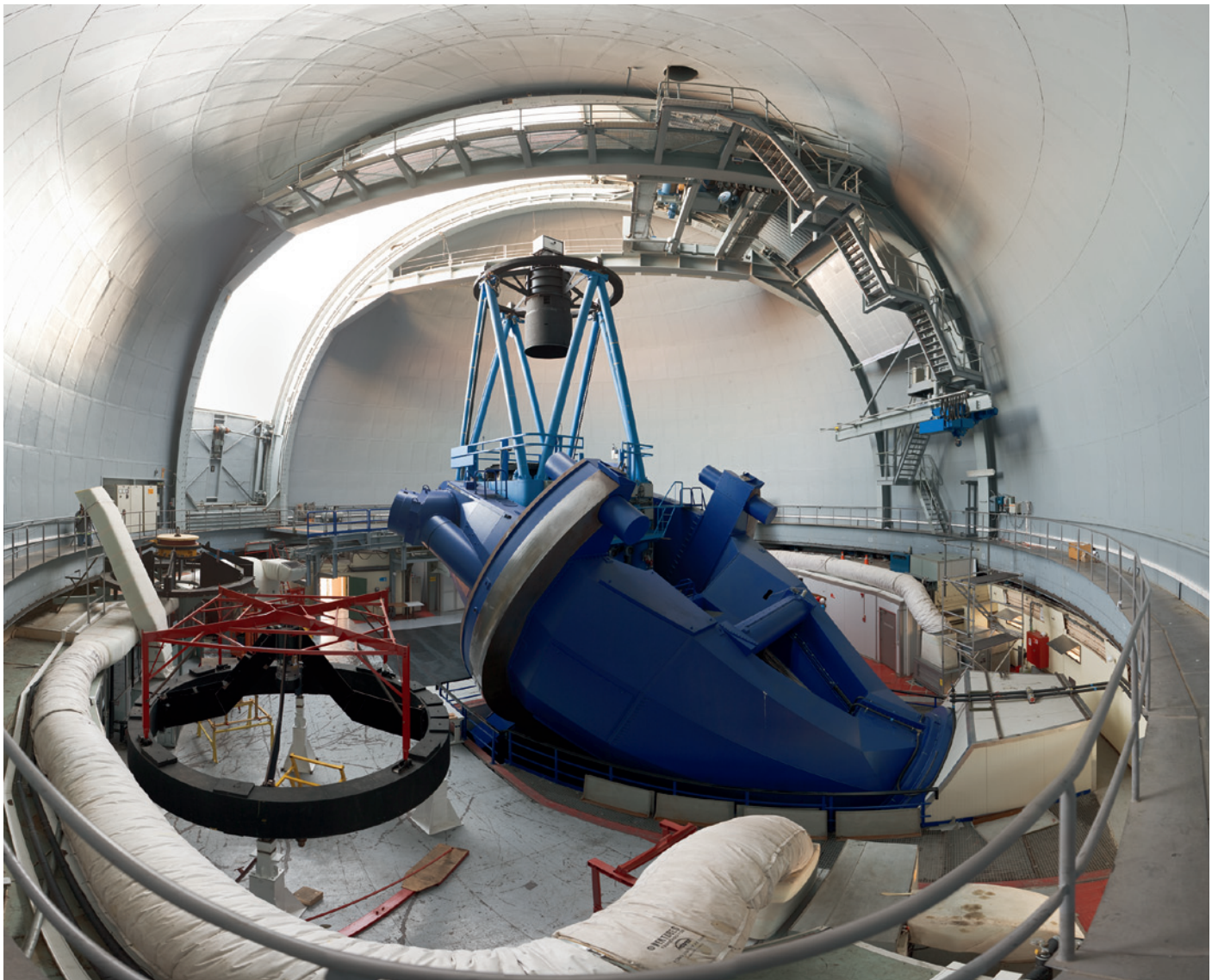
theses calibration errors, and invent an instrument that can overcome them.

#### Acknowledgements

We would like to thank the many people who helped making SAM a success, including, but not limited to, T. Evans, A. Kraus, B. Norris, H. Sana, N. Huelamo, D. Ehrenreich and C. Lidman. Special thanks go to N. Kornweibel, J. Argomedo, T.-G. Lowell and N. Ageorges.

#### References

- Chauvin, G. et al. 2004, A&A, 425, L29
- Evans, T. et al. 2011, ApJ, 2011, in press
- Huelamo, N. et al. 2011, A&A, 528, L7
- Kraus, A. & Ireland, M. 2011, ApJ, in press (arXiv:1110.3808)
- Lacour, S. et al. 2011, A&A, 532, A72
- Lagrange, A.-M. et al. 2010, Science, 329, 57
- Marois, C. et al. 2008, Science, 322, 1348
- Monnier, J. et al. 1999, ApJ, 512, 351
- Norris, B. et al. 2011, Nature, in press
- Olofsson, J. et al. 2011, A&A, 528, L6
- Sana, H. et al. 2011, arXiv 1109.6654



Wide-angle view of the inside of the dome of the ESO 3.6-metre telescope at the La Silla Observatory. The white tubes around the perimeter are part of the dome air-conditioning system.





A VST OmegaCAM colour-composite image of the spiral galaxy NGC 3628 formed from exposures in Sloan *g*, *r* and *i* filters. This Sb galaxy is at a distance of about 12 Mpc and, with M65 and M66, forms the Leo Triplet, a group of interacting galaxies. NGC 3628 is viewed almost edge-on and the dust clouds in the disc are very prominent. See [eso1126](#) for more details.



# Resolving the Inner Regions of Circumstellar Discs with VLT/NACO Polarimetric Differential Imaging

Sascha P. Quanz<sup>1</sup>  
 Hans Martin Schmid<sup>1</sup>  
 Stephan M. Birkmann<sup>2</sup>  
 Daniel Apai<sup>3</sup>  
 Sebastian Wolf<sup>4</sup>  
 Wolfgang Brandner<sup>5</sup>  
 Michael R. Meyer<sup>1</sup>  
 Thomas Henning<sup>5</sup>

<sup>1</sup> Institute for Astronomy, ETH Zurich, Switzerland

<sup>2</sup> ESA/ESTEC, Noordwijk, the Netherlands

<sup>3</sup> Department of Astronomy/Department of Planetary Sciences, University of Arizona, Tucson, USA

<sup>4</sup> Institute of Theoretical Physics and Astrophysics, University of Kiel, Germany

<sup>5</sup> Max-Planck Institute for Astronomy, Heidelberg, Germany

Planets originate from circumstellar discs of gas and dust around young stars. A better knowledge of the physical and chemical conditions in these discs is necessary in order to understand the planet formation process. As most planets form in the inner few tens of astronomical units these disc regions are of particular interest. However, the overwhelming brightness of the central star makes it very challenging to image directly those disc regions. Polarimetric Differential Imaging (PDI) is a powerful technique that overcomes these challenges. Without using a coronagraph, which would block not only the central star, but also part of the interesting inner disc region, PDI allows high-contrast imaging observations at small inner working angles.

The rapidly increasing number of known exoplanets reveals an unexpected diversity in properties, which in part challenges fundamentally our understanding of the planet formation process. Many exoplanets orbit their stars at separations where no counterparts exist in the Solar System, e.g., gas giant planets orbiting at very small or very large separations from their host stars. In order to understand how planets form one needs to understand the physical and chemical conditions in the natal circumstellar discs

surrounding the young stars. Furthermore, the conditions in these discs will also dictate whether, and to what extent, a newly-formed planet might interact with the disc and thereby perhaps change its orbital separation.

Recent direct-imaging surveys suggest that gas giant planets around solar-type stars are in general rare at orbital separations in excess of  $\sim 50$  astronomical units (AU; e.g., Chauvin et al., 2010). At least some early-type stars, on the other hand, are able to form gas giant planets even beyond this limit, as the remarkable examples of the HR8799 system (Marois et al., 2010) and Fomalhaut b (Kalas et al., 2008) have demonstrated. Still, as suggested already by the Solar System, most planet formation appears to take place in the inner few tens of AU, and it is exactly those regions of a circumstellar disc that one needs to study to learn about the relevant processes.

The classical direct-imaging approach to observe circumstellar discs at optical or near-infrared (NIR) wavelengths is to use a coronagraph and/or a reference star that is subtracted from the science target, thus subtracting the bright light from the central star and revealing the much fainter disc emission. This approach suffers from two significant limitations: (1) the coronagraph blocks out not only the central star, but also a significant fraction of the inner disc region; and (2) the reference star never matches the science target perfectly so that disturbing subtraction residuals remain, rendering the inner disc region often useless for scientific analyses.

## Polarimetric differential imaging

One elegant way to overcome these limitations is PDI, a technique that allows high-contrast imaging of circumstellar discs at very small inner working angles, i.e., very close to the star. PDI takes advantage of the fact that direct stellar light is essentially unpolarised, while stellar photons that undergo single scattering from the dust grains on the surface layer of a circumstellar disc are polarised. The VLT's high-resolution NIR imager NAOS–CONICA (NACO), installed at Unit Telescope 4 (UT4), offers a PDI mode. A

Wollaston prism splits the incoming light into two orthogonal, linearly polarised beams (the ordinary and extraordinary beam,  $I_{ord}$  and  $I_{ext}$ , respectively), which are simultaneously imaged onto the detector. A half-wave plate enables the observer to change the orientation of the polarisation direction with respect to the detector without rotating the Wollaston prism and without changing the field of view. Measurements are typically carried out for at least four angles ( $0^\circ$ ,  $45^\circ$ ,  $90^\circ$  and  $135^\circ$ ). The Stokes  $Q$  image can then be obtained from the differences of the  $I_{ord}$  and  $I_{ext}$  images at angles of  $0^\circ$  and  $90^\circ$  while the Stokes  $U$  image is computed correspondingly from the images taken at the other two angular positions ( $45^\circ$  and  $135^\circ$ ). To obtain the final image showing the polarised flux  $P$ , one combines the square root of the quadratic sum of the  $Q$  and  $U$  Stokes parameter images.

Inspection of the formula for the computation of  $Q$  reveals why PDI is so powerful: by subtracting the ordinary and extraordinary beams from each other, the unpolarised contribution from the central star cancels out almost perfectly because both beams have been imaged simultaneously. The result is the spatially resolved polarisation signal from the disc. For completeness we mention that one can also compute the fractional polarisation, i.e., images that show what fraction of the light at a given pixel is polarised, and also the position angle on the sky of the polarisation vector.

## NACO PDI observations

We used NACO in PDI mode to image the circumstellar discs around the young, early-type stars HD100546 and HD97048 in the  $H$  and  $K_s$  filters, i.e., at wavelengths  $\sim 1.7$  and  $2.2 \mu\text{m}$  (Quanz et al., 2011a; Quanz et al., 2011b). The final polarised flux images are shown in Figure 1. For the first time we were able to image directly the scattered light coming from the surface layer of these discs from regions as close as  $\sim 0.15$  arcseconds to the central stars. As mentioned above, these regions are typically not accessible with any other direct-imaging technique. To put our results in a broader perspective, we show, in Figure 2, a sketch comparing



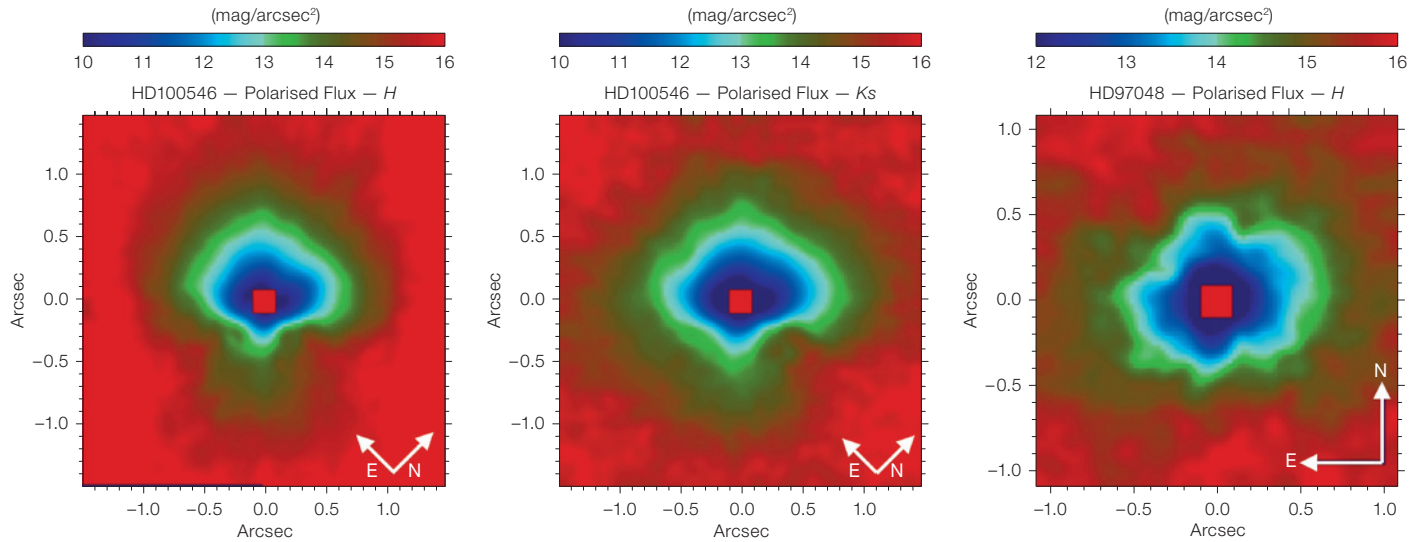


Figure 1. Polarised flux images of the circumstellar discs surrounding HD100546 (left: *H*-band; middle: *Ks*-band) and HD97048 (right: *H*-band). Note that 0.5 arcseconds correspond to ~ 50 AU projected separation in the case of HD100546 and ~ 80 AU in case of HD97048. The central region in each image has been masked out as the core of the PSF was saturated. Adapted from Quanz et al. (2011a, 2011b).

and Fomalhaut. It shows that our data can probe those regions of the circumstellar discs where planetary bodies might form.

Analysis of circumstellar discs

But what exactly can we infer from our images? The most obvious information is certainly the spatial extent and geometric orientation, i.e., inclination and position angle, of the disc emission and its appar-

ent brightness. From our images we can also measure how the disc brightness changes as a function of the disc radius  $r$  and derive disc surface brightness profiles. These profiles indicate whether the disc surface is “flared”, i.e., the disc scale height increases with radius, or rather “flat”. In case of HD97048 the measured profiles drop off roughly as  $r^{-2}$ , but there are indications of distinct “breaks” in surface brightness that appear roughly at 50 AU and 110 AU. Such breaks could

the two circumstellar discs as we have observed them with NACO/PDI, with the dimensions of the Solar System and the two extrasolar planetary systems HR8799

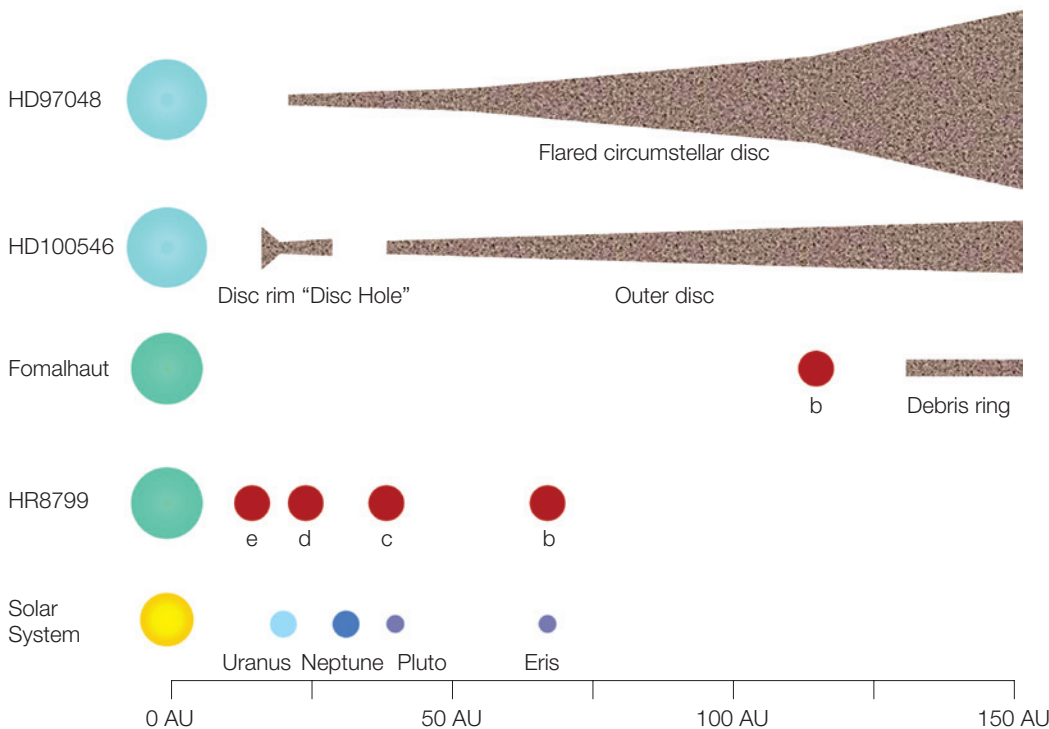
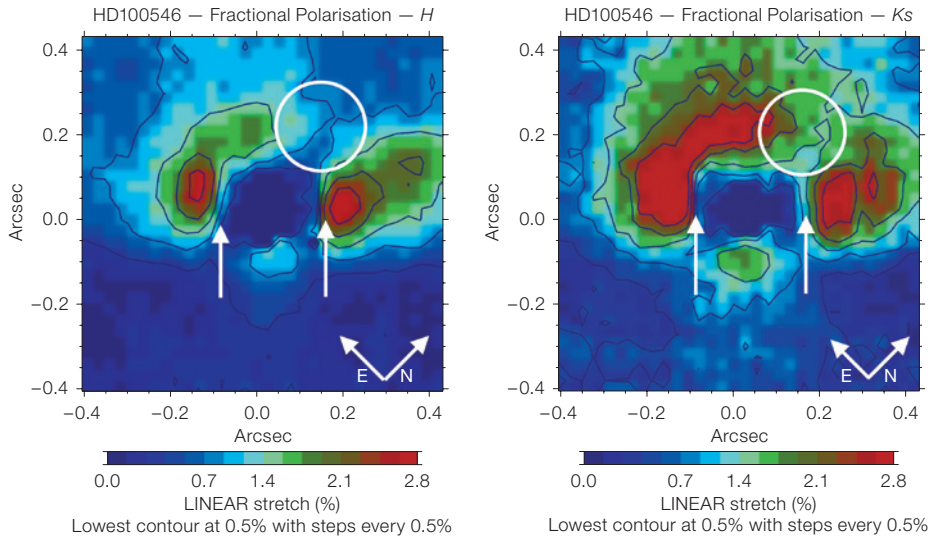


Figure 2. Schematic comparing the circumstellar disc regions of HD100546 and HD97048 resolved with NACO/PDI to the dimensions of the Solar System and the planetary systems around the A-type stars HR8799 and Fomalhaut. The sizes of the objects are not to scale. The inner six Solar System planets (Mercury to Saturn) are not shown.



**Figure 3.** Images showing the fractional polarisation of the inner disc regions of HD100546 (*H*-band left, *Ks*-band right). Note that 0.4 arcseconds corresponds to  $\sim 40$  AU projected separation. The circles show the position of the “disc hole”, while the arrows indicate the position of the “disc rim”. Adapted from Quanz et al. (2011a).

as it suffers from instrumental polarisation effects that change with the parallactic angle of the source (Witzel et al., 2010).

Soon, a new second generation instrument will be installed at the VLT that also has PDI modes: SPHERE (Beuzit et al., 2006). With its high-performance adaptive optics (AO) system, SPHERE will not only provide much better Strehl ratios, but a more stable point spread function (PSF) than NACO. In particular, ZIMPOL — a high precision optical imaging polarimeter — will yield an unprecedented polarimetric accuracy and open a new pathway for studying circumstellar discs from the ground in the *V*-, *R*- and *I*-bands. Furthermore, IRDIS — the NIR double beam imager — has also a PDI mode and is well suited to complement the ZIMPOL data with images at longer wavelengths. The current suite of VLTI instruments resolve the innermost few AU at NIR and mid-infrared wavelengths, while the Atacama Large Millimeter/sub-millimeter Array (ALMA) will probe the (sub-)millimetre thermal emission from cool dust grains in the disc midplane and the molecular gas content of the disc with comparable spatial resolution. In combination with these instruments, SPHERE will allow us to refine our understanding of circumstellar discs and uncover part of the physical and chemical conditions under which planets are presumably forming.

#### References

- Apai, D. et al. 2004, *A&A*, 415, 671
- Benisty, M. et al. 2010, *A&A*, 511, 75
- Beuzit, J.-L. et al. 2006, *The Messenger*, 125, 29
- Chauvin, G. et al. 2010, *A&A*, 509, 52
- Kalas, P. et al. 2008, *Science*, 322, 1345
- Marois, C. et al. 2010, *Nature*, 468, 1080
- Quanz, S. et al. 2011a, *ApJ*, 738, 23
- Quanz, S. et al. 2011b, *A&A* submitted
- Witzel, G. et al. 2010, *The Messenger*, 142, 5

be signs that the disc is somehow perturbed at these separations or that the properties of the dust grains are suddenly changing. For comparison, the radial profile of HD100546 is steeper and drops off roughly with  $r^{-3}$ , but does not show any signs for discontinuities.

Furthermore, our images allow us to search for structures in the inner regions of the circumstellar discs. An example for the HD100546 disc is shown in Figure 3 and is also depicted in the cartoon in Figure 2. First, we find indications for a “hole” in the north-eastern part of the disc at a projected separation of  $\sim 30$  AU. In both filters the amount of polarised flux shows a local minimum here. The reason for this hole is unknown, but signatures of ongoing planet formation are a tempting interpretation. Secondly, closer inspection of the images reveals that very close to the central star the amount of polarised flux rapidly decreases from its maximum. Previous studies (e.g., Benisty et al. 2010) suggested that HD100546 disc has a gap roughly between 4–15 AU and that a giant planet might be orbiting within this gap. While our images cannot reveal the planet itself they support the idea that the disc has a rim at 15 AU (the maximum in our images) and is relatively low in scattering dust particles close to the star.

Finally, polarisation measurements of circumstellar discs allow us to constrain the properties of the dust grains — size and

composition — that we are probing. As we are observing the surface layer of circumstellar discs and as the dust grains on this layer are the dominant opacity source, the properties of the dust grains will determine how much stellar light is scattered, absorbed or transported in deeper disc layers. Hence, the surface grains strongly affect the energy budget of the discs, which in turn impacts on the physical conditions for planet formation. Knowing also the inclination of the disc and the disc-flaring angle we can compute how the intensity of the polarised flux changes as a function of the scattering angle. These scattering functions depend on the dust grain properties. If we have images in more than one filter we can furthermore see how the colour of the polarised light changes as a function of the disc radius. This is an additional probe to obtain information about the dust grain properties.

#### Potential and future of PDI

Despite the huge amount of information that PDI can offer for the inner regions of circumstellar discs, it has not yet been fully exploited with VLT/NACO. In addition to HD100546 and HD97048 there is only one additional circumstellar disc studied with NACO/PDI, TW Hya, which also shows signs of breaks in its radial surface brightness profile (Apai et al., 2004). However, NACO, as a Nasmyth focus instrument, is not perfect for PDI studies



# X-shooter Finds an Extremely Primitive Star

Elisabetta Caffau<sup>1,2,3,4</sup>  
 Piercarlo Bonifacio<sup>2</sup>  
 Patrick François<sup>2,5</sup>  
 Luca Sbordone<sup>1,2</sup>  
 Lorenzo Monaco<sup>3</sup>  
 Monique Spite<sup>2</sup>  
 François Spite<sup>2</sup>  
 Hans-G. Ludwig<sup>1,2</sup>  
 Roger Cayrel<sup>2</sup>  
 Simone Zaggia<sup>6</sup>  
 François Hammer<sup>2</sup>  
 Sofia Randich<sup>7</sup>  
 Paolo Molaro<sup>8</sup>  
 Vanessa Hill<sup>9</sup>

<sup>1</sup> Zentrum für Astronomie der Universität Heidelberg, Landessternwarte, Heidelberg, Germany

<sup>2</sup> GEPI, Observatoire de Paris, CNRS, Université Paris Diderot, Meudon, France

<sup>3</sup> ESO

<sup>4</sup> Gliese Fellow

<sup>5</sup> Université de Picardie Jules Verne, Amiens, France

<sup>6</sup> INAF, Osservatorio Astronomico di Padova, Italy

<sup>7</sup> INAF, Osservatorio Astrofisico di Arcetri, Firenze, Italy

<sup>8</sup> INAF, Osservatorio Astronomico di Trieste, Trieste, Italy

<sup>9</sup> Université de Nice-Sophia Antipolis, Observatoire de la Côte d'Azur, CNRS, Laboratoire Cassiopée, Nice, France

Low-mass extremely metal-poor (EMP) stars hold the fossil record of the chemical composition of the early phases of the Universe in their atmospheres. Chemical analysis of such objects provides important constraints on these early phases. EMP stars are rather rare objects: to dig them out, large amounts of data have to be considered. We have analysed stars from the Sloan Digital Sky Survey using an automatic procedure and selected a sample of good candidate EMP stars, which we observed with the spectrographs X-shooter and UVES. We could confirm the low metallicity of our sample of stars, and we succeeded in finding a record metal-poor star.

According to the standard Big Bang theory, the primordial matter of the Universe

was made of hydrogen, helium and traces of lithium. Almost all of the other (heavier) elements (metals), including those forming our bodies, were subsequently created in quiescent and explosive stellar nucleosynthesis. The first stars were formed by the condensation of clouds from the matter of the primordial Big Bang: the absence of metals in these condensing clouds makes their cooling more difficult, favouring the formation of high-mass stars. Such stars evolved rapidly, and disappeared in explosions (supernovae) that enriched the surrounding matter in metals. If low-mass stars (less than  $0.8 M_{\odot}$ ) had also been formed (e.g., Clark et al., 2011; Greif et al., 2011), they would still remain on the main sequence today, and, owing to their very slow and moderate evolution, their atmospheres would still display their initial abundances: the Big Bang abundances. No such star has been observed as yet.

The first stars, formed from primordial matter, composed only of material produced in the Big Bang nucleosynthesis, played an essential role in the first epochs of the Universe: the most massive ones produced the re-ionisation of the Universe and synthesised the first metals. The chemical composition of their descendants brings unique information about these first stars. The most ancient stars of the Milky Way galaxy are the direct descendants of the first stars and contain a fossil record of the first epochs of the Universe. For four decades, astronomers have been looking for stars with chemical compositions as close as possible to the primordial material, in order to understand the very first step of the build-up of the chemical elements, and also to establish whether stars with this primordial composition still exist. It is therefore essential to find and analyse these primitive stars.

In the Milky Way galaxy, a few low-mass, extremely metal-poor stars have been found: here the primordial matter has been slightly enriched in metals by the ejecta of the first stars. Among them, three stars are known to be extremely deficient in iron (less than 1/10 000 of the solar abundance): HE 0107-5840 (Christlieb et al., 2002), HE 1327-2326 (Frebel et al., 2005) and HE 0557-4840

(Norris et al., 2007). These stars are usually designated by the name of the first author of the discovery paper, thus: Christlieb's star, Frebel's star, and Norris's star. But in these stars the extreme deficiency in iron is *not* matched by a similar deficiency in lighter elements such as carbon and oxygen, which are enhanced by two to three orders of magnitude. It has been then suggested that the formation of such low-mass, iron-poor stars has been made possible only by the presence of some extra C and O (Bromm & Loeb, 2003). A sample of only three stars, however, is too small to draw any firm conclusions and needs to be extended.

## A good selection

To look for very rare objects, a first selection has been performed on a very large sample of low-resolution spectra from the Sloan Digital Sky Survey (SDSS; York et al., 2000). A selection method has been built and applied to the SDSS spectra. The selection, described in Caffau et al. (2011c), is based on an automatic abundance determination, where the stellar parameters are derived from the SDSS photometry, while the metallicity is derived from line profile fitting of the metallic features present in the spectra. The most metal-poor objects ( $[Fe/H] < -2.5$ ) are inspected by eye. We applied this selection to SDSS, Data Release 7, resulting in a sample of very metal-poor candidates.

We had the opportunity to observe twenty of the most promising candidates at higher resolution. Fifteen were observed with the UVES spectrograph and six with the X-shooter spectrograph mounted at the Cassegrain focus of the Kueyen VLT Unit Telescope (Vernet et al., 2011), taking advantage of its high efficiency, and using the Franco-Italian guaranteed observing time (GTO). One of these stars, whose 2D spectrum taken with X-shooter is represented in Figure 1, seemed particularly interesting, since the only metallic lines clearly detectable were the strong Ca II K lines at 3933 Å and 3968 Å. Owing to the peculiarity of this interesting star, additional telescope time was requested from the ESO Director General's discretionary time to study the star's light at higher resolution with

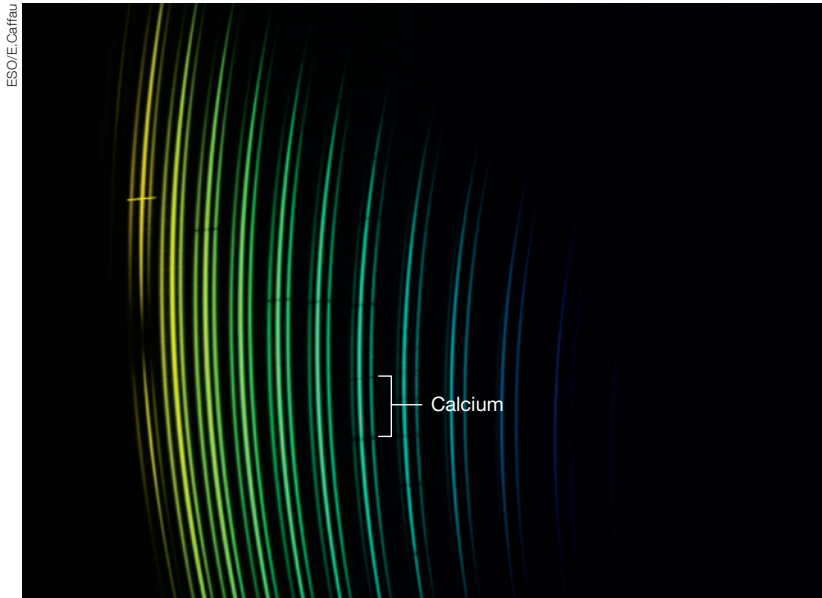


Figure 1. A 2D echellogram of the spectrum of SDSS J102915+172927 taken with X-shooter in the UVB range.

the UVES spectrograph to try to find other (faint) metallic lines in the spectrum. Figure 2 shows the three available spectra (SDSS, UVES, and X-shooter).

The high resolution analysis confirms the metallicity determination derived from the SDSS spectra. All the stars happen to be extremely metal-poor ( $[\text{Fe}/\text{H}] < -3$ ). For the stars above  $[\text{Fe}/\text{H}] > -3.5$ , there is a good agreement between the metallicity derived from low and high resolution

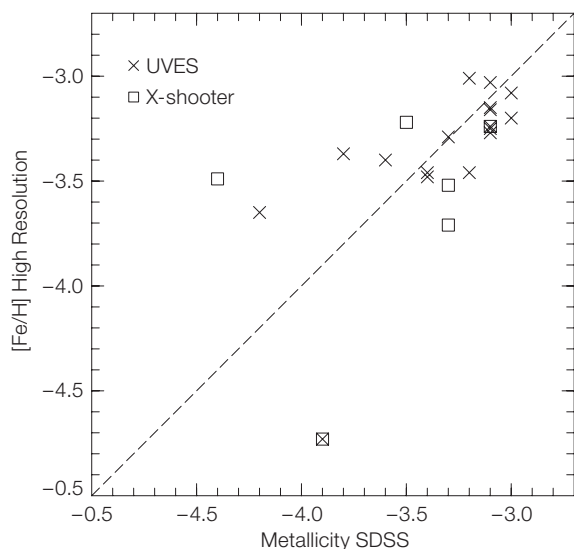


Figure 3. The metallicity derived from SDSS spectra for the sample of extremely metal-poor stars is here compared to the  $[\text{Fe}/\text{H}]$  values derived from higher resolution spectra (UVES data shown by crosses and X-shooter by squares).

spectra, within 0.5 dex. At lower metallicity, the disagreement is much larger, about 1 dex, but the low metallicity derived from SDSS spectra is still confirmed (see Figure 3).

### An extremely metal-poor star indeed!

The star SDSS J102915+172927 in the constellation of Leo is faint, with a  $g$ -band magnitude of 16.92, a  $g-z$  colour of 0.59 mag (0.53 after reddening correction) and is compatible with the colour of a turn-off star. Its distance is about 1.3 kiloparsecs (kpc). The stellar orbit is elongated,

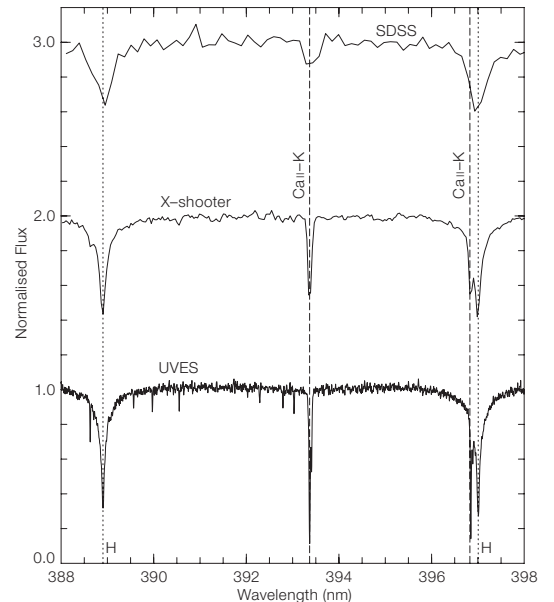


Figure 2. The SDSS, X-shooter and UVES spectra (from top to bottom) of SDSS J102915+172927 in the region of the CaII K and H lines.

so the star belongs to the halo. This star has a mass smaller than that of the Sun and therefore a slow evolution rate, so that its photosphere still displays the unaltered chemical composition of the cloud of interstellar matter from which it formed: a cloud made of the primordial matter of the Big Bang, slightly enriched by the ejecta of the first massive stars. The star is old, probably more than 13 billion years, following several arguments: such stars belong to old populations; comparable stars are directly found to be old by radiochronometry; and the matter of the Galaxy has been submitted to efficient mixing processes so that the formation of these stars had to take place before the rapid enrichment in metals by the ejecta of numerous supernovae.

The star turns out to be extremely metal-poor: it is less iron-poor than two of the three well-known stars quoted before, but it has not been affected by an inflow of C and N, so it is also C-poor. Oxygen is not measured in the star, but since the star is not enhanced in C and N, we assume that it is not O-rich. Metal-poor stars show a constant ratio  $[\text{O}/\text{Fe}]$  of about 0.4 dex, irrespective of their metallicity. We assume for this star  $[\text{O}/\text{Fe}] = +0.6$ , adding +0.2 dex to the expected value, to be conservative.



Stars have generally been classified taking into account only their iron abundance (the most easily measured abundance). We are compelled to use here a more general parameter, the metallicity,  $Z$  (used in stellar structure theory).  $Z$  is the mass fraction of elements heavier than helium (i.e., the mass fraction of metals). The metallicity of the Sun is around  $Z = 0.0153$  (Caffau et al., 2011a). The metallicity of SDSS J102915+172927 is less than  $6.9 \times 10^{-7}$  (i.e., about  $4 \times 10^{-5}$  times the Solar metallicity). The metallicities of the other three well-known EMP stars are larger than  $10^{-5}$ . The metallicity of SDSS J102915+172927 is much lower, and hence nearer to the Big Bang metallicity (see Caffau et al., 2011b).

#### How was this star formed?

A large and massive cloud condenses easily and rapidly into a massive star, but it is difficult for a small cloud to form a low-mass star rapidly, so that a slowly condensing cloud of primordial matter is at risk of being contaminated by the ejecta of massive supernovae (SNe). The main difficulty is to find efficient mechanisms that can cool the gas cloud during its collapse. Without such a mechanism the thermal energy of a small cloud is sufficient to halt its collapse. Metals are efficient cooling agents, and thus, because of an observed absence of stars with a metallicity  $Z < 1.5 \times 10^{-5}$ , it has been suggested that low-mass stars cannot form from the primitive interstellar medium until it has been significantly enriched in metals.

Different theories exist as to the physical mechanism providing the cooling. Bromm & Loeb (2003) postulate the need for a minimum amount of carbon and oxygen that can provide efficient cooling through the fine structure transitions of ionised carbon and neutral oxygen. Another theory postulates that dust grains are instead responsible for the cooling and make it possible for a cloud of large mass to fragment and form low-mass stars (Schneider et al., 2011). The issue is far from being settled and competing theories exist, predicting that low-mass stars can form even without any metals to guarantee the cooling (Clark et al., 2011; Greif et al., 2011).

Element	A(X) 3D	[X/H] 3D	[X/Fe] 3D	[X/H] 1D	Number of lines	A(X) <sub>⊙</sub>
Li	≤ 1.1				1	1.03
C	≤ 4.2	≤ -4.3	≤ +0.7	≤ -3.8	G-band	8.50
N	≤ 3.1	≤ -4.8	≤ +0.2	≤ -4.1	NH-band	7.86
Mg I	2.95	-4.59 ± 0.10	+0.40	-4.68 ± 0.08	4	7.54
Si I	3.25	-4.27 ± 0.10	+0.72	-4.27 ± 0.10	1	7.52
Ca I	1.53	-4.80 ± 0.10	+0.19	-4.72 ± 0.10	1	6.33
Ca II	1.48	-4.85 ± 0.11	+0.14	-4.71 ± 0.11	3	6.33
Ti II	0.14	-4.76 ± 0.11	+0.23	-4.75 ± 0.11	6	4.90
Fe I	2.53	-4.99 ± 0.12	+0.00	-4.73 ± 0.13	44	7.52
Ni I	1.35	-4.88 ± 0.11	+0.11	-4.55 ± 0.14	10	6.23
Sr II	≤ -2.28	≤ -5.2	≤ -0.21	≤ -5.1	1	2.92

Table 1. The chemical abundances of SDSS J102915+172927 (A(X) for 12 + log (A/H) and [X/H] or [X/Fe] for log abundances relative to Solar) derived from the UVES spectrum.

The abundances in SDSS J102915+172927 (Table 1) and the assumption [O/Fe] = +0.6 strongly support the idea that, at least in some cases, low-mass stars can also form at lower carbon and oxygen abundances than the current estimates for the critical values in the theory of Bromm & Loeb (2003). The metallicity of SDSS J102915+172927 is compatible with the critical metallicity predicted in the case of dust cooling (Schneider et al., 2011). It is clearly interesting to see if stars of much lower metallicity can be found, and would thereby yield support to theories that do not predict any critical metallicity for the formation of low-mass stars.

#### Where has the lithium gone?

Another very interesting finding is the lack of lithium in SDSS J102915+172927. Such an old star should have a composition similar to that of the Universe shortly after the Big Bang, thus including traces of lithium, with a few more metals. But we found that the proportion of lithium in the star was at least fifty times less than expected in the material produced by the Big Bang. The warm, unevolved old stars in the Galactic halo display a constant abundance of lithium — the Spite Plateau (Spite & Spite, 1982). The upper limit for lithium in SDSS J102915+172927 is well below the value of the Spite plateau. The reasons for this lack of lithium are not understood: it could be the extension of the “meltdown” described by Sbordone et al. (2010). Lithium is also depleted in the most iron-poor star HE 1327–2326 (Frebel et al., 2005). What is certain is that, in order to destroy the lithium produced in the Big Bang, the material we are observing in these stars

must have been processed at temperatures exceeding two million degrees.

#### How many of these stars are there?

Stars similar to SDSS J102915+172927 are probably not very rare. Between 5 and 50 stars with similarly low, or even lower, metallicity than SDSS J102915+172927 are expected to be found among the candidates accessible from the VLT, and many more in the whole SDSS sample. The high efficiency of X-shooter, and of its integral field unit mode, holds the promise that a large number of candidates can be scrutinised in a limited amount of time.

We are still involved in the Italian GTO for X-shooter, and we hope to continue observing the best candidates during the next few semesters. We have also applied for more observation time with both X-shooter and UVES, to increase the sample of extremely metal-poor stars.

#### References

- Bromm, V. & Loeb, A. 2003, *Nature*, 425, 812
- Caffau, E. et al. 2011a, *Sol. Phys.*, 268, 255
- Caffau, E. et al. 2011b, *Nature*, 477, 67
- Caffau, E. et al. 2011c, *A&A*, 534, 4
- Christlieb, N. et al. 2002, *Nature*, 419, 904
- Clark, P. C. et al. 2011, *Science*, 331, 1040
- Frebel, A. et al. 2005, *Nature*, 434, 871
- Greif, T. H. et al. 2011, *ApJ*, 737, 75
- Norris, J. E. et al. 2007, *ApJ*, 670, 774
- Sbordone, L. et al. 2010, *A&A*, 522, 26
- Schneider, R. et al. 2011, *MNRAS*, in press, arXiv1109.2900
- Spite, M. & Spite, F. 1982, *Nature*, 297, 483
- Vernet, J. et al. 2011, *A&A* in press, arXiv 1110.1944
- York, D. G. et al. 2000, *AJ*, 120, 1579

# Evolution of the Observed Ly $\alpha$ Luminosity Function from $z = 6.5$ to $z = 7.7$ : Evidence for the Epoch of Re-ionisation?

Benjamin Clément<sup>1,2</sup>  
 Jean-Gabriel Cuby<sup>1</sup>  
 Frédéric Courbin<sup>3</sup>  
 Adriano Fontana<sup>4</sup>  
 Wolfram Freudling<sup>5</sup>  
 Johan Fynbo<sup>6</sup>  
 Jesús Gallego<sup>7</sup>  
 Pascale Hibon<sup>8</sup>  
 Jean-Paul Kneib<sup>1</sup>  
 Olivier Le Fèvre<sup>1</sup>  
 Chris Lidman<sup>9</sup>  
 Richard McMahon<sup>10</sup>  
 Bo Milvang-Jensen<sup>6</sup>  
 Palle Moller<sup>5</sup>  
 Kim K. Nilsson<sup>5</sup>  
 Laura Pentericci<sup>4</sup>  
 Bram Venemans<sup>5</sup>  
 Victor Villar<sup>7</sup>  
 Jon Willis<sup>11</sup>

<sup>1</sup> Laboratoire d'Astrophysique de Marseille, Université Aix-Marseille & CNRS, France

<sup>2</sup> Steward Observatory, University of Arizona, Tucson, USA

<sup>3</sup> Laboratoire d'Astrophysique, EPFL, Observatoire de Sauverny, Switzerland

<sup>4</sup> INAF Osservatorio Astronomico di Roma, Monteporzio, Italy

<sup>5</sup> ESO

<sup>6</sup> Dark Cosmology Centre, Copenhagen, Denmark

<sup>7</sup> Departamento de Astrofísica, Facultad de CC. Física, Universidad Complutense de Madrid, Spain

<sup>8</sup> SESE, Arizona State University, Tempe, USA

<sup>9</sup> Australian Astronomical Observatory, Epping, Australia

<sup>10</sup> Institute of Astronomy, Cambridge, United Kingdom

<sup>11</sup> Department of Physics and Astronomy, University of Victoria, Canada

Probing the first billion years of the Universe is one of the last frontiers in cosmology. Ly $\alpha$  emitters (LAEs) are galaxies that can be detected out to very high redshifts during the epoch of re-ionisation. The evolution of their luminosity function with redshift is a direct probe of the Ly $\alpha$  transmission of the intergalactic medium (IGM), related to the amount of neutral hydrogen. We report on the results of a search for LAEs at  $z = 7.7$  using HAWK-I at the VLT with a narrowband filter centred at

1.06  $\mu\text{m}$ . We did not find any LAE candidates, which allows us to infer robust constraints on the LAE luminosity function at  $z = 7.7$ . Depending on which luminosity functions at  $z = 6.5$  are referred to, our results may reflect a significant quenching of the IGM Ly $\alpha$  transmission, possibly from a strong increase in the neutral hydrogen fraction between these two redshifts.

The quest for distant objects has made spectacular progress since the discovery of the first astrophysical object at a redshift  $> 6$ , a Ly $\alpha$  emitter at redshift 6.56 (Hu et al., 2002). For finding high-redshift galaxies, astronomers mainly use two techniques based on optical and infrared imagery data. The Lyman-break technique uses the redshifting of the Ly $\alpha$  forest to locate strong absorption breaks in broadband photometry of galaxies (Lyman break galaxies – LBGs), while the narrowband (NB) technique looks for a photometric excess in NB filters due to the redshifted Ly $\alpha$  line. NB filters are usually designed to coincide with regions of low OH emission of the night sky, leading to discrete redshift values. At  $z = 5.7$  and  $z = 6.5$ , the largest samples of LAEs were obtained with the SuprimeCam on the Subaru Telescope (Ouchi et al., 2010; Hu et al., 2010; Kashikawa et al., 2010). Large samples of LBGs at redshift  $> 7$  have been recently assembled from Hubble Space Telescope (HST) observations with the new WFC3 near-infrared camera. Similarly, quasars at high redshift are found using the Lyman-break technique in multi-colour datasets over very wide fields, such as the Sloan Digital Sky Survey. Finally, gamma-ray bursts (GRBs) have been discovered at very high redshift and nicely complement the other methods by probing the faint end of the galaxy luminosity function.

## Probing the epoch of re-ionisation

Observations of the cosmic microwave background (CMB) allow astronomers to constrain the history of re-ionisation. Polarisation measurements of the CMB from WMAP show a large optical depth due to Thomson scattering of CMB photons from free electrons in the early Universe, suggesting that the re-ionisation

started 500 million years after the Big Bang at redshift  $10.6 \pm 1.2$  (Komatsu et al., 2011). Conversely, the strong increase of the optical depth in the Ly $\alpha$  forest of high-redshift quasars is a likely indicator that re-ionisation was mostly complete at a redshift of  $\sim 6$ . Determining how and at what pace the re-ionisation process took place when the Universe was 500 Myr to 1 Gyr old are the key questions that motivate the search for high-redshift objects.

Due to the resonant nature of the Ly $\alpha$  line ( $\lambda = 121.6$  nm), Ly $\alpha$  photons are easily affected by neutral hydrogen on their path to the observer and are scattered out of the line of sight. Thus, it has long been proposed that Ly $\alpha$  transmission by the intergalactic medium (IGM) could be used as a probe of its ionisation state during the re-ionisation epoch. One observational method of probing Ly $\alpha$  IGM transmission is to study the evolution of the LAE luminosity function (LF) with redshift. Various results show that the Ly $\alpha$  LAE LF remains surprisingly unchanged from  $z \sim 2$  to  $z \sim 6$ . Ouchi et al. (2010) and Kashikawa et al. (2011) infer from their NB observations that the evolution of the LAE LF between  $z = 5.7$  and  $6.5$  can be attributed to a reduction of the IGM Ly $\alpha$  transmission of the order of 20%, which can in turn be attributed to a neutral hydrogen fraction  $x_{\text{HI}}$  of the order of 20% at  $z = 6.5$ . Hu et al. (2010) have recently questioned this result and report significantly different LF parameters. They report lower number counts and no evolution in luminosity between  $z = 5.7$  and  $z = 6.5$ . These somewhat discrepant observational results could tentatively be attributed to cosmic variance or to differences in the selection criteria and in extrapolations of the spectroscopic samples to photometric samples. New data at redshift  $\sim 6$  will help in resolving the current contention, while data at higher redshifts can bring new constraints at still poorly explored redshifts.

This paper (see Clément et al. [2011] for full details) presents new results on the LAE luminosity function at  $z = 7.7$ , from observations carried out at the VLT with the HAWK-I instrument (Casali et al., 2005).



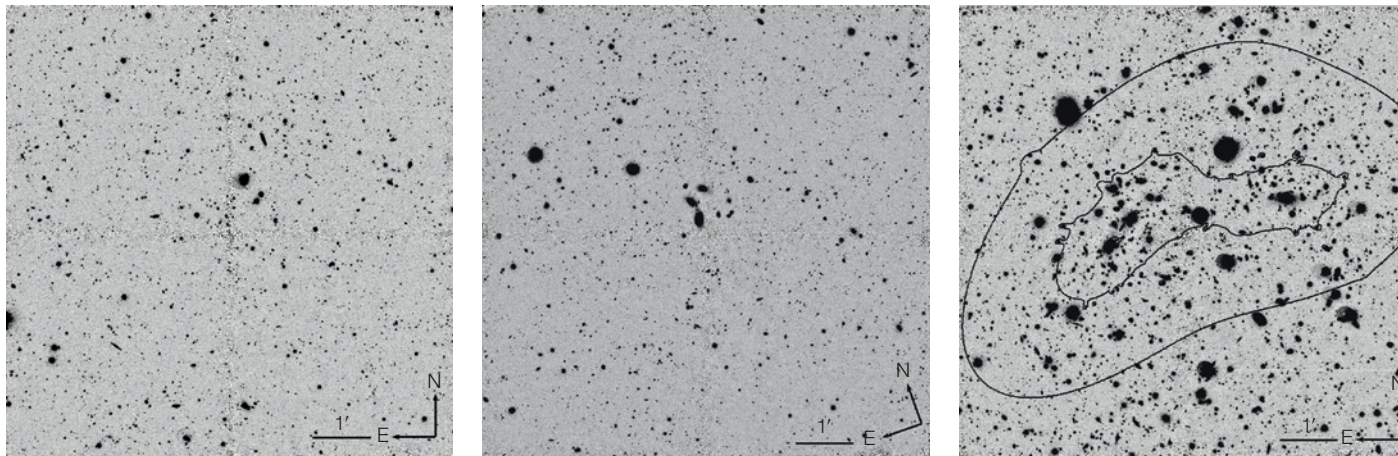


Figure 1. Images of the CFHTLS-D4 (left panel), GOODS-S (middle panel), and Bullet Cluster (right panel) fields as in the final HAWK-I *NB1060* image stacks. The inner and outer black contours on the Bullet Cluster image represent the regions where the gravitational amplification is respectively greater than 2.5 and greater than 1.2 for a source at a redshift of 7.7.

### Narrowband observations at 1.06 $\mu\text{m}$

Thanks to its wide field of view (7.5 by 7.5 arcminutes), excellent throughput and image quality, HAWK-I is ideally suited to searching for faint near-infrared (NIR) objects such as very high-redshift galaxies. The main dataset was obtained through a dedicated ESO large programme between September 2008 and April 2010. It is primarily based on observations using a NB filter at 1.06  $\mu\text{m}$  (hereafter referred to as *NB1060*). In addition, we include in our analysis HAWK-I science verification NB data taken in 2007. High-redshift galaxies can be extremely faint, and thus an efficient way to detect the faintest objects is to make use of massive galaxy clusters as gravitational telescopes. The amplification provided by gravitational lensing of background sources by foreground galaxy clusters allows us to probe luminosities that are intrinsically fainter than in the field, but at the expense of areal coverage due to space distortion.

We performed a careful analysis of the relative merits of blank field and cluster fields and determined that observing two clusters and two blank fields would be optimal in terms of high-redshift LAE yield, while mitigating the effects of cosmic variance. Our selected fields were

Abell 1689 and 1E0657-56 (Bullet Cluster) for the cluster fields, the northern half of the GOODS-S field and a subarea of the one square degree CFHTLS-D4 field for the two blank fields. The fields were chosen for the wealth of the available archival data. For one field, Abell 1689, it proved hard to assemble a consistent multi-wavelength dataset covering the full 7.5 by 7.5 arcminute HAWK-I field of view; this field will therefore be analysed separately and is not included in the present analysis. Figure 1 presents finding charts of the three fields studied here.

Our large programme data consists of more than 110 hours of on-sky integration time, of which  $\sim 80$  hours are *NB1060* data. Figure 2 shows the overall transmission curves of the HAWK-I broadband and NB filters corresponding to these observations. The *NB1060* filter has a central wavelength of 1062 nm, a full width at half maximum (FWHM) of  $\Delta\lambda \sim 10$  nm and is designed to match a region of low OH emission from the night sky. The filter width samples the Ly $\alpha$  line between  $z = 7.70$  and  $z = 7.78$ . For each field, the *NB1060* data are acquired over two epochs separated by one year, allowing us to discard transient objects that could be detected in a one-epoch stack, and not in the other. The three *NB1060* final images have exquisite image qualities ranging from 0.53 to 0.58 arcseconds. The  $3\sigma$  *NB1060* point source detection limits are 26.65, 26.65, and 26.50 for the GOODS-S, CFHTLS-D4, and Bullet Cluster respectively, in AB magnitudes.

### Candidate selection

We do not expect  $z = 7.7$  LAEs to be detected in any of the filters blueward of the Ly $\alpha$  line redshifted to 1.06  $\mu\text{m}$ . First, negligible amounts of radiation are expected to escape the galaxy and to be transmitted by the IGM below the Lyman limit at 91.2 nm, which is redshifted to  $\sim 790$  nm. In addition, all the radiation between the Ly $\alpha$  and Ly $\gamma$  lines at  $z = 7.7$  is entirely redshifted beyond the Gunn–Peterson trough at  $\sim 850$  nm observed in the spectra of high-redshift quasars and which corresponds to the end of the re-ionisation at  $z \sim 6$ . Only the blue part of the Ly $\alpha$  forest, just above the Lyman limit, could be transmitted to Earth. In practice, considering the limiting magnitudes of our optical and *NB1060* images, absorption of 2 magnitudes or so will result in no detections in any of the optical bands.

We used SExtractor for source detection and photometric measurements. We built a master catalogue of all the *NB1060* detected objects, measuring their magnitudes in each of the optical and NIR broadband images by running SExtractor in double image mode. We then searched for objects in this master catalogue that are not detected in the optical images at a signal-to-noise ratio above two. Because the *NB1060* bandpass is located within the bandpass of the Y filter (see Figure 2), the Ly $\alpha$  line may be detected in the Y filter when data in this filter are available. To estimate the *Y-NB1060* colour as a function of redshift, we generated simple synthetic models of LAE spectra and find that for objects with redshifts correspond-

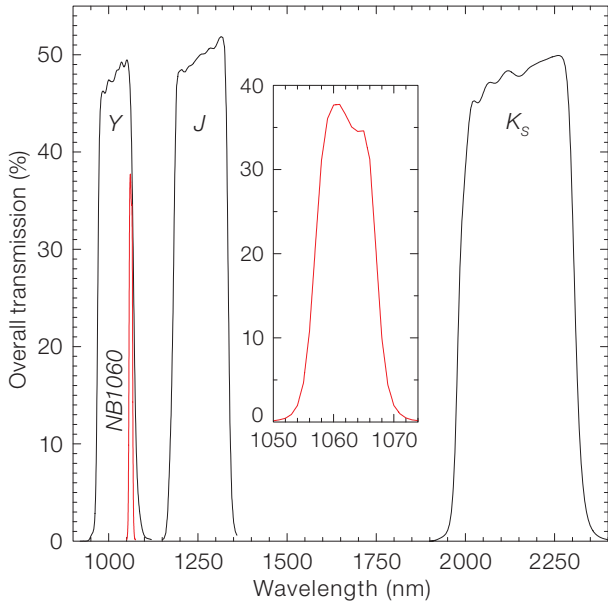


Figure 2. Transmission curves of the HAWK-I broad-band and narrowband filters corresponding to the observations made as part of our large programme. The red curve and the inset show the profile of the NB1060 filter centred at the wavelength of 1060 nm.

ing to the Ly $\alpha$  line falling in the NB1060 filter, the Y-NB1060 colour must be greater than 2 mag. To secure the presence of an emission line in the NB1060 filter, we further require a  $1\sigma$  narrowband excess over the flux measured in the J-band. Finally, we restrict the analysis to sources having a signal-to-noise ratio greater than five in the NB1060 final images and greater than two in image stacks corresponding to different observing epochs. The corresponding colour criteria used for the selection of candidates differ among the three fields depending on the depth of the optical images available in each of them.

After a rigorous inspection of potential candidates, we eventually concluded that we do not detect any LAE candidates down to a NB1060  $5\sigma$  magnitude of  $\sim 25.9$  to 26.1.

### Constraints on the $z = 7.7$ Ly $\alpha$ LF

The comoving volume sampled by our images corresponds to a grand total of  $\sim 2.4 \times 10^4$  Mpc $^3$  for the three fields. To constrain the LF of  $z = 7.7$  LAEs and compare our results with others, we

make use of the Schechter formalism in which the number of galaxies in a given luminosity bin is described by a function with three parameters: a characteristic luminosity  $L^*$ , a volume density normalisation factor  $\phi^*$  and  $\alpha$ , the faint-end slope, characterising how steeply the LF increases at low luminosities. From a Poisson distribution, one can easily compute single-sided confidence levels (CL) for the upper limits of the expected number of objects that correspond to a measured number of objects. By example, in our situation of zero detection, the 99.99% CL corresponds to upper limits of the mean number of objects of 10.36. Therefore, with zero detection and assuming pure Poisson statistics, one can exclude, at a given confidence level, the LF parameters that would yield an expected number of objects with our survey parameters.

However, considering the somewhat limited area covered by our observations, we need to consider the effects of cosmic variance in our statistical analysis. Because it fits the SDSS data well (Yang & Saslaw, 2011), we chose to adopt the negative binomial distribution (NBD) as an *ad hoc* representation of the probability density function of low galaxy number counts. The NBD can be conveniently expressed as a Poisson random variable whose mean population parameter is itself random and distributed as a Gamma

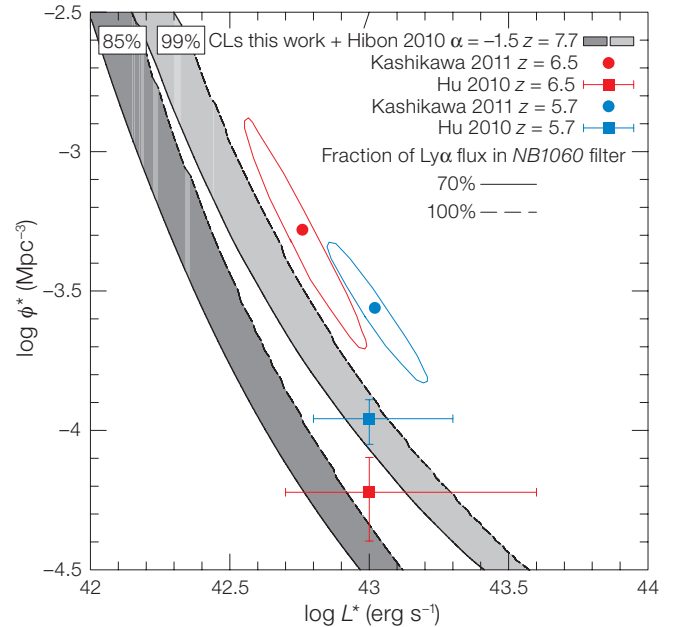


Figure 3. Parameters of the  $z = 7.7$  luminosity function excluded at 85% and 99% confidence levels from our data. We report the best-fit LF parameters at  $z = 5.7$  (blue) and  $z = 6.5$  (red) from Kashikawa et al. (2011) (as filled circles) and from Hu et al. (2010) (filled squares with error bars). The ellipses correspond to the  $3\sigma$  confidence levels. The plain (dashed) black lines correspond to the 85% and 99% confidence levels assuming a conversion factor of 70% (100%) between the NB1060 and Ly $\alpha$  fluxes.

distribution of variance equal to the relative cosmic variance.

We report in Figure 3 the parameters  $L^*$  and  $\phi^*$  excluded at 85% and 99% CL together with the best-fit parameters of the LAE LF at redshifts 5.7 and 6.5 from various sources. The faint-end slope  $\alpha$  is fixed at  $\alpha = -1.5$ . We report the upper exclusion zones derived from the absence of detections in the HAWK-I observations only (this work) combined with the null spectroscopic confirmation of the five brightest  $z = 7.7$  LAE candidates presented in Hibon et al. (2010).

The various LF parameters reported in the literature at redshifts 5.7 and 6.5 present some significant differences. Ouchi et al. (2010) and Kashikawa et al. (2011) convincingly claim that the evolution, mostly in luminosity, of the  $z = 6.5$  LF from the lower redshift LFs at  $z = 3.1$  and  $z = 5.7$  is a signature of re-ionisation, due to a neutral hydrogen fraction  $x_{\text{HI}}$  of



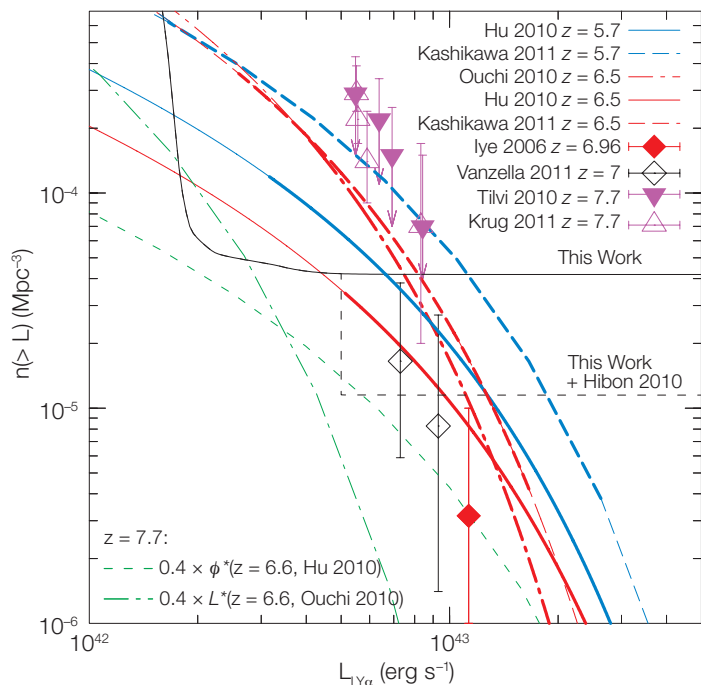


**Figure 4.** Cumulative Ly $\alpha$  luminosity functions. The blue lines show the cumulative LFs at  $z = 5.7$  and the red lines at  $z = 6.5$  from Hu et al. (2010) (as plain lines) and from Kashikawa et al. (2011) (as dotted lines). The red dotted-dashed line corresponds to the LF at  $z = 6.5$  from Ouchi et al. (2010). The transitions to thin lines indicate the range of the luminosities probed by the observations. The plain line and the dotted black line delimit the parameter space probed by our observations. The green dotted and dotted-dashed lines correspond to two scenarios for the evolution of the LAE LF between  $z = 6.5$  and  $7.7$ . The red filled diamond and the black open diamonds correspond to the spectroscopic confirmation of LAEs at  $z \sim 7$  from Iye et al. (2006) and Vanzella et al. (2011), respectively. The magenta downward-pointing filled triangles are the photometric candidates at  $z = 7.7$  from Tilvi et al. (2010) and the open triangles for the candidates from Krug et al. (2011).

the order of 20% at  $z = 6.5$ . Conversely, the evolution of the LF parameters between the same two redshifts deduced by Hu et al. (2010) is mostly in density; accordingly, they do not infer a signature of re-ionisation. How useful are our results in this context?

From Figure 3, we infer that we can safely exclude a scenario with no evolution of the LF parameters at  $z = 7.7$  at more than 99% CL from the Kashikawa et al. (2011) values at  $z = 6.5$ . With this LF, we should have found  $\sim 12$  LAEs on average in the three HAWK-I fields. The LF parameters of Hu et al. (2010) would pre-

dict  $\sim 2.5$  LAEs at  $z = 6.5$  and can be similarly excluded at more than 90% CL when including the null spectroscopic confirmation of the brightest LAE candidates of Hibon et al. (2010). Our results therefore clearly show that the  $z = 7.7$  LAE LF does evolve from the lower redshifts, but in the absence of concordance between the data at lower redshifts, it is difficult to ascribe this evolution to the galaxy properties or to re-ionisation.

### Two scenarios for the LF evolution

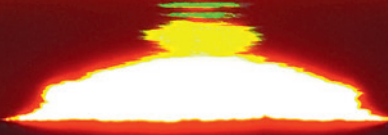
To assess what the consequences of our results might be, we consider two phenomenological scenarios for the evolution of the LAE LF between redshifts 6.5 and 7.7, either in density or in luminosity. We report these two scenarios in Figure 4 and compare them to cumulative Ly $\alpha$  luminosity functions from Hu et al. (2010) and Kashikawa et al. (2011), assuming a faint-end slope fixed at  $\alpha = -1.5$ . We also show the parameter space probed by the HAWK-I observations (this work) and the null spectroscopic confirmation of Hibon et al. (2010). In the first scenario, we consider a  $\sim 60\%$  evolution in density from the  $z = 6.5$  datapoint of Hu et al. (2010). Such an evolution is well reproduced by some models combining the evolution of large-scale structures and of

the intrinsic galaxies properties. However, the ultraviolet LF of high-redshift LBGs evolves mainly in luminosity, and such a density evolution for LAEs should therefore be treated with caution. As can be seen in Figures 3 and 4, this scenario would fit most of the observational data available up to redshift 7. The main conclusion from this test case is that to be consistent with our results, it does not require invoking a change in the Ly $\alpha$  IGM transmission and therefore a change in the neutral hydrogen fraction of the IGM. In the second scenario, conversely, we consider a 60% change in luminosity from the  $z = 6.5$  LF of Ouchi et al. (2010). This scenario clearly requires, by construction, a significant quenching of the IGM Ly $\alpha$  transmission. Although strongly model-dependent, a high neutral hydrogen fraction of the IGM (e.g.,  $x_{HI} \sim 60\%$ ) would then be required.

In conclusion, our results indicate a significant evolution of the LAE luminosity function at  $z = 7.7$  from lower redshifts. However, we cannot safely decide on whether we are “seeing” signatures of re-ionisation in our results, as this depends on which assumptions we use for the LFs at lower redshifts.

### References

- Bouwens, R. J. et al. 2011, ApJ 737, 90
- Casali, M. et al. 2005, The Messenger, 119, 6
- Clément, B. et al. 2011, arXiv:1105.4235
- Hibon, P. et al. 2010, A&A, 515, A97+
- Hu, E. M. et al. 2002, ApJ, 568, L75
- Hu, E. M. et al. 2010, ApJ, 725, 394
- Iye, M. et al. 2006, Nature, 443, 186
- Kashikawa, N. et al. 2011, ApJ, 734, 119
- Komatsu, E. et al. 2011, ApJS, 192, 18
- Krug, H. et al. 2011, arXiv:1106.6055
- Ouchi, M. et al. 2010, ApJ, 723, 869
- Tilvi, V. et al. 2010, ApJ, 721, 1853
- Vanzella, E. et al. 2010, ApJ, 730, L35+
- Yang, A. & Saslaw, W. C. 2011, ApJ, 729, 123



Upper: Even for Paranal the double green flash is a rare occurrence. This photo was taken by Gianluca Lombardi on 28 March 2011 as the Sun was setting on a cloudy horizon seen from Cerro Paranal. See Picture of the Week 1147 for details.

Lower: Their Royal Highnesses, the Prince and Princess of Asturias – the Spanish Crown Prince and Princess, visited Paranal on 24 November 2011. The Prince and Princess of Asturias are seen fourth and fifth from the left and are accompanied by the ESO Director General, Tim de Zeeuw (third from left), members of the Spanish delegation and ESO staff. See Release eso1146 for full details of the visit.





## Fornax, Virgo, Coma et al.: Stellar Systems in High Density Environments

held at ESO Headquarters, Garching, Germany, 27 June – 1 July 2011

Magda Arnaboldi<sup>1</sup>

<sup>1</sup> ESO

The workshop focused on recent observational progress in the understanding of stellar systems in the nearby clusters Fornax, Virgo, Coma et al. and provided a forum for comparing the results from theory and observations on galaxy evolution in high density environments at redshift zero.

Over the decade, the nearby galaxy clusters — Fornax, Virgo, Coma, Hydra and Centaurus, to name a few — have been the favourite targets of imaging and spectroscopic surveys like the Hubble Space Telescope Advanced Camera for Surveys (HST ACS), nearby cluster surveys (Virgo, Fornax and Coma surveys), the Next Generation Virgo cluster Survey (NGVS) at the Canada France Hawaii Telescope (CFHT), the SAURON and ATLAS-3D surveys of nearby galaxies and the 2dF Fornax cluster survey.

The strong scientific motivation for these extensive observational studies is driven by the presence of the oldest stellar populations and the products of the final collapse of massive stellar systems from star clusters with masses of  $10^3 M_{\odot}$  to the brightest cluster galaxies with masses of  $10^{13} M_{\odot}$ . On account of their proximity, which ensures excellent intrinsic spatial resolution in comparison with more distant galaxy clusters and allows the observations of individual stellar sources that are not accessible further away, nearby clusters are excellent laboratories in which to study the physical properties of old stellar populations by resolving individual star clusters reaching down to single stars.

In addition to the study of the stellar component, by using several tracers for measuring the distances of the different galaxies in these clusters, it is possible to construct the volume distribution and set constraints on how and when the different components, dark matter and baryons, come together to form the structures that we now see. The various galaxy morphological types can also be



Figure 1. Photo of the participants at the workshop, taken in the grounds of ESO Headquarters in Garching during a coffee break on a sunny morning in June.

placed within the 3D structure of these clusters and information can be collected on the effect of high density environments on the morphology and evolution of individual galaxies. The measurements of the physical parameters of galaxies, on all mass scales and surface brightness levels, can then be compared with predictions from theoretical models for the evolution of galaxies and larger-scale structures. In this sense, the study of nearby clusters complements those focused on clusters at high redshift: it provides independent constraints which allow models for galaxies and structure evolution to be tested further.

There is an important tradition of workshops dedicated to nearby clusters at ESO, and more than 120 participants (see Figure 1) gathered at ESO Headquarters to join in the discussions. As it happened, the ESO workshop Fornax, Virgo, Coma et al. took place 27 years after the ESO workshop on the Virgo cluster in 1984 (Richter & Binggeli, 1985). Twenty-seven years ago, the Virgo cluster was labelled the “Rosetta stone” for many problems in extragalactic astronomy in the foreword section of the workshop proceedings. Clearly, the enthusiasm of the participants during the intensive sessions and the vibrant discussion

which took place at the end of the workshop indicate that the Virgo cluster and the other nearby clusters continue to fulfil the expectations formulated in 1984.

### Workshop programme

Given the ambitious scientific programme, the sessions ran over five days of the week, including several exciting poster sessions, where the authors presented short two-minute talks on their work, 24 invited talks and 22 oral contributions. The poster announcing the workshop is shown in Figure 2. The complete programme of the workshop, including the presentations (in PDF format) is available<sup>1</sup>, and is linked to the Astrophysics Data System (ADS).

The workshop started during the afternoon of Monday, 27 June, with a session dedicated to invited reviews on topics important as background for the properties of stellar systems in high density environments that were to be addressed during the following sessions. The five reviews presented the general observational properties of clusters, the morphology of clusters at high redshifts from high resolution numerical simulations, galaxies and their black holes, active galactic nuclei (AGN) feedback and the size evolution of massive galaxies. The next day was dedicated to an overview of the surveys of nearby clusters at different wavelengths, from X-ray, optical

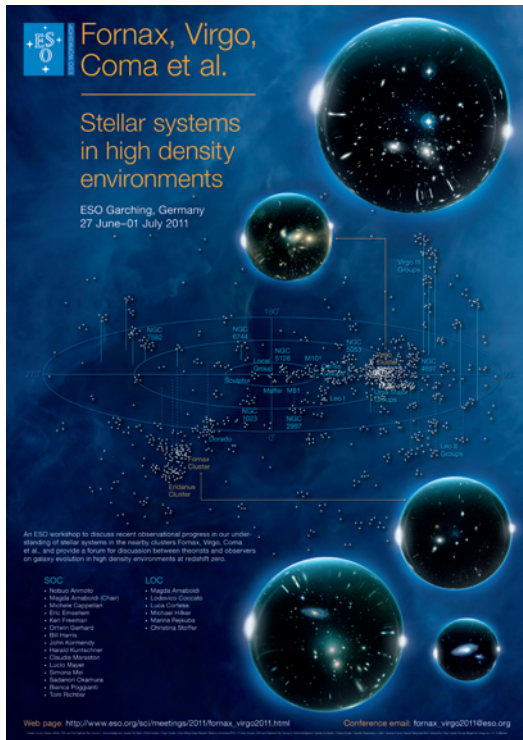


Figure 2. The poster of the ESO workshop, Fornax, Virgo, Coma et al.: Stellar systems in high density environments. It illustrates the large-scale structures in the local Universe and examples of galaxies in a range of luminosities and sizes. This poster will appear as background in the Warner Brothers series *The Big Bang Theory*.

- What is the distribution of dwarf spheroidals and UDCs in nearby clusters?
- What produces low luminosity galaxies ( $M_V > -16$ ) that are common to both groups and clusters? Are there enough low-luminosity irregulars to explain the many observed low-luminosity dwarf ellipticals?
- What is the relation between UCDs and bulges in compact dwarf galaxies?
- What are the most important scientific goals for future integral field unit spectroscopic surveys?

These questions represent a forward look in this area of research, which builds on 27 years of extragalactic studies in the nearby clusters since the ESO workshop on the Virgo cluster. Identifying these key questions sets an ideal bridge to the future as it highlights those exciting research areas that can be tackled by the European Extremely Large Telescope (E-ELT), as the high angular resolution and collecting power of an extremely large telescope are essential ingredients for the study of stellar populations at distances larger than 10 Mpc.

Again, the nearby clusters Fornax, Virgo, Coma et al. will be the first obvious targets for this new exciting era in extragalactic astronomy with many new amazing discoveries to be expected.

#### Acknowledgements

The LOC members Lodovico Coccato, Luca Cortese, Michael Hilker, Marina Rejkuba and Christina Stoffer are acknowledged for their hard work and support. The support by ESO students, and by Fei Zhao in particular, during question time is gratefully acknowledged. The intense and stimulating scientific programme of the workshop was defined by the SOC whose members were: Magda Arnaboldi, Noubuo Arimoto, Michele Cappellari, Eric Emsellem, Bill Harris, Ken Freeman, John Kormendy, Harald Kuntschner, Ortwin Gerhard, Claudia Maraston, Lucio Mayer, Simona Mei, Bianca Poggianti, Sadanori Okamura, Tom Richtler.

#### References

Richtler, O.-G. & Binggeli, B. (eds) 1985, ESO Workshop on the Virgo Cluster of Galaxies

#### Links

<sup>1</sup> Conference presentations available at: [http://www.eso.org/sci/meetings/2011/fornax\\_virgo2011/programme\\_final.html](http://www.eso.org/sci/meetings/2011/fornax_virgo2011/programme_final.html)

and near-infrared, to millimetre and radio wavelengths. On Wednesday the workshop started with a session dedicated to the faint end of the galaxy luminosity function with presentations on the physical properties of globular clusters, ultra-compact dwarfs (UCDs), and dwarf galaxies. It then moved on from photometry to kinematics and from the faint to the bright end of the galaxy luminosity function. Several topics were covered in this session: the inner and outer halo dynamics of early-type galaxies; the role played by merger events in shaping both light and kinematics in these objects; and the mass determination in massive galaxies using X-rays.

On the following day, the topics of the morning session covered the bright end of the luminosity function of galaxies in the nearby clusters and their physical properties. In the afternoon session, the subject shifted to the studies of the intra-cluster light (ICL), with presentations of results coming from both observations and numerical simulations. On the last day of the workshop, the morning session was dedicated to the discussion of the gas properties of galaxies with emphasis on the ram pressure stripping of gas experienced by galaxies as they

fall into the potential well and through the hot diffuse X-ray halo in the nearby clusters. Finally the workshop ended with a lively discussion chaired by Ortwin Gerhard and Roger Davies.

The discussion was structured around several questions which came about during the working sessions. These questions covered nearly all the topics presented at the workshop and are listed below:

- Is the current observational understanding of how the most massive galaxies form reconciled with the hierarchical formation paradigm? Are the observed distributions of angular momentum, colour gradients, alpha-element-to-iron ratio ( $\alpha/\text{Fe}$ ) and galaxy sizes compatible with these predictions?
- Where does the high metallicity in the hot coronae in clusters come from?
- Are S0 galaxies stripped or starved spirals?
- Does harassment cause significant star formation in gas driven to the centre of galaxies?
- How important is the star formation outside galaxies as seen in H $\alpha$  filaments and stripped gas?
- How do we learn from the ICL about galaxy evolution?



## Feeding the Giants: ELTs in the Era of Surveys

held in Ischia (Napoli), Italy, 29 August – 2 September 2011

Annalisa Calamida<sup>1</sup>  
 Aprajita Verma<sup>2</sup>  
 Isobel Hook<sup>1,2</sup>  
 Joe Liske<sup>3</sup>  
 Markus Kissler-Patig<sup>3</sup>

<sup>1</sup> INAF, Osservatorio Astronomico di Roma, Monteporzio, Italy

<sup>2</sup> Department of Physics, University of Oxford, United Kingdom

<sup>3</sup> ESO

Over the next decade, an incredible wealth of data will become available through many ongoing and forthcoming survey facilities. At the same time, the three Extremely Large Telescope (ELT) projects (the European ELT [E-ELT], the Thirty Meter Telescope [TMT] and the Giant Magellan Telescope [GMT]) will open a new parameter space of unprecedented sensitivity and spatial resolution. Motivated by exploring synergies between these two approaches, the workshop drew together both the survey and the ELT communities to define the first strategies to maximise the success of both aspects. The workshop was jointly organised by OPTICON and the INAF Observatory of Rome, the University of Oxford and ESO, and was held on the island of Ischia, near Naples.

The aim of the workshop was to address two broad questions: along with surveys conducted by current and forthcoming observatories, how will the upcoming dedicated survey facilities profit from follow-up by the ELTs; and to what extent do the three ELT projects require surveys to prepare for scientific breakthroughs? Both points were intensively discussed by about eighty international participants (from Europe, USA, Australia and Asia) over the five-day conference. We explored a range of forthcoming and ongoing facility projects and surveys, ELT instrumentation, as well as targeting a wide range of science areas (including exoplanets, stellar populations, galaxy formation and evolution, and cosmology) to address these two questions.

### The facility sessions

To set the scene, the conference opened with a comprehensive review of the facility landscape at the expected time of ELT operations, given by Patrick Roche, followed by invited reviews of the three ELT projects by Roberto Gilmozzi (E-ELT), Patrick McCarthy (GMT) and Timothy Davidge (TMT). All three projects are progressing well, undergoing cost and technical readiness reviews with planned first light early in the next decade.

The status of many ongoing and forthcoming facilities was then presented in detail by invited reviewers.

Thijs de Graauw presented a status update of the ALMA project, with the first call for proposals receiving around 900 applications; early science with the sixteen 12-metre antennas started on September 30. The Square Kilometer Array (SKA), presented by Lister Staveley-Smith, will be ready to enter the pre-construction phase in early 2012, and major science will already be possible with SKA1 in 2020 (10% of the full SKA). The synergies between these two facilities and the three ELTs were illustrated, highlighting, in particular, the comparable angular and spectral resolutions that will allow astronomers to perform multi-wavelength studies of astrophysical phenomena and objects, such as the gaseous evolution and dynamics of galaxies, star formation and discs around protostars.

The Large Synoptic Survey Telescope (LSST), presented by Philip Marshall, will have first light in 2018, and many of its projects would benefit from ELT follow-up, for example in providing spectra of newly detected transients, such as distant and exotic supernovae, or stellar velocity measurements in newly discovered low-mass Milky Way dwarf satellites.

Timo Prusti illustrated the advanced status of the Gaia project, which will be ready for launch in June 2013. This facility will provide astronomers with astrometry, photometry and radial velocities for at least one billion stars in the Milky Way, which will serve as an excellent astrometric reference frame with sub-milliarcsecond

accuracy down to magnitudes of  $V \sim 20$  for precise target selection with the ELTs.

Three other survey facilities, the Visible and Infrared Survey Telescope for Astronomy (VISTA), the VLT Survey Telescope (VST) and the Synoptic All Sky Infrared Survey (SASIR) were also presented during the first day's session. VISTA and VST are already in operation and conducting large public surveys addressing a variety of scientific questions.

Euclid, an M-class mission in the ESA Cosmic Vision Programme project, was also presented. This facility will survey the sky through optical and near-infrared imaging and slitless spectroscopy, with the primary goal of precision cosmology. These wide and deep surveys will deliver a wealth of other science including the discovery of rare objects that will be ideal targets for follow-up with ELTs.

### The science sessions

The following days of the workshop were devoted to seven science sessions, namely Solar System, Exoplanets, Stars and Milky Way, Stellar Astrophysics, Nearby Galaxies, Time Variability, Galaxy Evolution and Cosmology, each one introduced by an invited review. Roger Blandford opened the session presenting the scientific landscape of the next decade and future perspectives in light of limited resources.

Franck Marchis reviewed the current state of the art of Solar System science, which primarily originates from space missions that have probed the inner Solar System. Only one NASA mission, New Horizons, aimed at surveying Trans-Neptunian Objects (TNOs) is scheduled in the future, and another will observe Jupiter (Juno). There are no space missions towards the outer Solar System foreseen by countries that have just recently become involved in space studies. In this context, the ELTs, with their unprecedented angular resolution and sensitivity, will give access to the outer part of the Solar System from the ground. High angular imaging coupled with spectroscopy in the near infrared, for example, will allow the study of the surface

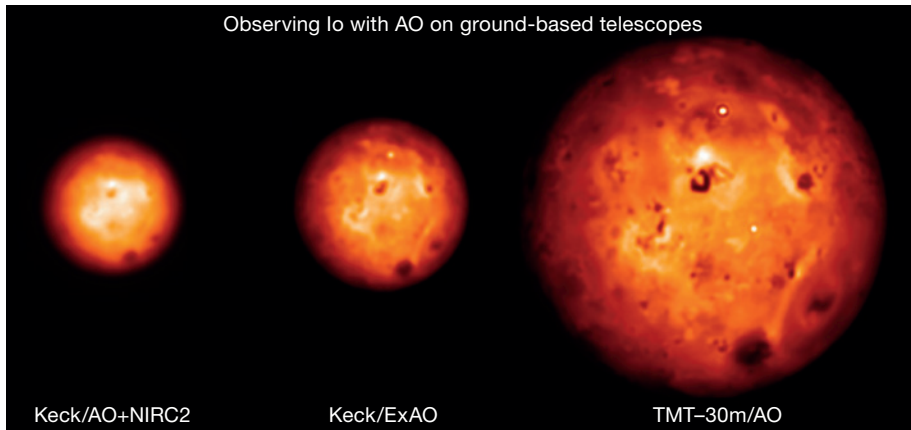


Figure 1. Simulations of the Jovian satellite Io as observed using adaptive optics with the Keck telescope using two techniques and with adaptive optics on the TMT. From Marchis et al., 2005.

composition and the volcanic activity of the Jovian satellite Io (see Figure 1), and to monitor the atmosphere of the satellite of Saturn, Titan, and of TNOs. On the other hand, mid-infrared spectroscopy will allow the analysis of molecular species in the atmospheres of Titan, Uranus and Neptune. Moreover, about half a million asteroids and comets are known today, and the sample will quickly increase thanks to the future ground- and space-based survey facilities. This large sample will require a spectroscopic follow-up by the ELTs, covering the wavelength range from the ultraviolet to the near-infrared (NIR), in order to provide an accurate taxonomic classification of these objects.

The topic of exoplanets was reviewed by Anne-Marie Lagrange, who showed how the ELTs will allow both indirect detection of low-mass Earth-like planets down to the habitable zone and direct detection of giant and Neptune-like planets. The characterisation of planets discovered by survey missions, through transits, direct imaging or spectroscopy, is a key science driver for the ELTs. These observations will allow the physical properties of the exoplanets to be constrained, such as mass, atmospheric composition and even weather in giant planets, on the path towards remote detection of exo-life.

In the field of stellar astrophysics, Manuela Zoccali showed in her review how large-scale surveys will be needed, with high

spatial and spectral resolution, to characterise the Milky Way Bulge. The ELTs will be crucial for studying the abundances of the most metal-poor Bulge stars to check, for instance, whether they were the first stars to form in the Galaxy. Great advances will come from facilities such as Gaia, Skymapper, RAVE, Hermes, SOFIA, and LSST, which will provide accurate astrometry and multi-wavelength photometry. These data, together with the high-resolution spectroscopy at high angular scales provided by the ELTs, will allow different Galactic stellar components (thin and thick disc, Bulge and halo) to be disentangled, thereby allowing us to constrain how the Milky Way and other galaxies formed and evolved.

Giuseppe Bono highlighted in his review how the uncertainties in the distance measurements still strongly affect the age estimates of Galactic clusters, giving absolute ages with an accuracy of only about 1–2 gigayears. The precise estimate of absolute and relative ages of stellar clusters in the Milky Way is fundamental to constrain the formation scenario of the Galaxy and to provide a lower limit to the age of the Universe. The high-resolution images collected by the future ELTs with the help of adaptive optics techniques will provide deep and accurate optical–NIR colour–magnitude diagrams (CMDs) of both Galactic clusters and Local Group stellar systems. These will be crucial to fully exploit the potential of diagnostics, such as the white dwarf cooling sequence or the bending of the lower main sequence, in providing absolute and relative ages.

For nearby galaxies, Carme Gallart's review illustrated that targeted surveys, together with ELT deep photometry and low/intermediate resolution spectroscopy, will be essential. The ultimate goal will be to derive star formation histories of galaxies in different environments. In order to derive accurate star formation histories, CMDs reaching the old main sequence turn-offs will be needed. With the ELTs this goal will be achieved in galaxies belonging to nearby groups, while for a representative sample of galaxies in the Virgo cluster (at a distance of about 16 megaparsecs), issues such as the effect of galaxy interactions on star formation might be addressed. More importantly, the ELTs will allow resolution of stars in these distant galaxies at surface brightness values currently not accessible to any other ground- or space-based facility. Furthermore, low-resolution spectroscopy of red giant branch stars will allow the chemical composition of old stellar populations to be traced out to the distance of the Virgo and Fornax galaxy clusters, while low-resolution spectroscopy of luminous super-giants will provide accurate chemical compositions for stars in galaxies well beyond these clusters.

Driven by technological innovation, wide-field astronomy has witnessed a resurgence, with a multitude of surveys being carried out and planned for the next decade; these surveys can investigate time-variable sources in the Universe. In his invited review, Shrinivas Kulkarni highlighted that, along with depth and area, cadence should be a standard parameter in the description of a survey, as this is the quantity that drives the frontiers in the research of time-variable phenomena. Ongoing surveys have largely filled in the gap between the rare but bright supernovae (SNe) and the faint but common classical novae with a host of objects (core-collapse SNe, thermo-nuclear SNe, calcium-rich transients, red novae, SNIa explosions, SNe and gamma-ray burst [GRB] afterglows), but the domain of short time-scales (less than one day) remains largely unexplored. While a number of surveys are planned, the subject would benefit from a co-ordinated multi-facility and multi-wavelength approach to make real



progress in understanding time-variable phenomena.

The ELTs will play a pivotal role in identifying and characterising transients (on all timescales) that are faint in the optical/NIR, up to about six magnitudes fainter than is currently possible. Optical–NIR follow-up of transient sources (e.g., pulsars, SNe/GRB afterglows) and their faint progenitors or host galaxies, identified by, for example, LSST, FERMI, SWIFT, GLAST and LOFT, will open a new era in understanding the properties of transient sources as well as opening new fields, such as the connection of short time-scale GRBs to gravity wave experiments, mapping the magnetospheres and magnetic fields of pulsars via polarimetric observations and faint probes of the (very) high-redshift intergalactic medium.

In his invited review, Carlos Frenk discussed both theoretical predictions of galaxy formation and evolution models and the observational advances made in these fields. Together with sensitive concurrent facilities, the ELTs will play a crucial role in galaxy evolution both at the highest redshifts and at the faintest flux levels, as well as in unprecedented spatial resolution via adaptive-optics assisted observations. The session on galaxy evolution and cosmology comprised talks on a range of multi-wavelength approaches to the topic covering detailed analysis at high spatial resolution of the dynamical state of galaxies, infrared photometric and spectroscopic surveys with Spitzer, Herschel and SPICA, sensitive radio measurements of star-forming galaxies with the SKA and its pathfinders, and the search for galaxies at the highest redshifts.

The synergies between large-area sensitive surveys with future facilities, including the James Webb Space Telescope (JWST) and SKA, in finding large samples of galaxies at high redshift were discussed, as well as the complementarity in spatial resolution to ALMA. With the ELTs we will be moving to detailed studies of large samples of galaxies. The ELTs will push the redshift barrier to the earliest galaxies, providing key constraints on the sources of first light. They will potentially reach objects dominated by Population III stars and probe the evolution of the



Joseph Caruana

Figure 2. The conference photo taken at the venue on Ischia on 31 August 2011.

intergalactic medium out to the era of re-ionisation.

A session of the workshop was also devoted to future instrumentation. The session comprised talks devoted to wide-field spectrographs for 4-metre-, 8-metre- and ELT-class telescopes (WEAVE, MOBIE and MANIFEST) from both the technological perspective and the key scientific motivations. In addition, the multi-conjugate adaptive optics module MAORY for the E-ELT (see Diolaiti, 2010) was discussed, with an emphasis on the possibility of correcting the image quality over a field of view as large as possible. HARMONI, an optical to near-infrared integral field spectrograph for the E-ELT (see Thatte, 2010) was also presented. As well as a pixel scale that suits seeing-limited conditions, HARMONI's finest pixel scale can make use of adaptive optics to achieve diffraction-limited observations with this telescope, providing a strong complementarity to ALMA. *The Messenger* 140 provides summaries of all the E-ELT instrument concepts.

The workshop also issued a statement in support of JWST, since the majority of astronomers were particularly concerned by the risk of cancellation of the JWST project, and by the impact that the loss

of scientific capability would have on the astronomical community worldwide.

### Closing discussion

The discussion was organised as a World Café<sup>1</sup>. Astronomers were divided into tables of about seven for three rounds of 20-minute discussions around proposed questions. Each table had a leader who took notes and summarised the discussion at the end. Gerry Gilmore summarised the discussion and provided conclusions for the Café.

Many interesting points were raised during this open and relaxed discussion, in particular, regarding how to deal with future observing programmes, data mining of surveys, and sharing technology and capability. It was emphasised how the follow-up of surveys with the ELTs will be crucial in the search for optical–NIR counterparts of extragalactic sources detected in the submillimetre, radio and X-ray, in characterising the faintest stars and brown dwarfs in the Milky Way and in the Local Group galaxies, in providing transit spectroscopy of newly detected exoplanets, or in identifying sources of gravitational waves. On the other hand, the impact of the ELTs will be maximised by surveys producing accurate astrometry and radial velocities of large samples of exoplanets and stars in the Milky Way, or by wide-field imaging

and spectroscopic surveys identifying the first galaxies, rare quasars, supernovae and gamma-ray bursts.

A lively discussion arose on data policy and data mining for surveys and ELTs. Most participants agreed that proprietary time should be at the minimum level but sufficient to guarantee intellectual ownership and a satisfactory progress of the surveys and the ELTs. Others proposed to have the data public from the beginning. In order to facilitate data mining, it was proposed that all data provided by the surveys and the ELTs should be Virtual Observatory compliant from the outset. Another interesting discussion was about ELTs sharing their development efforts through common documentation, complementary instrumentation capabilities, sharing information on site monitoring and sharing observing time.

The third part of the discussion dealt with how to retain diversity and how to involve young people in the era of flagship projects. Astronomers agreed that a large fraction of open time should be available

at the ELTs, together with encouraging some explicitly high-risk projects. It was noted that is very important to retain a broad range of facilities, including 4-metre- and 8-metre-class telescopes, to be used as survey facilities, to promote small projects, and to train young astronomers. All the long-term flagship projects should try to involve more students and young researchers, allowing them to attend science working committees, and communicating the outcome of the major high-level decisional meetings to them. Furthermore, it was proposed that at least one young astronomer should be included in each of the ELT science committees. More resources should be allocated to provide for longer term contracts to leave young astronomers more time to develop new and creative ideas.

Richard Ellis, in summarising the conference, highlighted the opportunity to establish a better coordination of facilities, instrumentations and programmes and that we should further strengthen these collaborations in the future. He also

emphasised the power of emerging countries and public outreach for investments in astronomical research and that diversity in facilities and astronomical capabilities should be retained together with large-scale projects. Ellis reminded us that we cannot plan the future in detail and so optimism, versatility and creativity remain the key attributes for success.

All the presentations and the conference picture are available at the conference website: <http://www.eso.org/sci/meetings/2011/feedgiant>.

#### References

- Diolaiti, E. 2010, *The Messenger*, 140, 28  
 Marchis, F., Spencer, J. R. & Lopes, M. C. 2005, in *10 after Galileo*, eds. R. M. C. Lopes and J. R. Spencer, Springer, p.287  
 Thatte, N. 2010, *The Messenger*, 140, 26

#### Links

- <sup>1</sup> More about the World Café format at: <http://www.theworldcafe.com/>

Report on the ESO/MPE/MPA/ExcellenceCluster/LMU Joint Astronomy Workshop

## The Formation and Early Evolution of Very Low-mass Stars and Brown Dwarfs

held at ESO Headquarters, Garching, Germany, 11–14 October 2011

Monika Petr-Gotzens<sup>1</sup>  
 Leonardo Testi<sup>1</sup>

<sup>1</sup> ESO

The topics discussed at the workshop ranged from the structure and fragmentation of molecular clouds to the formation of individual very low-mass objects, their multiplicity, physical structure, mass distribution and early evolution. Each topic was introduced by two reviews on the status of our theoretical and observational understanding of the field, followed by presentations of new results and discus-

sions. In this report we provide a brief summary of some of the areas discussed at the workshop.

Very low-mass (VLM) stars ( $< 0.4 M_{\odot}$ ) and brown dwarfs (BDs) are faint objects with low effective temperatures which are difficult to detect due to their low luminosities ( $\leq 0.01 L_{\odot}$ ). On the other hand, these objects are the major constituents of the stellar population of any galaxy and outnumber higher-mass stars by factors of hundreds to thousands. Current wide area surveys in nearby molecular clouds, from optical to far-infrared wavelengths, provide exciting new information on the process of the formation and early evolu-

tion of VLM stars and BDs. We report on the ESO/MPE/MPA/LMU/ExcellenceCluster joint workshop dedicated to recent theoretical and observational advances made in the field of study of the formation and early evolution of brown dwarfs and very low-mass stars.

It was demonstrated in several talks that, with the help of new and powerful ground- and space-based facilities (e.g., VISTA and Herschel respectively), we are starting to discover young VLM stars and BDs and their precursors in numbers large enough to allow statistical analyses of their properties. In addition, detailed studies of individual objects and small samples are now effectively being



carried out with large optical/infrared telescopes and millimetre arrays (e.g., VLT/X-shooter and ALMA). On the theoretical side, the latest modelling results were discussed and confronted with the observations. Approximately 120 participants came together in Garching (see Figure 1) for lively discussions in five sessions on the dedicated topics summarised below.

### Structure of molecular clouds: Formation and properties of cores

Substantial progress in understanding the formation of pre-stellar cores has been made thanks to the Gould Belt survey of nearby molecular clouds performed with the Herschel Space Observatory. The emerging picture is of the important role of filaments as the prime places for pre-stellar core formation (review talks by P. Myers and P. Andre). The typical structure of a filament, based on the analysis of more than 100 filaments in different molecular clouds, is that of a narrow, steep density profile with a characteristic width of roughly 0.1 parsecs. Observational evidence was presented for the formation of a pre-stellar core from velocity-coherent gas flows along the filament directions (talk by A. Hacar). It was further argued that pre-stellar cores are formed from the fragmentation of the densest parts of the filaments and that filament fragmentation forms the basis of the (sub)stellar initial mass function by setting the mass distribution of pre-stellar cores. It was also shown that Herschel observations of the Perseus and Serpens clouds suggest that the spatial density distribution of pre-stellar cores is scale-free, a result consistent with the spatial density distribution of young stellar objects in nearby molecular clouds (talk by E. Bressert). These findings support the ideas of the existence of a column density threshold for the formation of cores and stars and that the global properties of the outcome of the star formation process in nearby clouds is closely linked to the fragmentation process of molecular clouds.

However, the unambiguous identification of the precursors of BDs and VLM stars remains elusive: very low luminosity pre-stellar cores remain undetected; and low



Figure 1. Group picture of the workshop participants in the entrance hall of ESO Headquarters.

luminosity Class 0 sources with  $L \lesssim 0.8 L_{\odot}$  appear under-abundant in a large survey of protostars in the Orion star-forming region (talk by W. Fischer).

### From cores to stellar systems: Fragmentation, properties and multiplicity of protostars

In this session several models for the formation of VLM stars and BDs were reviewed and discussed by M. Bate, A. Boss, S. Basu and D. Stamatellos. New numerical simulations, including radiative feedback from protostars, show reduced core fragmentation and produce much fewer BDs than in previous simulations. Very low-mass stars and BDs may also be formed in fragmenting massive circumstellar discs involving subsequent ejections from these discs. Ejections are frequent events and may happen even at early evolutionary stages, leading to ejected low-mass clumps. However, it was pointed out that massive discs around Class 0 sources are not observed and that radiative feedback

tends to inhibit disc fragmentation. This problem could be overcome if radiative feedback is episodic, with long periods of quiescence. The detection and physical characterisation of very low luminosity objects (VeLLOs) remains an observational challenge, but a few candidates were presented (in talks by M. Dunham and T. Huard). Progress in this respect is expected to be made soon with ALMA, which provides excellent sensitivities at submillimetre wavelengths and at high spatial resolution.

The observed properties of low-mass protostars/proto brown dwarfs are clearly a key to understanding their formation. Protostellar/brown dwarf multiplicity was discussed by several speakers (G. Duchene, A. Kraus, P. Viana Almeida and R. Parker). It has been established over the last couple of years that the binary frequency declines with primary mass, a trend that continues down into the substellar regime. For the youngest objects, it seems that there is a lack of 100–500 AU separation Class I binaries (not specific to a particular primary mass range), while a high fraction is observed at larger separations. Also, Class 0 objects show a low binary frequency at separations  $< 2000$  astronomical units (AU).

### Revealing and understanding the low-mass end of the stellar initial mass function

The third session was introduced by a critical review from G. Chabrier of different theoretical scenarios of VLM star and BD formation and the confrontation with recent observations of the initial mass function (IMF). The large number of accumulating observational studies targeting the IMF in various star-forming regions was then summarised in a second review talk by K. Luhman, suggesting that the low-mass IMF shows in general very little, if any, variation. On the other hand, the measured IMF is subject to substantial biases as a consequence of different observational approaches, such as the use of different stellar evolutionary models to convert the observed magnitudes to (sub)stellar masses, different spectral classification schema, or the restriction of the analysis to photometric data alone.

Several observational results based on recently completed or ongoing wide-field imaging surveys, such as UKIDSS/GCS or VISTA/Orion, in various star-forming regions showed the detection of numerous candidate VLM objects impressively, down to the lowest-mass T-type dwarfs (talks by N. Deacon, N. Lodieu, C. Alves de Oliveira, K. Muzic and J. J. Downes). Evidence was presented that shows no difference in the spatial distribution of stars, VLM stars, BDs and planetary-mass objects (talks by A. Bayo, K. Pena Ramirez). The typical ratio of low-mass stars to brown dwarfs is 4–5 (P. Dawson) with some scatter from one star-forming region to another. However, the explicit shape of the substellar IMF is still under discussion. During the workshop the essential concern was raised that the faintest (i.e. usually the lowest mass) objects detected in most of the surveys ( $< 13 M_{Jup}$ ) are only photometric candidates, and spectroscopic follow-up is urgently required. It was also pointed out by various speakers that the true (low-mass) end of the IMF has not yet been found.

### The circum(sub)stellar environment: Discs, outflows and accretion processes

The large body of evidence for a “T Tauri-like” phase in the early evolution of VLM stars and BDs was emphasised in many talks (e.g., by L. Hartman and A. Natta). Recent studies also suggest outflow, accretion variability and disc properties similar to those of more massive pre-main sequence stars. These findings, although generally consistent with the idea that objects as low as  $\sim 50 M_{Jup}$  can form in a similar fashion to more massive stars, cannot yet rule out different formation channels (ejection from multiple systems or fragmenting discs) starting to play a more significant role in the low-mass and brown dwarf regimes.

The key role of high sensitivity and simultaneous broadband spectroscopy with instruments like X-shooter at the VLT was pointed out as an important step to understanding the complex interplay between discs, accretion and outflow in these objects (talk by J. M. Alcalá). The statistical analysis of the accretion signatures in large population studies is starting to show evidence for different timescales depending on the mass of the central stars (talks by A. Natta and C. F. Manara). The intriguing discovery of a population of very long-lived accretors in the regions around very massive clusters in the Magellanic Clouds and in the inner regions of the Galaxy was also presented (talk by G. De Marchi).



Figure 2. Stamp depicting a young brown dwarf with an outflow, issued by the Republic of Ireland Post to celebrate the International Year of Astronomy in 2009, was shown several times at the meeting.

Sensitive surveys seem to suggest that circumstellar discs around VLM stars and BDs are at least as common as in T Tauri stars, and their properties appear to be similar (talks by S. Mohanty, D. Jaffe and M. Gully Santiago). The current millimetre observations do not yet allow us to resolve the disc sizes and place strong constraints on the ejection models, but it is expected that ALMA will soon allow these constraints to be lifted. Brown dwarf discs are also an interesting case study to test disc evolution theories in a very low density regime. In particular, probing grain growth in very low-mass discs, such as those found around BDs, will allow us to put strong constraints on dust evolution models. The rapid and ubiquitous dust grain evolution observed in discs around solar and slightly subsolar-mass stars are not predicted in the BD regime, but ALMA will soon tell us whether these predictions are verified or not (talk by L. Testi).

### Early evolution of very low-mass stars and brown dwarfs

Finally, during the last day of the workshop an overall picture of the early evolutionary stages of very low-mass stars and brown dwarfs was laid out in talks by I. Baraffe and L. Spezzi. As opposed to the assumption of steady mass accretion limited to the protostellar stage, as in previous pre-main sequence evolutionary models, new models now consider episodic and significant mass accretion rates also during the early phases of pre-main sequence evolution (talks by Baraffe and S. Offner). Episodic accretion acts on the internal structure of very low-mass stars and brown dwarfs, making them more compact (smaller radii) and hence appear less luminous, i.e. older, in the Hertzsprung–Russell diagram.

New average lifetimes for different evolutionary phases were constrained from Spitzer’s Cores to Discs and Gould Belt surveys resulting in a revised Class 0 lifetime estimate of  $\sim 1/5$  of the Class I lifetime ( $\sim 0.44$  Myr), while the classical T Tauri phase (Class II) represents the dominant phase during the pre-main sequence evolution of low-mass stars



(talk by L. Spezzi). As spectroscopic confirmation of a low effective temperature is often the final proof for a *candidate* substellar mass object, it is essential to build up spectral libraries for the lowest-mass objects. Some large sample spectroscopic projects, as well as detailed observations of individual objects, have been carried out, or are currently underway, as mentioned in talks by S. Antonucci, J. Patience and J. Bochanski.

In summary, the workshop stimulated a very successful exchange of ideas and new results, and was very well received by the participants. The success of the workshop and its smooth and efficient practical organisation would have not been possible without the dedicated work of ESO students and fellows (Joana Ascenso, Giacomo Beccari, Eli Bressert and Sebastian Daemgen) and Christina Stoffer, who all provided excellent sup-

port before, during and after the meeting. The workshop gratefully acknowledges the receipt of financial support from ESO, the LMU/Excellence Cluster and from MPE. Most of the talks and posters are available from the workshop webpage<sup>1</sup>.

#### Links

<sup>1</sup> Workshop webpage: <http://www.eso.org/sci/meetings/2011/vlms2011.html>

## Brazilian Teachers and Students Visit Paranal and ALMA

Michael West<sup>1</sup>

<sup>1</sup> ESO

With Brazil poised to become the first non-European member of ESO, new opportunities exist to strengthen ties between the Brazilian astronomical community and ESO.

At the invitation of ESO’s Director General, a group of ten Brazilian teachers and students travelled to Chile in August 2011. All are members of the Louis Cruls Astronomy Club from the city of Campos in Rio de Janeiro state, and were led by Professor Marcelo Souza of Universidade Estadual do Norte Fluminense and with the support of Dr José Monserrat Filho, Advisor for International Cooperation from the Brazilian Space Agency.

Accompanied by the head of the Office for Science in Chile, the group visited the ALMA and Paranal sites during the week of 21–27 August. Seeing the ALMA array and the VLT up close was a dream come true for this enthusiastic group of amateur astronomers. Other highlights of the visit included an opportunity to chat with the ESO astronomer and fellow countryman, Claudio Melo, and to get an insider’s look at the VLT and ALMA operations.

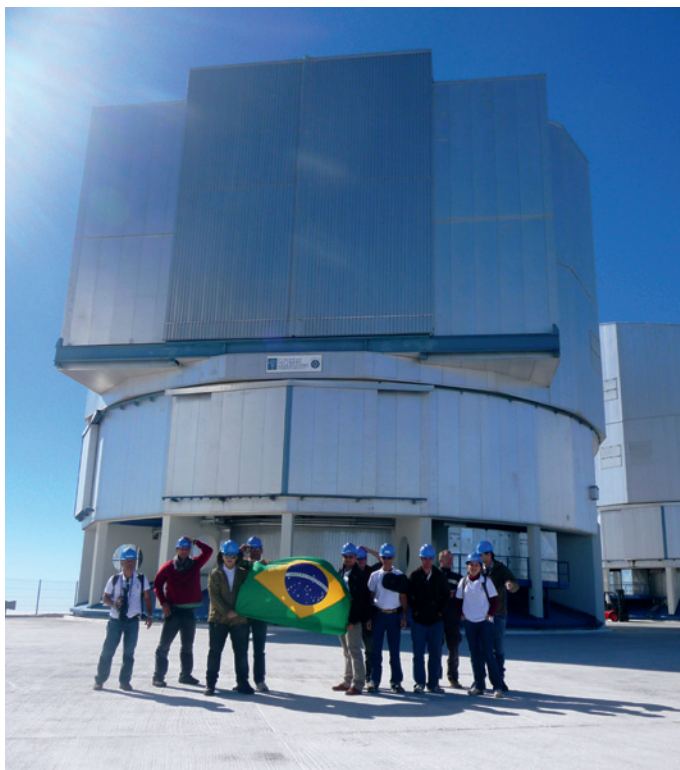


Figure 1. Teachers and students from the Brazilian Louis Cruls Astronomy Club during their visit to Paranal.

Brazil’s first astronaut, Marcos Pontes, has inspired millions of young Brazilians to consider scientific careers. “Brazil has a very bright future in science and technology,” he said, “but for this to come true, you have to have young people working in this area.” Thanks to the

opportunity to visit the ESO and ALMA facilities in Chile, today’s student members of the Louis Cruls Astronomy Club may be inspired to become tomorrow’s professional astronomers and engineers in Brazil.

# ESO Presence at the Astronomical Society of Brazil Annual Meeting

Jochen Liske<sup>1</sup>

<sup>1</sup> ESO

The 36th annual meeting of the Astronomical Society of Brazil (Sociedade Astronômica Brasileira SAB<sup>1</sup>) was the first meeting since Brazil's notice of accession to ESO at the end of 2010. The organisers of this event took the opportunity to offer their community a wide-ranging overview of ESO by inviting four speakers to present high-level synopses of key ESO activities. The meeting was held from 4–8 September 2011 in the beautiful setting of the holiday resort town of Aguas de Lindoia, about 180 kilometres from Sao Paulo.

The importance of Brazil's joining ESO was underlined by the Director General, Tim de Zeeuw, opening the proceedings on the first night of the meeting with an overview of ESO's facilities and activities.

On the third day of the conference, the estimated 300 participants, the vast majority of whom represented the future of Brazilian astronomy, were treated to a special session dedicated to ESO. To begin with, Wolfgang Wild provided an excellent description of the Atacama Large Millimeter/submillimeter Array (ALMA), its science goals and the project status. The equivalent overview for the

Rafael Santucci, IAG/USP



Figure 1. The ESO Director General Tim de Zeeuw fielding questions after his inaugural address to the Astronomical Society of Brazil.

European Extremely large Telescope (E-ELT) was presented by Jochen Liske. Simon Lilly from ETH, Zurich, then supplied a review of ESO from the perspective of a community member and telescope user. He related his own experiences in engaging with ESO, both as a committee member and as PI (Principal Investigator) of a Large Programme at the VLT, and encouraged the audience to get involved in ESO's decision-making processes. This was followed by a thorough review of ESO's Public Surveys and the Science Archive Facility by Thomas Szeifert. Last, but by no means least, Luca Pasquini reviewed the VLT and La Silla instrumentation programmes, highlighting opportunities for the Brazilian community.

In addition to these dedicated ESO presentations, Francois Hammer presented an instrument concept for the E-ELT, while other speakers reported on recent results from the VLT, including Rodolfo Smiljanic, a Brazilian ESO Fellow. These ESO-related presentations were received with a high level of interest getting the astronomical relations between Brazil and ESO off to a great start.

## Links

<sup>1</sup> Sociedade Astronômica Brasileira webpage: <http://www.sab-astro.org.br/>

## First ESO Public Release of Data Products from the VISTA Public Surveys

Magda Arnaboldi<sup>1</sup>

Jörg Retzlaff<sup>1</sup>

on behalf of the ESO Archive Science Group

<sup>1</sup> ESO

The ESO Science Archive Facility now provides community access to the first release of data products from the near-infrared 4-metre Visual and Infrared Sur-

vey Telescope for Astronomy (VISTA) public survey projects. Following one and a half years of successful scientific operations of the VISTA telescope, the VISTA public surveys have returned nearly 6 TB of reduced data products, which can be queried for and downloaded by the international community via dedicated query interfaces.

The survey programmes on VISTA are a suite of well-coordinated and challenging scientific projects that range from a

pencil-beam survey with deep observations of extragalactic fields to whole hemisphere surveys (Arnaboldi et al., 2007). These survey projects were approved during the 79th ESO Observing Programme Committee meeting in November 2007 and effectively started surveying the southern sky in April 2010, following the successful commissioning of the VISTA telescope at the La Silla Paranal Observatory. A summary of the scientific goals and observing strategies of these surveys is available on the ESO web pages<sup>1</sup>.



As stated in the ESO Council document on the VLT/VLTI science operations policies, the Science Archive is the collection point for the survey products and the primary point of publication/availability of these products to the ESO community. The policies that ESO implemented to manage the survey projects on behalf of the community entail the submission and publication of data products according to an agreed cadence before any new telescope time allocation is granted to the continuation of each survey. The first of such review milestones was set one and a half years after the start of scientific operations at the VISTA telescope. Most of the survey teams have now submitted the agreed-upon data products, the first of which are now publicly available for community access and scientific investigation.

The current data release covers mostly the period from February 2010 to September 2010. It primarily consists of astrometrically and photometrically calibrated mosaicked and co-added images, each covering 1.5 square degrees, their weight maps and associated single band source lists in the different bands of each survey. The data products from the first VISTA public release can be queried for and retrieved<sup>2</sup>. A summary table of the current

Survey project	Release content	Sky coverage (sq.deg)	NIR filters
VVV	Contiguous patch of Bulge and Disc region including multi-epoch data in <i>Ks</i>	520	ZYJHKs
VIDEO	XMM-LSS field	1.5	YJHKs
VMC	2 pointings in the LMC, one overlapping with 30 Doradus and the other with the South Ecliptic Pole	3.0	YJKs
VHS	VHS DES: 120 seconds in <i>JHK</i> VHS ATLAS: 60 seconds in <i>YJHKs</i> VHS GPS: 60 seconds in <i>JKs</i>	1910 –	YJHKs

Table 1. Summary of the content of the first VISTA public survey data release.

release is provided in Table 1.

The mechanism set in place by the Phase 3 process for the reception, validation, and publication of data products from public survey projects ensures a high level of homogeneity and uniform standards for the data products accessible via the ESO archive query interface. Each data release is accompanied by an accurate release description<sup>3</sup> which provides information on the area coverage, the content of the release (i.e. bands, depth, etc) and additional details on the calibrations and results from quality control. This information supports the scientific use of the products by the international community beyond the initial goals identified by the survey teams.

By accessing the first VISTA public release, the ESO community benefits from the joint efforts by ESO, the PIs of the VISTA public survey projects and their collaborators, including the data centres at CASU<sup>4</sup> and WFAU<sup>5</sup>.

#### References

Arnaboldi, M. et al. 2007, *The Messenger*, 127, 28

#### Links

- Goals of VISTA public surveys: <http://www.eso.org/sci/observing/policies/PublicSurveys/sciencePublicSurveys.html>
- VISTA public surveys query form: [http://archive.eso.org/wdb/wdb/adp/phase3\\_vircam/form](http://archive.eso.org/wdb/wdb/adp/phase3_vircam/form)
- Description of public surveys data release: [http://www.eso.org/sci/observing/phase3/data\\_releases.html](http://www.eso.org/sci/observing/phase3/data_releases.html)
- Cambridge Astronomy Survey Unit: <http://casu.ast.cam.ac.uk>
- Edinburgh Wide Field Astronomy Unit: <http://horus.roe.ac.uk/vsa/index.html>

Announcement of the Workshop

## Astronomical Data Analysis 7th Conference

14–18 May 2012, Cargèse, Corsica, France

Held regularly since 2001, the Astronomical Data Analysis (ADA) conference series is focused on algorithms and information extraction from astrophysical datasets. During this year's conference ADA-VII, sessions will be dedicated to advanced algorithms in astronomical pipelines, asteroseismology, exoplanet detection, large-scale structure, cosmic microwave background, restoration, hyperspectral data analysis and compressed sensing. As in previous ADA conferences, there will be a full week of

tutorials (7–11 May 2012) on various topics of advanced data processing, preceding the conference itself.

The ADA conference is strongly interdisciplinary, allowing researchers coming from different fields to interact. There are generally five or six keynote speakers, who are leaders in their respective fields, half being astronomers and the other half being mathematicians, statisticians or electrical engineering researchers. Each session has at least one invited

speaker, and half of the talks are contributed talks. A full poster session is also included in the programme.

The Cargèse conference centre can host 80 participants during the conference week and 40 participants during the tutorial week.

More details can be found at the conference web page: <http://ada7.cosmostat.org/> or by email to: [ada7.cargese@gmail.com](mailto:ada7.cargese@gmail.com)

## Introduction of Calibration Selection via the ESO Science Archive Facility and Discontinuation of PI Packages

CalSelector is a new archive service that, starting from the results of a query for raw science files, groups together the raw science files that need to be calibrated together (e.g., an infrared jitter sequence) and associates and returns all the raw and static calibrations needed to process the raw science files. Excerpts from the relevant night logs and an XML representation of the calibration cascade are also added as ancillary files to the request. The set of raw and static calibrations needed to process the raw science files is defined by the calibration plan of the instrument and instrument mode. The calibration plans are distributed as part of the instrument documentation<sup>1</sup>.

Only Paranal instruments are supported for this first release. The associations of calibration files with raw science files

become available only after the calibrations are certified for quality. This typically takes of the order of two working days. An upcoming release of the tool is foreseen to allow the association of uncertified calibrations, with essentially no delay with respect to the data acquisition. The tool currently provides associations for all data acquired since June 2009. For some instruments the coverage extends back to 2008. We are currently working to extend the coverage as far back in the past as possible.

More information and instructions on CalSelector are available on the Science Archive web pages<sup>2</sup>.

With the deployment of the CalSelector service, the generation of PI Packs (the collection of raw science and calibration

files, master calibrations and some science products associated with a PI proposal) is discontinued as of 4 November 2011. PI Packs created before that date will remain available online<sup>3</sup> but will no longer be updated. PI Packs created between 1 October and 4 November 2011 will only contain raw data.

### Links

<sup>1</sup> Instrument calibration plans available as: <http://www.eso.org/sci/facilities/paranal/instruments/instrumentName/doc> e.g., for HAWK-I: <http://www.eso.org/sci/facilities/paranal/instruments/hawki/doc>

<sup>2</sup> Information and use of CalSelector: <http://www.eso.org/sci/archive/calselectorInfo.html>

<sup>3</sup> Existing PI Packs available at: <http://dataportal.eso.org/rh/pipacks>

Announcement of the Joint ESO/IAG/USP Workshop

## Circumstellar Dynamics at High Resolution

27 February – 2 March, 2012, Rafain Hotel and Convention Center, Foz do Iguaçu, Brazil



The dynamics of circumstellar (CS) envelopes is an active research frontier that has benefited greatly from the advent of

high-resolution observational techniques in the spectral, spatial and temporal domains. The observational discoveries and theoretical results emerging from this field have broad implications for many astrophysical topics, ranging from cosmology (via a better understanding of the progenitors of gamma-ray bursts, for instance), to star and planet formation (through a better description of CS disc dynamics in which viscosity plays a key role). The diverse and complex CS environments revealed by these observational techniques are particularly evident near hot high-mass stars, where stellar radiation plays a large, if not crucial role, in continuously shaping the immediate environment.

This workshop aims at bringing together the active community of hot stellar astrophysics, both theoreticians and observers, addressing the common topic of what can be learned from high resolution observa-

tions. Oral sessions during the meeting will be devoted to: theory and observations of CS discs and outflows; delta Sco and Be stars as laboratories for CS disc physics; dynamics of CS material and tidal interactions in hot binaries; massive star formation out of a dynamic environment; and magnetospheres of hot stars.

The scientific organising committee is composed of: A. C. Carciofi (São Paulo, co-chair), D. Baade (ESO), J. E. Bjorkman (Toledo, USA), A. Damiani (São Paulo), W. Dent (ALMA), A. Domiciano de Souza (Nice), Th. Rivinius (ESO, co-chair), S. Stefl (ESO), J. Vink (Armagh) and G. Wade (Ontario).

The registration deadline is 13 January 2012.

Further details are available at: <http://www.eso.org/sci/meetings/2012/csdyn> or by email to: [csdyninfo@eso.org](mailto:csdyninfo@eso.org)



## Fellows at ESO

### Olja Panić

There is nothing that makes our differences so insignificant as the infinite starry sky above our heads. Just a glance at it, and I see millions of reasons to do astronomy twinkling back at me reassuringly. Perhaps this glance was what has kept me going through many difficult moments in my life, as the starlight lit the way ahead.

As dawn broke one September day in 2000, I left Bosnia, my friends and family, with no more than 2500 euros to my name, but with disproportionately more ambition and enthusiasm. I went to nearby Italy and enrolled in an undergraduate degree course in astronomy at the University of Bologna, the world's oldest university. This was an endeavour that changed my life completely: from a life with no prospects in a country torn apart by a recent war, to a beautiful medieval city in Italy where my new life began to develop, and offering so much more. My interest in the chemistry that takes place in the cold dark corners of the Universe led me to do my MSc research in Florence, where I modelled the physics and chemistry of the dense prestellar cores.

Five years later, I was changing countries once more. I had just received my MSc degree cum laude and not more than two weeks later I took up a PhD position in Leiden. I followed the advice of my MSc thesis supervisors, who told me that Leiden was the best place for astrochemistry. To date they tell anecdotes about my fearless attitude of aiming only at the top places. I enjoyed my life in the Netherlands, the place that my husband and I soon called home, and the exciting research I was carrying out. Throughout my PhD I travelled a lot, an aspect of being an astronomer that I enjoy: exploring different cultures and traditions, speaking foreign languages and building collaborations with experts of varied personal and scientific backgrounds.

In my PhD thesis I investigated the structure of discs around young stars with high angular resolution observing techniques, mainly using millimetre interferometers. The three-dimensional structure of these discs holds keys to the condi-



Olja Panić

tions in which planets are formed, what the physical regimes of the gas and dust are during this process, and what chemical material will be delivered to the new planetary systems. In my papers, I brought modelling closer to observations by observing and modelling both gas and dust, a challenging and not frequently applied approach, in spite of the close interdependence of the gas and dust in discs.

For my next step, my heart was set on ESO, and ESO alone. In 2009 I received my PhD degree and though broken-hearted to leave Holland, I moved to my present job – that of a Fellow at ESO's Headquarters. Here, I am studying protoplanetary discs further, modelling discs and deriving observational constraints on their structure from both infrared and millimetre interferometry.

The stimulating environment at ESO, with the instrumentation experts at one's fingertips and a big star and planet formation community in Garching and Munich, has allowed me to grow as a researcher and expand my observational expertise. For almost two years I have been organising star formation seminars, regularly bringing together dozens of people to discuss the newest science results. A great thing about my job at ESO is that I spend three months a year on duty in Chile, where I have a unique

opportunity to participate in the commissioning and science verification of the Atacama Large Millimeter/submillimeter Array (ALMA). In my view ALMA represents the same for our modern world as the Egyptian pyramids or Machu Picchu did for their epochs – a pinnacle of our civilisation and technology created in the attempt to reach toward the heavens. If ever the stars in the sky are not enough to motivate me, a glance at the synchronous dance of the ALMA antennas certainly is.

After ESO I will spend five years at Cambridge University, where I will study both protoplanetary discs and their later stages, the debris discs.

### Dimitri Gadotti

I had forgotten about Jupiter's high proper motion!

It was the first night alone on my first observing run, studying to get a Master's degree. We had six nights at the 60 cm telescope of the Laboratório Nacional de Astrofísica, atop the pleasant hills of Minas Gerais, in Brazil, to obtain multi-band optical images of barred galaxies. At the beginning of each night the position of the telescope on sky had to be calibrated by eye, using the finder and a bright star with well-known coordinates. I did not want to get into much trouble with that, saw Jupiter at sunset, and decided to use it as my calibrator, since it could be easily identified with the finder. This was a bad idea of course, as Jupiter moves fast, and the coordinates I could get from the Astronomical Almanac did not correspond to the time when I put the planet at the centre of the finder! As a result, to my dismay I couldn't find any of the targets!

After realising the mistake, and correctly calibrating the telescope, everything went smoothly, and I can still clearly remember the excitement running through my veins when, one by one, "my" galaxies were parading on the computer monitor. The privilege of witnessing their spectacular beauty was all mine! I was utterly alone, cold, in pitch black darkness, and Pink Floyd was playing loudly. I knew I was doing something I would never let go of.

Years later, I'm at the helm of the VLT, a truly impressive technological feat, performing complicated spectroscopy of the transit of extrasolar planets, and it works superbly well.

I also obtained my PhD degree in Brazil, at the University of São Paulo, on the formation and evolution of stellar bars in galaxies. This led me to work on the secular building of galaxy bulges, a subject that is receiving considerable attention now. After São Paulo, I continued my work on bars at the Laboratoire d'Astrophysique de Marseille. Just before I came to work at ESO in Chile, I worked for four years as a researcher in the cosmology group at the Max-Planck Institute for Astrophysics, in Garching, just across the street from ESO Headquarters. Ironically, when I received the offer of the ESO fellowship, it was not to just cross the street, but to move twelve thousand kilometres away and spend 80 nights per year on Paranal – I was thrilled!

Working as support astronomer at Paranal for FORS2, CRIRES, X-shooter,



Dimitri Gadotti

FLAMES and UVES, even if a very demanding job, both mentally and physically, has been a refreshing and very rewarding experience. Supporting observing programmes outside my field

of expertise, which is the formation, evolution and structure of galaxies, has not only been fun, but also given me a chance to become much more complete as an astronomer. Paranal provides me with a chance to be involved in programmes on topics that range from Solar System bodies to high redshift quasars. Programmes such as the rapid time-monitoring of comets and supernovae allow me to see such objects, unlike galaxies, evolve before my eyes. In addition, the exchange of ideas, and the exciting atmosphere of discovery and challenge that permeates the control building during a regular night, has helped my own research on multiple occasions.

Understanding the intricate evolution of galaxies and their substructures is the main focus of my research. The current instrument suite at Paranal is paramount in providing us with the data we need to fulfill this wish. New instruments, already scheduled to come to the mountain, are even more revealing and challenging. I can only be thankful that my career path has led me here.

## Personnel Movements

### Arrivals (1 October–31 December 2011)

#### Europe

Reckmann, Fabian (DE)	Construction Technician
Davis, Timothy (GB)	Fellow
Spezzi, Loredana (IT)	Fellow
Muller, Nicolas (FR)	Optical Engineer
Argomedo, Javier (CL)	Software Engineer
Niederhofer, Florian (DE)	Student
Feldmeier, Anja (DE)	Student
Ferreira, Leticia (BR)	Student
Feltre, Anna (IT)	Student
Sciocluna, Peter (GB)	Student
Costigan, Gráinne (IE)	Student
Sanchez, Joel (MX)	Student

#### Chile

Barkats, Denis (FR)	System Astronomer
Vlahakis, Catherine (GB)	Commissioning Scientist
Wesson, Roger (GB)	Fellow
Manjarrez, Guillermo (MX)	Student
Saulder, Christoph (AT)	Student
Kim, Taehyun (KR)	Student

### Departures (1 October–31 December 2011)

#### Europe

Austin-May, Samantha (GB)	Deputy Head of Human Resources
Igl, Georg (DE)	Quality Engineer
Checucci, Alessio (IT)	Software Engineer
Santander Vela, Juan de Dios (ES)	Software Engineer
Boehnert, Alex (DE)	Student
Sartoris, Barbara (IT)	Student

#### Chile

Gillet, Gordon (DE)	Electronics Engineer
Aguila, Luis (CL)	Electrical Technician
Arcos, Juan Carlos (CL)	Warehouse Assistant
Saguez, Claudio (CL)	Warehouse Supervisor
Costa, Jaime (CL)	Electrical Engineer
Pizarro, Andres (CL)	Safety Engineer
Quitana, Rolando (CL)	Procurement Officer
Beletsky, Yuri (BY)	Operations Astronomer
Kurz, Richard John (US)	ALMA Project Manager
Mateluna, Reneé Cecilia (CL)	Student
Alamo, Karla Adriana (MX)	Student
Jilkova, Lucie (CZ)	Student





ESO

European Organisation  
for Astronomical  
Research in the  
Southern Hemisphere



## E-ELT Project Manager and Head of the E-ELT Division

The European Organisation for Astronomical Research in the Southern Hemisphere (ESO) is the foremost intergovernmental astronomy organisation in Europe and the world's most productive astronomical observatory. ESO operates three unique world-class observing sites in the Atacama Desert region of Chile: La Silla, Paranal and Chajnantor. The ESO headquarters are located in Garching, near Munich, Germany. ESO is the focal point for Europe's participation in the Atacama Large Millimeter/submillimeter Array (ALMA) consortium, which is currently constructing a large submillimetre array in the Chilean Andes.

The concept and design of the European Extremely Large Telescope (E-ELT) is currently underway at ESO. This revolutionary new ground-based telescope concept will have a 40-metre-class main mirror and will be the largest optical/near-infrared telescope in the world: "the world's biggest eye on the sky". The start of E-ELT construction is planned for 2012, with the start of operations planned for early in the next decade.

For its E-ELT Division at the Headquarters in Garching near Munich, Germany, ESO is opening the position of:

### E-ELT Project Manager and Head of the E-ELT Division

The E-ELT Project Manager is responsible for the successful completion to specification of the E-ELT construction and within the approved budget and schedule. As Head of the Division the successful candidate directs all ESO activities in it and reports to the Director of Programmes and to the ESO Director General. As a member of the ESO enlarged management team the Head of Division contributes directly to the development of the overall policy, strategic planning and maintains professional contacts at the highest level outside the Organisation. The Division consists of about 15 engineers and scientists who work in groups or teams, plus additional people drawn from the Directorate of Engineering and Directorate for Science.

#### Main Duties and Responsibilities:

- Delivering the E-ELT within time, cost and specification;
- Leads and manages the team based in Garching/Germany and in Chile;
- Releases all technical and managerial documentation generated within the project;
- Is the sole authority for approving change requests and requests for waiver, irrespective of their origin or urgency;
- Reports on a regular basis on progress, cost and schedule variations and risks to internal and external Committees;
- Supported by, and in consultation with ESO Administration and Human Resources, submits the annual forecast and manpower request to the Director of Programmes;
- Is the interface with the Directorates of Engineering, Operations and Science ensuring that the necessary resources to execute the project are available.

#### Experience:

- At least ten years of experience in constructing or operating scientific/high technology projects; experiences with such projects in astronomy or closely related fields would be an advantage;
- An established record of successful management and leadership in a large multi-disciplinary technology based project;
- Hands-on experience in the use of standard project management systems and tools.

#### Expertise in the following is essential:

- Strong leadership and organisational capabilities;
- Excellent motivational and communication skills;
- In-depth understanding of the budget and schedule controls needed for the timely, cost-effective completion;
- In placing and managing large contracts;
- In risk analysis, systems engineering procedures and in QA systems.

#### Key Competences:

- Translates complex aims into clear and manageable plans, identifying the resources required and timescales, contingencies and counter measures;
- Proactively identifies critical issues and ensures their timely resolution. Makes informed decisions that take into account the facts, goals, constraints, and risks;
- Balances conflicting demands and responds quickly to changes in priorities in-line with agreed overall objectives;
- Builds and manages collaborative working relationships within the organisation and with other teams and external partners;
- Ability to negotiate, influence and communicate in a clear and concise manner both in writing and verbally.

#### Qualifications:

The position requires a university degree in engineering, astrophysics or another of the physical sciences.

#### Language Skills:

The position requires very good working knowledge of English. Additional knowledge of other European languages would be an advantage.

#### Remuneration and Contract:

We offer an attractive remuneration package including a competitive salary (tax free), comprehensive pension scheme and medical, educational and other social benefits, as well as financial help in relocating your family and the possibility to place your child/children in daycare.

The initial contract is for a period of three years with the possibility of a fixed-term or indefinite extension based on technical and managerial achievements. The title or grade may be subject to change according to qualification and the number of years of experience.

#### Duty Station:

Garching near Munich, with frequent travel to Chile.

#### Career Path: VII

#### Application:

If you are interested in working in areas of frontline technology and in a stimulating international environment, please visit (<http://www.eso.org>) for further details.

Applicants are invited to apply online at <https://jobs.eso.org/>. Applications must be completed in English and should include a motivation letter and CV.

**Closing date for applications is 8 January 2012.**

For additional information, please contact the Director of Programmes, Dr. Adrian Russell at [arussell@eso.org](mailto:arussell@eso.org).

Although recruitment preference will be given to nationals of ESO Member States (members are: Austria, Belgium, Brazil, the Czech Republic, Denmark, Finland, France, Germany, Italy, the Netherlands, Portugal, Spain, Sweden, Switzerland and United Kingdom) no nationality is in principle excluded.

The post is equally open to suitably qualified female and male applicants.







Colour image of the double-barred spiral galaxy NGC 3368 (M96) formed from FORS1 images in *B*-, *V*- and *I*- bands. This galaxy of type SAB is situated at a distance of about 10 Mpc and has a weak active galactic nucleus. The images were identified in the ESO archive by Oleg Maliy from Ukraine, who participated in ESO's Hidden Treasures 2010 astrophotography competition. See Picture of the Week 1143 for more details.



ESO, the European Southern Observatory, is the foremost intergovernmental astronomy organisation in Europe. It is supported by 15 countries: Austria, Belgium, Brazil, the Czech Republic, Denmark, France, Finland, Germany, Italy, the Netherlands, Portugal, Spain, Sweden, Switzerland and the United Kingdom. ESO's programme is focused on the design, construction and operation of powerful ground-based observing facilities. ESO operates three observatories in Chile: at La Silla, at Paranal, site of the Very Large Telescope, and at Llano de Chajnantor. ESO is the European partner in the Atacama Large Millimeter/submillimeter Array (ALMA) under construction at Chajnantor. Currently ESO is engaged in the design of the European Extremely Large Telescope.

The Messenger is published, in hard-copy and electronic form, four times a year: in March, June, September and December. ESO produces and distributes a wide variety of media connected to its activities. For further information, including postal subscription to The Messenger, contact the ESO education and Public Outreach Department at the following address:

ESO Headquarters  
Karl-Schwarzschild-Straße 2  
85748 Garching bei München  
Germany  
Phone +49 89 320 06-0  
information@eso.org

The Messenger:  
Editor: Jeremy R. Walsh;  
Design: Jutta Boxheimer; Layout,  
Typesetting: Mafalda Martins;  
Graphics: Pedro Moura.  
www.eso.org/messenger/

Printed by Mediengruppe UNIVERSAL  
Grafische Betriebe München GmbH  
Kirschstraße 16, 80999 München  
Germany

Unless otherwise indicated, all images in The Messenger are courtesy of ESO, except authored contributions which are courtesy of the respective authors.

© ESO 2011  
ISSN 0722-6691

## Contents

### Telescopes and Instrumentation

M. Capaccioli, P. Schipani – The VLT Survey Telescope Opens to the Sky: History of a Commissioning-	2
K. Kuijken – OmegaCAM: ESO's Newest Imager	8
G. Zins et al. – PIONIER: A Four-telescope Instrument for the VLTI	12
S. Lacour et al. – Sparse Aperture Masking on Paranal	18

### Astronomical Science

S. Quanz et al. – Resolving the Inner Regions of Circumstellar Discs with VLT/NACO Polarimetric Differential Imaging	25
E. Caffau et al. – X-shooter Finds an Extremely Primitive Star	28
B. Clément et al. – Evolution of the Observed Ly $\alpha$ Luminosity Function from $z = 6.5$ to $z = 7.7$ : Evidence for the Epoch of Re-ionisation?	31

### Astronomical News

M. Arnaboldi – Report on the Workshop “Fornax, Virgo, Coma et al.: Stellar Systems in High Density Environments”	36
A. Calamida et al. – Report on the Workshop “Feeding the Giants: ELTs in the Era of Surveys”	38
M. Petr-Gotzens, L. Testi – Report on the ESO/MPE/MPA/ ExcellenceCluster/LMU Joint Astronomy Workshop “The Formation and Early Evolution of Very Low-mass Stars and Brown Dwarfs”	41
M. West – Brazilian Teachers and Students Visit Paranal and ALMA	44
J. Liske – ESO Presence at the Astronomical Society of Brazil Annual Meeting	45
M. Arnaboldi, J. Retzlaff – First ESO Public Release of Data Products from the VISTA Public Surveys	45
Announcement of the Workshop “Astronomical Data Analysis 7th Conference”	46
Introduction of Calibration Selection via the ESO Science Archive Facility and Discontinuation of PI Packages	47
Announcement of the Joint ESO/IAG/USP Workshop “Circumstellar Dynamics at High Resolution”	47
Fellows at ESO	48
Personnel Movements	49

Front cover: Colour image of the large globular cluster Omega Centauri taken with the newly commissioned VLT Survey Telescope (VST) and its 0.95 square degree (268 Mpix) camera, OmegaCAM. VST images in Sloan  $g$ ,  $r$  and  $i$  filters were combined. The data were processed using the VST-Tube pipeline developed by A. Grado and collaborators at the INAF-Capodimonte Observatory. See Release eso1119 and articles on VST and OmegaCAM on pp. 2 and 8. Credit: ESO/INAF-VST/OmegaCAM.